Université de Montréal

Mémoire intitulé :

New insights on ammonia metabolism in endothelial cells of the blood brain barrier

par Mariana Macedo de Oliveira

Programme des Sciences biomédicales
Faculté de Médecine

Mémoire présenté en vue de l'obtention du grade de Maitrise
en sciences biomédicales, Médecine expérimentale

Évalué par le jury suivant:
Dr. Pierre Haddad, Président rapporteur
Dr. Christopher Rose, Directeur de recherche
Dr. Jean-François Cailhier, membre du jury

Décembre, 2016

Résumé

L'encéphalopathie hépatique (HE) est un syndrome neuropsychiatrique complexe, une complication majeure de la maladie du foie. L'œdème cytotoxique est une complication grave de l'encéphalopathie hépatique, connu comme étant le résultat d'un gonflement des astrocytes. Les facteurs pathogéniques dérivés du sang tels que l'ammoniaque (NH_4^+) et le stress oxydatif (SO) sont connus pour être synergiquement impliqués. Les cellules endothéliales (CE) de la barrière hémato-encéphalique (BHE), régulant le passage vers le cerveau, sont les premières cellules à entrer en contact avec les molécules circulantes. L'effet de l'ammoniaque et du SO sur le transport et le métabolisme des CE n'a jamais été complètement exploré. Par conséquent, notre objectif était d'évaluer les effets de NH_4^+ et des espèces réactives de l'oxygène (ROS) sur les CE de la BHE en utilisant des systèmes de modèles *in vivo* et *in vitro*. Il a été démontré que le cotransporteur Na-K-2Cl (NKCC1) était impliqué dans la pathogenèse de l'œdème cérébral dans de nombreuses affections neurologiques. Le NKCC1 peut transporter NH_4^+ vers le cerveau et est régulé par les ROS. Par conséquent, l'expression de NKCC1 a été évaluée dans des CE primaires soumises à différentes concentrations de ROS et de NH_4^+ ainsi que dans des microvaisseaux cérébraux (MVC) isolés chez le rat BDL (*bile-duct ligated*), un modèle d'EH induit par une maladie hépatique chronique. Aucune régulation à la hausse de NKCC n'était présente chez les CE traitées ou les MVC. La glutamine synthétase (GS) est une enzyme qui joue un rôle compensatoire important dans la détoxification du NH_4^+ au cours de la maladie du foie. La GS est exprimée dans le muscle et le cerveau (astrocytes), mais n'a jamais été totalement explorée dans les CE de la BHE. L'expression et l'activité de la protéine GS ont été trouvées dans les CE de la BHE *in vitro* (CE primaires) et *in vivo* (MVC isolés de rats naïfs). Dans le modèle BDL, l'expression de GS dans les MVC n'était pas significativement différente des témoins (SHAM). Par ailleurs, nous avons traité des CE avec du milieu conditionné à partir de plasma de rats BDL et avons trouvé une diminution de l'expression de la protéine GS et de l'activité par rapport aux SHAM. De plus, les CE traitées avec NH_4^+ augmentaient en activité de GS tandis que les traitements avec SO avec et sans NH_4^+ diminuent l'activité de GS. Globalement, ces résultats démontrent pour la première fois que la GS est présente dans les CE, à la fois *in vivo* et *in vitro*. La GS est régulée à la baisse dans les CE traitées avec du plasma de BDL (mais pas dans les MVC de BDL). Il est intéressant de noter que le NH_4^+ stimule l'activité de GS dans les CE, alors que le SO inhibe l'activité de GS, ce qui justifie possiblement les résultats de nos études avec les milieux conditionnés. Nous supposons que le SO empêche la régulation à la hausse de GS de la BHE, en diminuant la capacité des CE à détoxifier l'ammoniaque et à limiter l'entrée d'ammoniaque dans le cerveau. Nous envisageons qu'une régulation à la hausse de GS dans les CE de la BHE pourrait devenir une nouvelle cible thérapeutique de l'EH.

Mots-clés : Encéphalopathie hépatique, hyperammoniémie, cellules endothéliales, œdème cérébral, glutamine synthétase, NKCC1

Abstract

Hepatic encephalopathy (HE) is a complex neuropsychiatric syndrome, which is a major complication of liver disease. Cytotoxic edema is a serious complication of HE, known to be the result of astrocyte swelling. Blood derived pathogenic factors such as ammonia (NH_4^+) and oxidative stress' (OS) are known to be synergistically implicated. Endothelial cells (EC) of the blood brain barrier (BBB) are the first cells regulating passage into the brain and to contact blood-derived molecules. The effect of ammonia and oxidative stress on EC transport and metabolism has never been thoroughly explored. Therefore, our aim was to evaluate the effects of NH_4^+ and reactive oxygen species (ROS) on EC of the BBB using *in vivo* and *in vitro* models systems. The Na–K–2Cl cotransporter (NKCC1) has been demonstrated to be involved in the pathogenesis of brain edema in numerous neurological conditions. NKCC1 can transport NH_4^+ into the brain and is regulated by ROS. Therefore, the expression of NKCC1 was evaluated in primary EC submitted to different concentrations of ROS and NH_4^+ as well as in cerebral microvessels (CMV) isolated from the bile-duct ligated (BDL) rat, a model HE induced by chronic liver disease. No upregulation of NKCC1 was present in either the treated EC or CMV. Glutamine synthetase (GS) is an enzyme with an important compensatory role in NH_4^+ detoxification during liver disease. GS is expressed in muscle and brain (astrocytes) but has never been thoroughly explored in ECs of the BBB. GS protein expression and activity was found in EC of the BBB *in vitro* (primary EC) and *in vivo* (CMV isolated from naive rats). In the BDL model, GS expression in CMVs was not significantly different from SHAM-operated controls. In addition, we treated ECs with conditioned medium from plasma of BDL rats and found a decrease in GS protein and activity when compared to SHAM. Furthermore, EC treated with NH_4^+ increased GS activity while treatments with ROS with and without NH_4^+ decreased GS activity. Overall these results demonstrate for the first time that GS is present in EC both *in vivo* and *in vitro*. GS is downregulated in EC treated with BDL plasma (but not in BDL CMV). Interestingly, NH_4^+ stimulates GS activity in ECs, while ROS inhibits GS activity, possibly justifying the results found from the conditioned medium studies. We speculate that ROS prevents the upregulation of GS in the BBB, decreasing the capacity of the EC to detoxify ammonia and to limit ammonia entry into the brain. We foresee that upregulating GS in ECs of the BBB could become a new therapeutic target for HE.

Keywords: Hepatic encephalopathy, hyperammonemia, endothelial cells, brain edema, glutamine synthetase, NKCC1

List of contents

List of tables

List of figures

List of abbreviations

ALF: Acute liver failure

BBB: Blood-brain barrier

BDL: Bile-duct ligation

CLD: Chronic liver disease

CHE: Covert HE

CNS: Central nervous system

EC: Endothelial cells

GA: Glutaminase

GS: Glutamine synthetase

HE: Hepatic encephalopathy

OHE: Overt HE

OP: Ornithine phenylacetate

PIC: Protease inhibitor cocktail

RBMEC: Rat brain microvascular endothelial cells

TNF: Tumor necrosis factor

WNK: with no lysine kinase

Acknowledgments

First, I would like to thank Dr. Christopher Rose for the opportunity of being part of his team, for his incentive, availability and inspiration.

Secondly, I would like thank Mélanie Tremblay for her precious advice and for teaching me numerous techniques that allowed me to complete my master's degree, Cristina Bosoi for her hard work and competence that provided the foundation for this project and Marc-André Clément for always being there, either to help me with the project or to refresh my ideas over a cup of coffee.

Finally, I would like to thank Rafaela Almeida for her advice and all the members of the Hepato-Neuro lab for sharing their knowledge and making this two years enriching and enjoyable.

Introduction

Hepatic encephalopathy

Hepatic encephalopathy (HE) is a serious neuropsychiatric disorder that affects up to 80% of patients with liver disease (Bajaj, 2008). A major complication of either acute and chronic liver disease, HE develops when the ailing liver can no longer perform properly, including detoxification, leading to a build up of toxins in the blood which affect the brain. HE has a range of symptoms going from attention and learning deficits and motor incoordination to stupor, coma and death. HE has an impact on the patients' survival, quality of life and neurological outcome following liver transplantation (Bajaj et al., 2011; Sotil et al., 2009; Stewart et al., 2007). Although HE patients present a major burden on health care systems (Neff, 2010a), there is still no optimal treatment available, and more research is needed to fully understand this syndrome and develop efficient treatments.

Liver

The liver is the second largest organ in the body, weighing approximately 2-3% of total body weight. The liver is morphologically divided in two main lobes (left and right) and two accessory lobes (quadrate and caudate) (Bismuth, 1982). The functional unit of the liver is the hepatocyte. Hepatocytes are epithelial cells grouped in interconnected plaques forming the hepatic lobules, with each lobule being served by branches of the hepatic artery, portal and hepatic veins and biliary ducts (figure 1).

Vascularity

The liver has a unique vascular setting in the body, since it receives both arterial and venous blood. The liver is fed by the common hepatic artery that separates into two branches (left and right arteries) that perfuse the respective lobes. The hepatic drainage arises via the intrahepatic vein that splits into three hepatic veins that drain into the inferior vena cava. The liver is also perfused by the portal vein, which is formed by the confluence of the mesenteric vein, splenic vein and other additional branches (coronary/left gastric, cystic and tributaries of the right gastric and pancreaticoduodenal veins). The portal vein transports blood rich in

nutrients and toxins from the gastro-intestinal tract (GIT), pancreas and spleen into the liver and is responsible for approximately 70-80% of all the blood entering the liver (Junqueira and Carneiro 2016). The biliary system typically follows the portal system and is composed by multiple intrahepatic ducts responsible for the formation and transport of the bile (Abdel-Misih and Bloomston, 2010).

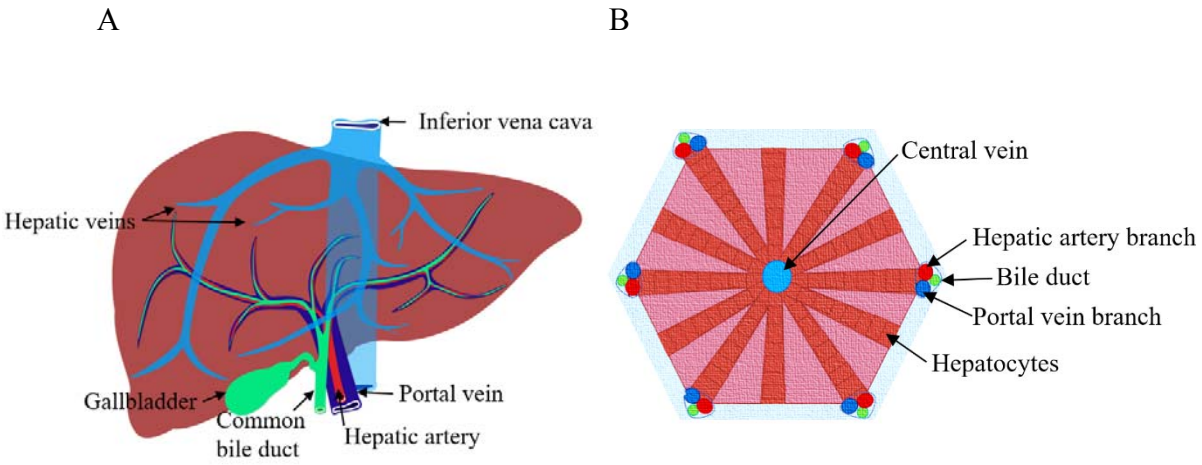

Figure 1: The liver anatomy
(A) gross liver anatomy, (B) hepatic lobule anatomy.

Function

The liver regulates several systemic processes in the body. It is responsible for adjusting metabolites in the blood, for processing and storing nutrients, for producing coagulation factors and plasmatic proteins, for detoxifying potentially harmful molecules and has a role in the digestion of lipids.

Bile production

The bile, secreted by the hepatocytes, is rich in water, bile acids, fats and bilirubin. It is responsible for fat emulsification which is central for lipid absorption in the small intestine. After production, the bile is stored, concentrated and enriched in bicarbonate by the gallbladder, to be further released into the duodenum for digestion during a meal. Different than that found in humans and other mammals such as mouse, cat and dogs, the rat does not possess a

gallbladder, but rats secrete large volumes and higher concentrations of bile in comparison to other animals (McMaster, 1922).

Detoxification

As a process of major importance, the neutralization of toxic substances by the liver is imperative for homeostasis. The most important toxin metabolized by the liver is ammonia, which is produced in the gut via nitrogen metabolism and urease bacteria.

Urea Cycle

The urea cycle is solely found in the liver and primarily responsible for ammonia detoxification through its generation of non-toxic urea which is then excreted by the kidney. A large portion of ammonia enters the liver via the portal vein and reaches the periportal hepatocytes where ureagenesis takes place (Figure 2).

The urea cycle involves carbamyl phosphate synthetase (CPS I), a periportal hepatocyte mitochondrial enzyme, which mediates the formation of carbamyl phosphate from NH_3, HCO_3^- and ATP. Glutamate and acetyl-CoA form N-acetyl-glutamate (NAG) by the action of the enzyme NAG synthetase. Carbamyl phosphate is then condensed with ornithine, forming citrulline by action of the ornithine transcarbamylase (OTC). Citrulline is then released into the cytosol, where it condenses with aspartate to form argininosuccinate via argininosuccinate synthetase (ASS). Argininosuccinate is then converted into fumarate and arginine by argininosuccinate lyase (ASL) in the cytosol. Fumarate is then oxidized in the tricarboxylic acid (TCA) cycle, and arginine is transformed into urea and ornithine by the enzyme hepatic arginase. Several factors of the cycle are regulated by protein intake (NAG, OTC) or by starvation (citrulline, arginase). (Yudkoff, 1999). The produced urea is then transported to the kidney where it is secreted.

Although high in capacity, the urea cycle has a low affinity for ammonia and therefore not all ammonia arising from the portal vein is detoxified promptly by periportal hepatocytes. As a result of that, the perivenous hepatocytes are equipped with the enzyme glutamine synthetase (GS), which will help to maintain physiological levels of blood ammonia through the amidation of glutamate into glutamine.

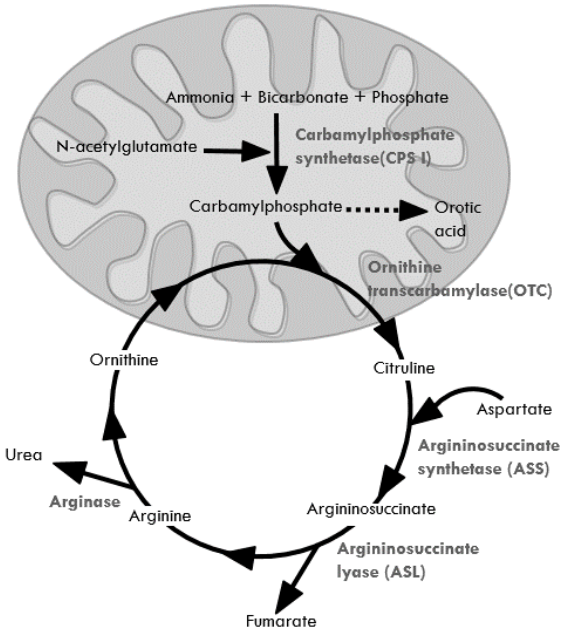

Figure 2: The urea cycle

The urea cycle is formed by series of reactions which are responsible for detoxifying ammonia. In the urea cycle, two molecules of ammonia enter in order to form urea. The first one forms carbamylphosphate inside the mitochondrion, the second one is included in aspartate, which is then converted into argininosuccinate.

Urea cycle disorder

Inborn errors of urea metabolism, known as urea cycle disorders (UCD), are associated with full or partial deficiency in any of the enzymes of the urea cycle. The incidence of UCDs is from 1:8000 to 1:44000, but these numbers might be underestimated due to undiagnosed cases in partial deficiency or abrupt death in infants. Among the affected enzymes, OTC deficiency is the most common and arginase deficiency the least (Allen, 2013).

Aside arginase deficiency, hyperammonemia is the hallmark of the syndrome, and the symptoms differ according to whether it is acute or chronic (Gropman et al., 2007). Infants with severe deficiency develop an acute hyperammonemia with quick development of symptoms leading to hyperammonemic encephalopathy after birth, starting with poor feeding and lethargy that can progress to coma (Burton, 2000). Chronic hyperammonemia presentation includes

headaches, confusion, lethargy, protein avoidance, behavioural changes and learning deficits (Häberle, 2011).

Central Nervous System

The central nervous system (CNS) is the most complex system in the body. It coordinates voluntary (speech, locomotion) and involuntary (breath, blink) movements, receives and responds to sensorial information and regulates several processes such as behaviour (day/night cycle) and growth. The CNS consists of the brain and spinal cord, and is responsible for centralized control upon the rest of the body. The brain is a complex structure and can be divided according to its embryological development into forebrain, midbrain and hindbrain (figure 3). The forebrain will form the cerebral hemispheres, thalamus and hypothalamus. The hindbrain will consist of the medulla, pons and cerebellum.

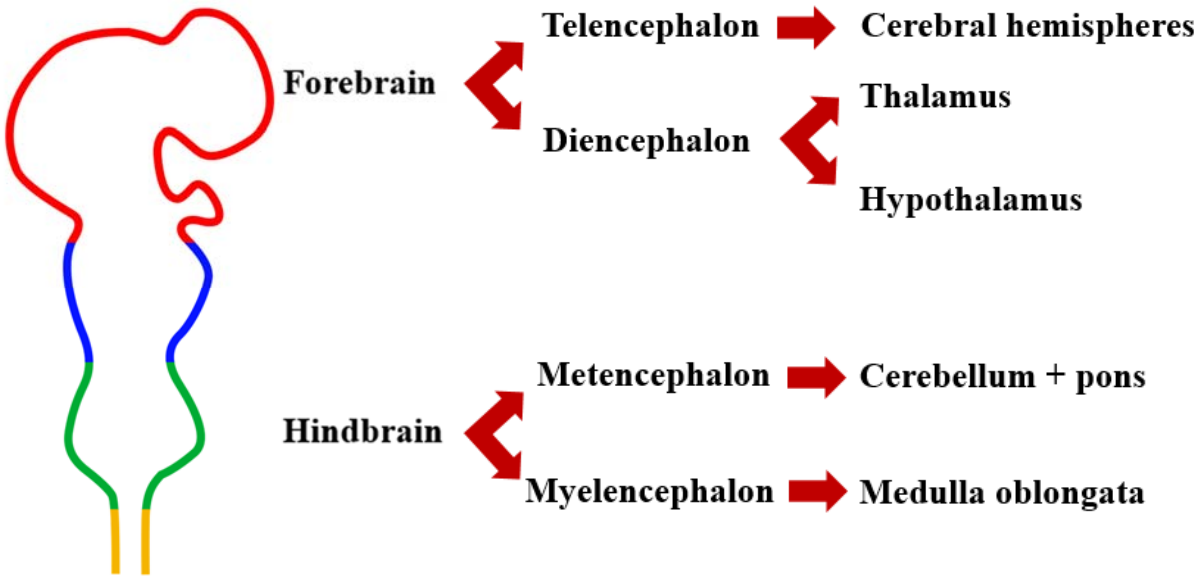

Figure 3: Early central nervous system

The CNS is composed of forebrain (red), midbrain (blue), hindbrain (green) and spinal cord (yellow). The forebrain involves the cerebral hemispheres, thalamus and hypothalamus and the hindbrain consists of the cerebellum, pons and the medulla oblongata. Image from (Nrets, https://commons.wikimedia.org/wiki/File: EmbryonicBrain.svg, «EmbryonicBrain», under CC BY-SA 3.0 license).

The telencephalon is the largest part of the brain, highly folded in humans, and presents numerous sulcus and gyri. It is divided into four lobes: frontal, parietal, temporal and occipital (figure 4). The frontal lobe controls several functions such as problem solving, behaviour, attention, movement coordination and personality. The frontal cortex can be further divided into pre-frontal cortex (PFC), which corresponds to the anterior part of the frontal lobe. The PFC receives highly processed information from other forebrain systems and is related with modulation of social behaviour, ability to retain concentration, expression of the personality, decision making and learning. The PFC is crucial for complex behaviour and impairments in this area have a significant impact on quality of life (Miller et al., 2002).

Positioned below the occipital lobe, the cerebellum is composed by external highly folded gray matter. It is generally divided into two lobes; the anterior and posterior lobes, plus a vermiform structure vertically oriented called the vermis. Although it might have a role in some cognitive activities, the main function of the cerebellum is to exert fine motor control allowing the body to move properly, influencing balance, posture, motor learning and coordination (Fine et al., 2002).

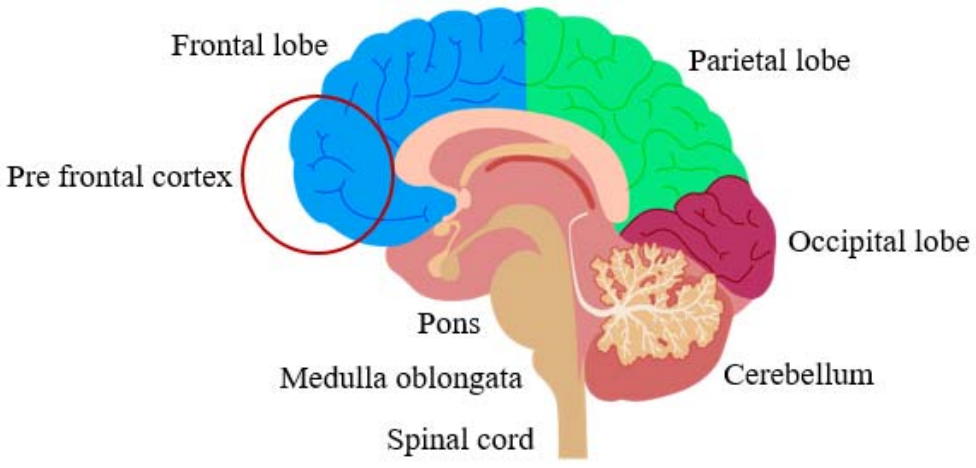

Figure 4: Brain's anatomy

Brain's structures showed in a sagittal plan. Temporal lobe is not visible due to the section plan. Image adapted from dreamstime image bank.

Vasculature

The brain is perfused by vertebral (2 branches) and carotid (4 branches) arteries which join an anastomotic structure called Circle of Willis. The Circle of Willis is at the base of the skull and the cerebral arteries (anterior, middle, posterior) come from it. The circulation of blood by anastomotic structures such as the Circle of Willis protects the effect of blockage of one cerebral artery and consequently compromise an entire lobe by allowing the circulation through collateral vessels. The cerebral arteries run close to the dura mater and then infiltrate into the meninges, becoming the penetrating arteries. These arteries are still in contact with a layer of the dura mater, and as they run deeper, they become arterioles and then capillaries (figure 5). The capillaries then make direct contact with the brain via astrocyte foot processes, becoming a part of the blood-brain barrier (BBB). Blood poor in oxygen is carried to the post-capillary veins converging into cerebral veins which merge into the sinuses (inferior, superior, straight, sigmoid, transverse, occipital), and finally join the jugular veins. Because the capillaries are the major site of molecule exchange, they present only a monolayer of endothelial cells and no muscular or collagen layers, making the presence of the BBB critical for the CNS protection.

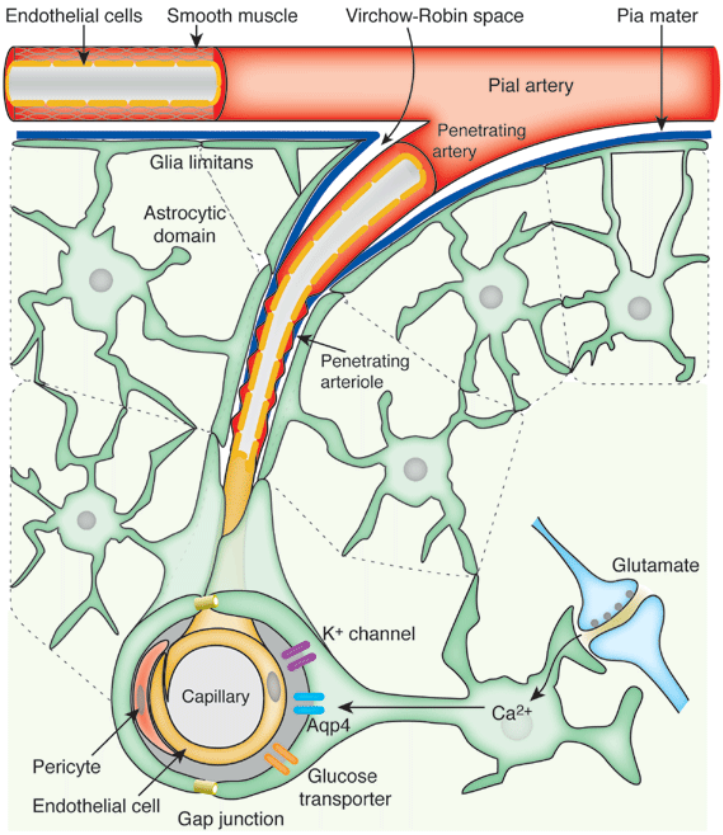

Figure 5: Brain's arterial vasculature

The Virchow-Robin space represents the area between the penetrating artery and the surrounding pia mater. Image from (Iadecola and Nedergaard, 2007).

Cell types

The brain is formed by several types of cells; neurons and glia (astrocytes, oligodendrocytes and microglia). Neurons are responsible for reception, transmission and the processing of inhibitory and excitatory stimuli. Via numerous transporters/pumps and ion channels, these cells generate and propagate electrical signals and transform them into chemical signals via the release of neurotransmitters. Regulating the brain's microenvironment and providing support to the neurons, the glial cells are far more numerous in the brain, accounting for up to 90% of the cells in the CNS. The glia family involves oligodendrocytes which produce the myelin sheath for the neurons in the CNS, the ependymal cells which produce the cerebrospinal fluid, the phagocytic microglial cells, a major part of the CNS immune system

and the astrocytes. Astrocytes are star-shaped cells responsible for support and communication between the neurons and blood capillaries and controls the ionic and molecular extracellular environment on the brain. The astrocytic foot processes transfer molecules and ions from the blood to the neurons. In addition, astrocytes synthesize molecules such as lactate which are transported and used as energy source by neurons (Pellerin et al., 1998). Finally, astrocytes play a role in protecting the brain by being part of the BBB, protecting the neurons and other central cells from potential blood-derived toxins.

Liver disease

Liver disease is a generic term which covers several types of hepatic insults. It presents a major burden for health systems with costs as great as 157 million dollars just related to in-hospital procedures (Canadian Liver Foundation 2013). Even with treatment being available, the Canadian Liver Foundation predicts an increase in death related to liver disease in the next years (Canadian Liver Foundation 2013).

Acute liver failure

Acute liver failure (ALF) encompasses a number of conditions which are marked by severe and rapid liver cell dysfunction and massive necrosis of hepatocytes, with the presence of coagulopathy and HE, without any pre-existing liver disease (Lee, 2012). Patients with ALF present at first non-specific symptoms such as malaise and nausea, which are followed by jaundice, quick onset of altered mental status and coma. ALF presents high morbidity and mortality rates, being often caused by viral hepatitis, autoimmune liver disease and drug-induced liver injury (Ostapowicz et al., 2002).

Chronic liver disease

Chronic liver disease (CLD) is responsible for over 80% of primary liver cancers, of which hepatocellular carcinoma (HCC) is the most frequent, and are a major public health problem worldwide. Just in Canada, 2748 deaths were attributed to CLD and liver cirrhosis (eleventh leading cause of death) in 2008. In addition CLD is the fifth leading cause of death in England and is among fifteen leading causes of death in the United States in the past decade (Government of Canada, 2013).

Having a slow progression (from 5 to 50 years), CLD is the most common type of liver disease. The hepatic injury regularly culminates in fibrosis and then cirrhosis, which is marked by tissue scaring with replacement of liver parenchyma by fibrotic tissue and distortion of tissue architecture. The main causes of CLD are excessive alcohol consumption, viral hepatitis and non alcoholic steatohepatitis (NASH) (Pellicoro et al., 2014), with NASH presently being the leading cause of liver disease in Canada (Canadian Liver Foundation 2013). CLD can lead to complications, regardless of the aetiology of the underlying disease. While compensated patients with liver disease have no indications of their condition, decompensated patients present symptoms due to cirrhosis. Due to stiffening of hepatic structures, CLD patients develop portal hypertension which consequently could cause variceal bleeding. In addition, many times these patients present with ascites (accumulation of fluid in the abdominal cavity), sarcopenia (loss of muscular mass), jaundice (development of yellow skin) and HE.

Types of HE

The American Association for the Study of Liver Disease (AASLD) and the European Association for the Study of the Liver (EASL) guidelines recommend that HE should be classified according with the type of underlying disease, severity of manifestations, time course, and precipitating factors (Vilstrup et al., 2014). Based on the type of liver disease from which it arises, HE can be classified as: type **A,** associated with **acute** liver disease (ALF); type **B,** associated with portal-systemic **bypass** without any existing liver disease and type **C,** associated with **chronic** liver disease (CLD).

Patients with type A are generally in critical state, presenting rapid progression of cerebral edema which, in up to 25% of the cases, evolves to life-threatening intracranial hypertension and might culminate in brain stem herniation and death (Bernal et al., 2007). Type B HE is associated with a congenital malformation rarely found in humans (Tivers et al., 2014), but it might develop when a transjugular intrahepatic portosystemic shunt (TIPS) is done in order to treat portal hypertension (Madoff et al., 2004). These conditions allow the blood from the gut to bypass the liver, resulting in an increase of toxins in circulation. Type B is also important as a surgical animal model of HE (Butterworth et al., 2009), presenting typical neurological features due to systemic build up of toxins, but without the underlying liver disease. Finally, HE type C is associated with cirrhosis and prevails in 50-70% of cirrhotic patients

(Bustamante et al., 1999). It can be subdivided according to its severity in covert (CHE) and overt HE (OHE).

CHE represent a mild form of HE, with no clinically obvious symptoms present. However, patients with CHE presents abnormal cognitive and neuropsychological skills, having a detrimental effect on ability of perform complex tasks such as driving and decreased life quality (Bajaj et al., 2011). Due to its subtle presentation, the assessment of CHE is challenging and requires the use of sensitive tools. Testing is done using psychometric tests such as PHES (Psychometric Hepatic Encephalopathy Score), referred as the "gold standard" for CHE assessment. PHES is a paper-pencil test in which patients are challenged for attention and processing speed, among other factors. Although highly sensitive and specific, paper-pencil tests are time-consuming. The EncephalApp Stroop is a free phone application that evaluates the patient's psychomotor speed and cognitive flexibility. With high accuracy, the Stroop test is simple to perform and easily evaluated (Patidar and Bajaj, 2015). In addition to psychometric testing, other tests, including the Critical Flicker Frequency (CFF) might help in CHE diagnosis as it is simple, quick and language independent (Torlot et al., 2013).

OHE is the clinically obvious form of HE. It is usually associated with the presence of a precipitant factor such as constipation, infections and GIT bleeding (Devrajani et al., 2009). It is also possible that no precipitant factors are found associated with an episode, characterizing a spontaneous case. OHE is classified according to the West-Haven criteria (Table 1). Currently, minimal HE (Psychometric or neuropsychological alterations without clinical evidence of mental change) and grade I (superficial lack of awareness, euphoria or anxiety, shortened attention span, altered sleep rhythm) are incorporated in CHE. OHE then comprises grades II (presence of lethargy or apathy, time disorientation, obvious personality change, inappropriate behaviour, motor incoordination and asterixis), III (somnolence to stupor, confusion, gross disorientation, bizarre behaviour but still responsive to stimuli) and IV (coma) (Vilstrup et al., 2014). In addition, the presence of OHE can be occasional (episodic HE), having more than one episode within 6 months (recurrent) or continuous (persistent HE).

Table 1: Classification of HE

Grades 0 (Minimal HE) and 1 from the West-Haven criteria, which have no obvious clinical signs of the syndrome, are now known as covert HE. The grades 2 to 4 are known as overt HE. Table from (Patidar and Bajaj, 2015)

<table>
<tr><th>Type</th><th colspan="2">Grade</th><th>Time course</th><th>Spontaneous/precipitated</th></tr>
<tr><td rowspan="2">A
(acute liver failure)</td><td>MHE</td><td rowspan="3">Covert</td><td rowspan="2">Episodic (one episode in 6 months)</td><td rowspan="2">Spontaneous (no precipitating factor found)</td></tr>
<tr><td>1</td></tr>
<tr><td rowspan="2">B
(porto-systemic bypass)</td><td>2</td><td rowspan="3">Recurrent (>1 episode in 6 months)</td></tr>
<tr><td rowspan="3">Overt</td><td rowspan="3">Precipitated</td></tr>
<tr><td rowspan="2">C
(cirrhosis)</td><td>3</td><td rowspan="2">Persistent (never returned to baseline)</td></tr>
<tr><td>4</td></tr>
</table>

Pathogenesis of HE

HE is known to be a multifactorial complex syndrome with the underlying mechanisms still not fully understood. Nonetheless, the hyperammonemia, oxidative stress, inflammation and infection are known to play important roles.

Ammonia

Although the pathogenesis of HE is believed to be multifactorial, ammonia toxicity is considered to be central in the development of this syndrome. In liver disease, the loss of hepatic tissue and consequently hepatic function, is responsible for impaired ammonia detoxification, leading to an increase in this toxin. In addition, alteration of the gut microbiota during liver disease, favors the dominance of ammonia-producing bacteria. (Bajaj et al., 2012; Chen et al., 2011).

Presentation

Ammonia exists as two forms, a weak acid (NH_4^+) and a weak base (NH_3) with the ratio of NH_3/ NH_4^+ being given by the Henderson-Hasselbalch equation:

$$NH_3/\ NH_4^+ = 10^{-(pKa-pH)}$$

Since ammonia has a pKa ~9.1, at pH 7,4 and at 37˚C, only 2% of the ammonia is presented as NH_3, while approximately 98% is presenting as NH_4^+ (Lockwood et al., 1980). Because NH_3 is a gas, it can freely cross biological membranes via diffusion. The ionic form, NH_4^+ can also cross biological membranes, but via specific transporters. Since NH_4^+ has similar ionic properties as potassium (similar radius and diffusion coefficient) it can be transported by potassium carriers, such as the sodium-potassium-chloride co-transporter (NKCC), ATPase transporters Na^+/K^+ and H^+/K^+ among others (Bosoi and Rose, 2009). In addition, ammonia can cross membranes through ammonia transporters: the Rhesus associated glycoprotein (RhCG and RhBG), found in several cell types, including brain capillaries (Huang and Liu, 2001; Nakhoul and Hamm, 2013).

Toxicity

The effect of ammonia on brain function is well documented. Once inside the brain, increased ammonia causes changes in pH, alterations in membrane potential by competing with K^+, and changes in cell metabolism, since ammonia is a common substrate and product for many reactions (Bosoi and Rose, 2009).

Astrocytes exposed to ammonia leads to cell swelling with ammonia-induced oxidative and nitrosative stress playing a role (Jayakumar et al., 2008). Ammonia also reduces mitochondrial function by several mechanisms. It affects the TCA cycle via the inhibition of α-ketoglutarate dehydrogenase and pyruvate dehydrogenase (Katunuma et al., 1966; Rama Rao and Norenberg, 2012) and the electron transport chain (Rao et al., 1997), resulting in impaired energy metabolism. In addition, ammonia influences the glutamate receptor N-methyl-D-aspartate (NMDA) leading to over-activation and excitotoxicity (Hermenegildo et al., 2000). In fact, ammonia treatment triggers a calcium dependent glutamate exocytosis in astrocytes, which

may represent the main mechanism for glutamate's toxicity in hyperammonemia (Görg et al., 2010a).

Furthermore, hyperammonemia has been demonstrated to be implicated in circadian rhythm impairments, as proven by the work of Ahabrach and colleagues in which Wistar rats were submitted chronically to an ammonium rich diet. Ammonia fed rats showed alterations in the rhythm of spontaneous ambulatory activity and hormonal secretion of cortisol and cortisone, which suggests that it is implicated in patients with CLD (Ahabrach et al., 2010). In another study, rats submitted to the same ammonia diet showed impaired brain activity, which was expressed by failure in different learning tasks (Arias et al., 2014).

Hyperammonemia is an important part of the pathogenesis of CLD, reaching levels around 150-250 μM, and its levels correlate with HE severity in patients (Ong et al., 2003; Qureshi et al., 2014). Ammonia-lowering therapies are shown to decrease brain edema in animal models of HE (Bosoi et al., 2011). Since hyperammonemia is present in most HE patients, ammonia lowering strategies are shown to improve cognitive functions, health related quality of life (Prasad et al., 2007) and prevent new episodes of overt HE (Sharma et al., 2009).

In ALF, ammonia concentrations rise quickly and are higher than in CLD, generally resulting in brain edema and intracranial hypertension. An ALF model consisting of pigs submitted to hepatectomy showed ammonia levels that were up to 1,2 mM and correlated with raised intracranial pressure (Zwirner et al., 2010). Death from brain edema and intracranial hypertension is also well recognized in human ALF, in which high ammonia levels (above 200 μg/dL) allied with HE are associated with rapid onset of brain herniation (Vaquero et al., 2003).

Oxidative stress

Oxidative stress is known to be involved in several neuropsychiatric syndromes. In HE, several factors might be responsible for oxidative stress generation, including the ailing liver, high levels of ammonia or the presence of other factors such as inflammation.

Presentation

Oxidative stress is presented when the ability of removing reactive oxygen species (ROS) is exceeded by the production of such molecules, due to an imbalance between anti-

oxidants and pro-oxidants respectively. ROS are highly reactive molecules containing oxygen such as nitric oxide (NO), hydrogen peroxide (H_2O_2) and the anions superoxide (O_2^-) and hydroxyl (OH^-). ROS are highly generated from the mitochondrial electron transport chain and as by-products of cellular enzymes such as NADPH oxidases, xanthine oxidase and nitric oxide synthase (Norenberg et al., 2004).

ROS in health

ROS are responsible for cell signaling and regulation of several functions, being involved in cell oxygen sensing, which is critical during limited oxygen availability (Guzy and Schumacker, 2006), effective immune response by activated phagocytes and skeletal muscle glucose uptake (Alfadda and Sallam, 2012), apoptosis and cell differentiation, among others. ROS are normally produced in the human body as a consequence of aerobic respiration and substrate oxidation, but elevated levels can cause deleterious effects. Therefore, the presence of antioxidants enzymes such as superoxide dismutase, glutathione peroxidase, and catalase are essential for the balance between pro and antioxidants (Matés et al., 1999).

ROS in HE

The influence of ROS on the pathogenesis of HE is well established, but the role of systemic and central ROS is a subject of debate. Görg and colleagues found increased oxidative stress in post-mortem brains of liver-diseased patients to be correlated with the presence of HE (Görg et al., 2010b), stressing the relationship of central ROS and HE. In this study, patients' brains presented increased levels of tyrosine-nitrated proteins, heat shock protein-27 and 8-hydroxyguanosine (RNA oxidation marker). On the other hand, different studies have showed that systemic levels of ROS are related to the presence of HE. Negru and colleagues found systemically increased levels of free radicals in HE due to alcoholic liver disease (Negru et al., 1999). Agreeing with that, blood levels of the antioxidant glutathione peroxidase and other antioxidant/oxidative markers were correlated with the presence of minimal HE in cirrhotic patients (Irimia et al., 2013; Montoliu et al., 2011; Sangeetha et al., 2016).

Treatments of HE

HE treatments focus on treating precipitating factors (e.g. GIT bleeding, infection and constipation among others) and lowering blood ammonia levels (table 2). Since CHE is highly underdiagnosed, currently only patients that present OHE episodes are treated. Various treatments are available to treat HE, such as non-absorbable disaccharide (lactulose) and antibiotics such as rifaximin. Lactulose, a laxative that decreases ammonia production by accelerating bowel movement, is the first-line treatment for HE. Besides its laxative function, it is assumed that lactulose acts on the growth of beneficial intestinal flora and decrease of intestinal pH (Jiang et al., 2015; Riggio et al., 1990). Patience compliance with lactulose treatment might present a challenge due to adverse effects (diarrhea, flatulence and abdominal pain) and the complicated dosage regimen which requires that the oral lactulose solution must be titrated in order to maintain two soft stools per day (Neff, 2010b). Rifaximin is a non-absorbable antibiotic which due to lower incidence of gastrointestinal effects, presents better patient compliance, which translates in less HE episodes and hospitalizations costs (Neff, 2010b). Even so, its high cost represents a drawback and obstacle from becoming the first line treatment for HE.

Table 2: HE treatments

Treatment	Type	Mechanism	Side-effects
Lactulose	non-absorbable disaccharide	Decrease in ammoniogenic bacteria	Diarrhea, nausea, abdominal pain
Rifaximin	Antibiotic	Decrease gut bacteria	Nausea, headache
L-ornithine L-aspartate (LOLA)	Metabolic ammonia scavenger	Stimulate urea cycle and glutamine synthesis	Nausea, vomiting
Ornithine phenylacetate (OP)	Metabolic ammonia scavenger	Increased excretion of ammonia by the kidneys	In evaluation
glycerol phenylbutyrate (GPB)	Metabolic ammonia scavenger	Increased excretion of ammonia by the kidneys	In evaluation
Leucine, isoleucine, valine	branched-chain amino acids	Decrease in ammoniogenic bacteria	fatigue
Neomycin, metronidazole	Antibiotics	Decrease in ammoniogenic bacteria	Nephrotoxic; neuropathy, nausea

Metabolic ammonia scavengers such as glycerol phenylbutyrate (GPB), L-ornithine L-aspartate (LOLA) and ornithine phenylacetate (OP) (table 2) have the potential of increasing ammonia's removal by alternative pathways, such as glutamine synthesis by the enzyme glutamine synthetase. Other ammonia scavengers such as sodium benzoate and sodium phenylacetate are generally used for urea cycle disorders, but can also be used for HE management when irresponsive to other treatments (Ah Mew et al., 1993; Misel et al., 2013). Finally, branched-chain amino acids (BCAA)-enriched formulations and probiotics might be used since they showed improvement of features of HE (Vilstrup et al., 2014). Most HE therapies have not been thoroughly tested. In addition to that, the fact that there is no ideal treatment for HE so far, depicts the importance of finding new therapeutic strategies.

Ammonia metabolism

Glutamine synthetase

In liver disease, the loss of hepatic detoxifying function causes hyperammonemia. The neurological complications caused by hyperammonemia are primarily associated with ammonia entering the brain. In the setting of liver disease, enzymes of nitrogen metabolism such as glutamine synthetase (GS), have an important role.

GS is a glutamate-ammonia ligase present in animals, plants and bacteria. With a molecular weight of 44 kDa, GS is the product of GLUL gene (Wang et al., 1996) which is highly conserved within living organisms (Spodenkiewicz et al., 2016). In humans, GLUL is found in chromosome 1 at 1q31 position (Helou et al., 1997), and its transcript has 1122 bp and comprises 6 exons encoding a 373 amino-acid polypeptide (human liver) (Häberle et al., 2005). In addition, three GLUL-like genes were described and a 54 kDa GS-like protein was isolated from human brain, although their function is not clear (Boksha et al., 2002; Wang et al., 1996). The enzyme is found in the cytoplasm of most mammalian cells, including brain (Matthews et al., 2010).

The 373 amino acid protein has three domains (figure 6): a N-terminal (residues 3-24), a β-grasp domain (25-112) and a catalytic domain (residues 113-373) (Krajewski et al., 2008). Four to six monomers together form a ring in a way that the catalytic domain of each subunit aligns with the β-grasp domain of the next (Boksha et al., 2002). Two rings are stacked oppositely-oriented and the functional GS becomes a octameric (human), decameric (canine) or dodecameric (bacteria) structure (Boksha et al., 2002; Krajewski et al., 2008). The number of monomers that form the ring depends on the type (GS type I is present in prokaryotes and GS type II in eukaryotes) and on the different isoforms of the enzyme inside each type. The ring orientation favors the position of the active sites toward substrates, with the bonds between the two stacked rings being weaker than the ones holding the monomers together.

A B C

Figure 6: Glutamine synthetase structure

Representation of GS structure from canine cells. (A) the subunit is colored from blue (N-terminus) to red. The blue-cyan corresponds to the β-grasp domain, and the rest represents the C-terminal catalytic domain. The magenta spheres correspond to magnesium ions. (B) The active sites in the second pentamer are placed between the ones in the first and are opposed. (C) the hydrogen bonding interaction between the two pentamer rings is represented. (Krajewski et al. 2008).

GS plays a key role in two major functions: detoxifying nitrogen metabolic waste and regulating brain neurotransmission. The detoxification of systemic ammonia occurs by a two-step reaction depending of ATP and Mg^{2+} or Mn^{2+} (figure 7). Besides that, GS can catalyze the conversion of glutamate + hydroxylamine into γ-glutamyl hydroxamate, which is the basis for the assays measuring GS activity. GS is responsible for half of the hepatic and likely most of the extra-hepatic detoxifying capacity in hyperammonemic conditions (Hakvoort et al., 2016), representing a high affinity (but low capacity) ammonia detoxifying mechanism. Aside from perivenous hepatocytes in the liver, GS has been found to be expressed in kidney, heart, skeletal muscle and in CNS (specially in astrocytes) (Anlauf and Derouiche, 2013; Iqbal and Ottaway, 1970).

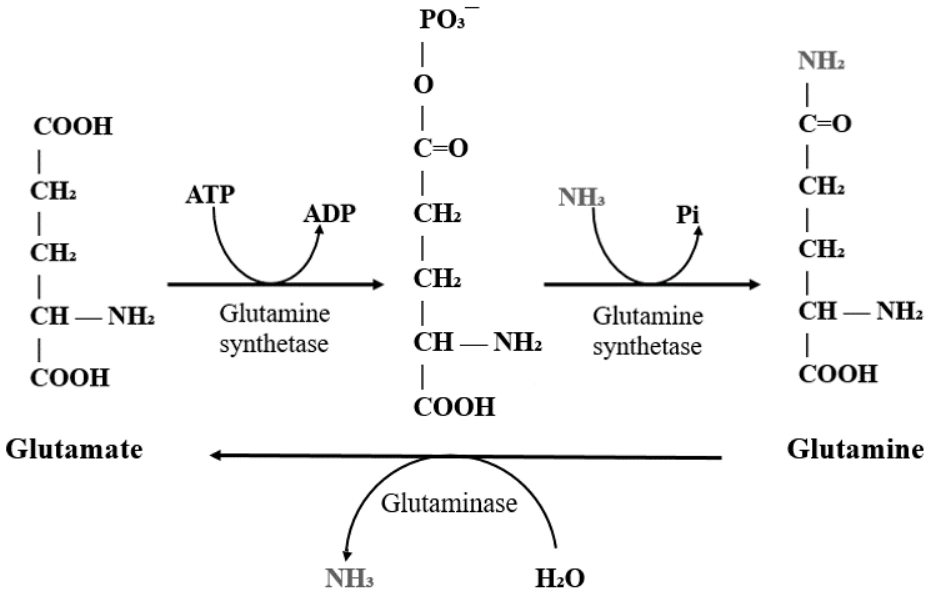

Figure 7: Glutamine synthetase reaction

GS catalyzes the two step amidation of glutamate into glutamine. First, glutamate is phosphorylated and forms γ-glutamyl phosphate, which then reacts with an ammonia molecule resulting in a glutamine. The inverse reaction is catalyzed by the enzyme glutaminase, which turns glutamine into glutamate and releases ammonia.

GS is present in astrocytes (Anlauf and Derouiche, 2013) and is responsible for regulation of neurotransmitter production and recycling (glutamine-glutamate cycle). After glutamate is released on the post-synaptic cleft, it is taken up by astrocytic transporters and converted into glutamine by GS, enter the tri-carboxylic acid (TCA) cycle or enter the cycle for GABA formation. Part of the recently formed glutamine is shuttled to the neuron, where it is converted into glutamate by the enzyme glutaminase (GA), completing the glutamate-glutamine cycle (figure 8) (Cooper and Jeitner, 2016). GS regulates excitatory neurotransmission by limiting glutamate availability. In addition, since glutamine is a major precursor for γ-aminobutyric acid (GABA) synthesis (Schousboe et al., 2013), GS also plays a role regulating inhibitory neurotransmission. Because of that, disruption of GS is known to cause severe neuropsychiatric disorders (Spodenkiewicz et al., 2016).

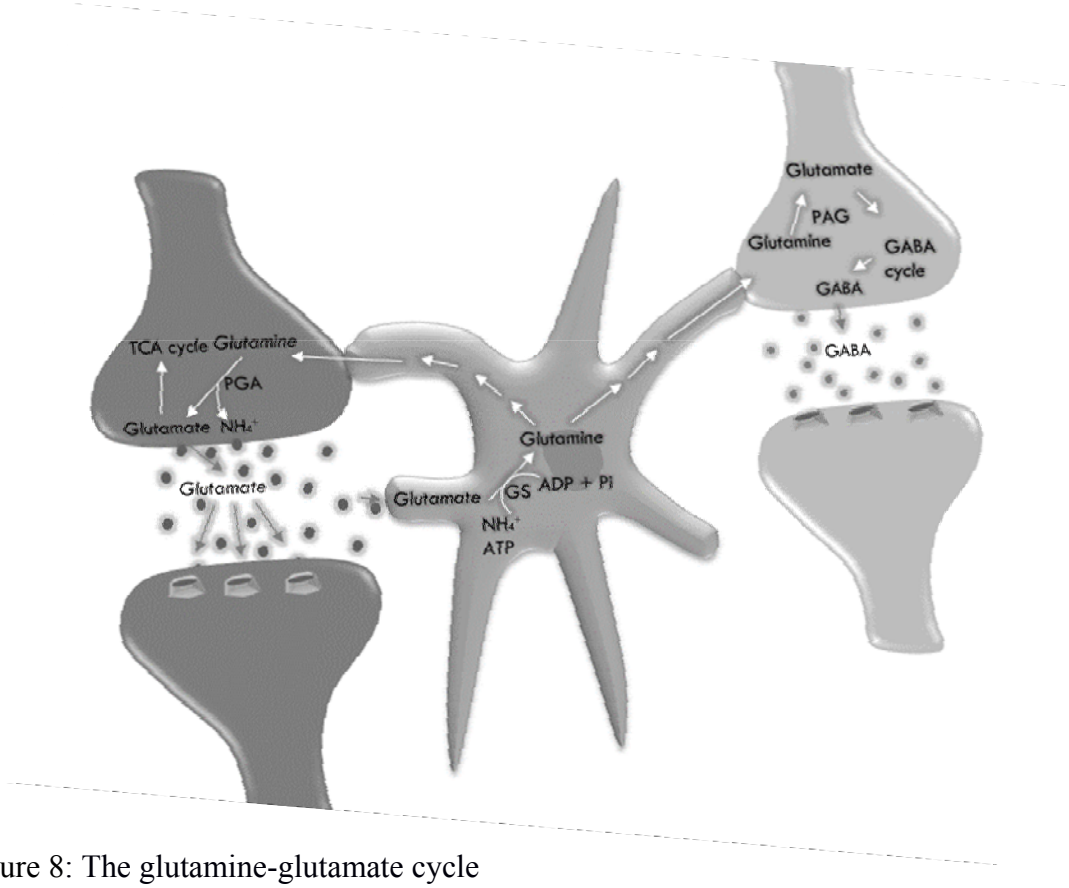

Figure 8: The glutamine-glutamate cycle

The glutamine produced at the astrocytes is transported to the neurons where it will be converted by the neuronal glutaminase into glutamate. Glutamate then is released or enters the GABA cycle.
Tri-carboxylic acid (TCA), phosphate-activated glutaminase (PAG), adenosine di-phosphate (ADP), adenosine tri-phosphate (ATP), phosphate (Pi).

Glutaminase

Glutaminase (GA) plays essential roles in cell nitrogen metabolism, being responsible for the deamidation of glutamine into glutamate, releasing an ammonia ion. Mammalian GA is encoded by two different genes, resulting in different isoforms: the kidney types (KGA and GAC) formed as spliced variants of the GLS gene (Elgadi et al., 1999) and liver types (LGA and GAB) formed by the gene GLS2 (Martín-Rufián et al., 2012). Kidney type GA has the ability of being activated by phosphate and therefore is also known as phosphate activated glutaminase (PAG) (Kvamme et al., 2000). Although classified as kidney or liver type, GA is present in several cell types and tissues such as pancreas, immune system, heart and brain, with

brain tissue possessing all GA isoforms except for GAC. In addition, the levels of each type of GA depend on the cell type and the individual species (Márquez et al., 2012).

The GA is a dimeric protein which has approximately 54 kDa. It is composed by 2 chains containing 305 residues each, with 8 helices (H) that comprise 23% of the amino acid content, or 71 residues and 23 beta sheet strands (S) that comprise 21% or 95 residues of the protein (figure 9). A N-terminus is formed starting from H3, and the GA structure is stabilized by four disulfide bonds. An active site cleft is located on the protein surface surrounded by S6, S7, S10, S11, H4, H6 with the catalytic residues being Cys-156, His-197, and Asp-217, localized in a catalytic pocket (Hashizume et al., 2011).

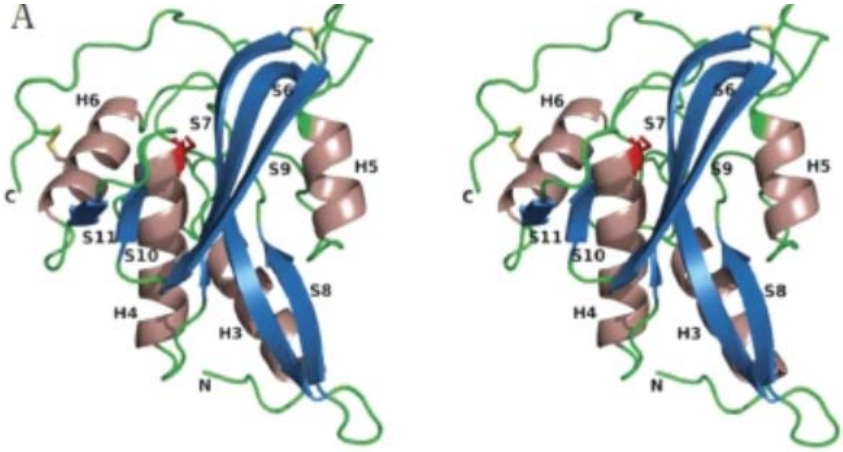

Figure 9**:** The overall structure of protein glutaminase

Ribbon diagrams drawn in left and right stereo from different directions. Disulfide bonds are in yellow with labeled residue numbers. The catalytic residue, Cys-156, is in red. Image from (Hashizume et al., 2011).

GA plays important roles in different organs. In the gut, it transforms glutamine from the diet into ammonia and glutamate, which will then reach the liver. The liver itself has glutaminase activity in order to feed the urea cycle with ammonia. Finally, in the brain GA is present in neurons (Olalla et al., 2002), where it is responsible for converting glutamine from the astrocytes into the excitatory neurotransmitter glutamate, acting in fine tuning with GS.

The blood-brain barrier

The blood-brain barrier (BBB) is the most important biological barrier in the body. Highly regulated, it physically and biochemically limits the transport of molecules into the brain thereby creating a unique controlled micro-environment. The BBB restricts the transcellular passage of charged, non-lipophilic and large molecules, acting as a shield from blood-derived harmful molecules, allowing for the CNS to properly function. In addition, enzymes within the cells of the BBB can metabolize and prevent certain molecules from entering the brain (Brownson et al., 1994). The BBB is composed by astrocyte foot processes wrapped around a monolayer of endothelial cells with the adjacent pericytes (Figure 10).

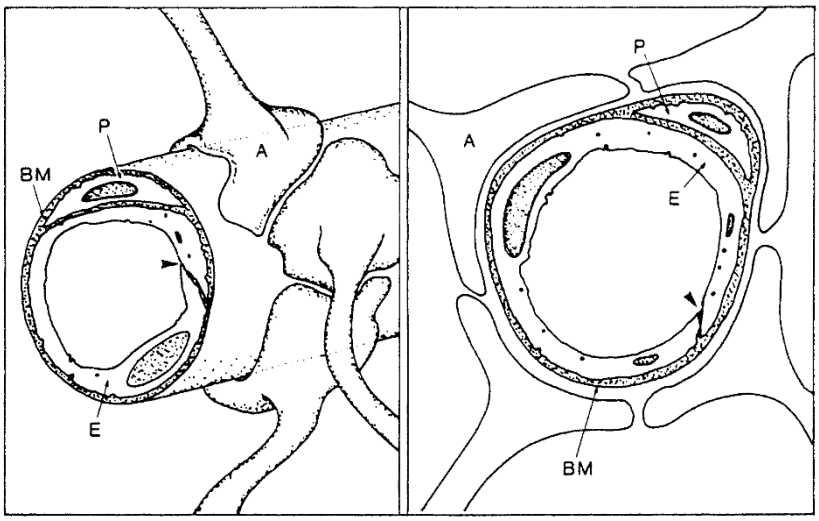

Figure 10: The blood-brain barrier

The BBB is composed by endothelial cells (E) and pericytes (P) sharing a basement membrane. Both structures are wrapped around astrocytic foot processes (A). Picture from (Allt and Lawrenson, 2001)

Endothelial cells

Endothelial cells (EC) have a central role in the composition of the BBB. These cells are in direct contact with the systemic circulation and regulate the entrance of certain molecules. Unlike the cells of other capillaries outside the CNS, the endothelial cells from the BBB are not

fenestrated, have very little vesicular transport and possess specific junctional complexes, which restricts the passage of molecules into the ECs (Liu et al., 2012; Stewart, 2000). These cells also have high mitochondrial density in order to produce enough energy to sustain active transport systems (Oldendorf and Brown, 1975). Ions (K^+, Cl^-, Na^+), proteins (albumin), amino acids, nutrients (glucose) and other molecules have to be actively carried into the ECs by transporters, pumps and receptor mediated transcytosis (Wang et al., 2009b). In addition, outward transporters such as ATP-binding cassette (ABC) transporters, are known to expulse potentially harmful molecules therefore protecting the brain (Elali and Hermann, 2011).

Astrocytes

In addition to providing nutrients to neurons, astrocytes are an integral part of the BBB. Their foot processes involve the endothelium and are known to provide structural stability (Caley and Maxwell, 1970). Furthermore, astrocytes interact with the endothelium and are responsible in regulating the barrier phenotype. Cultured astrocytes induce tightening of the endothelium when implanted into leaky areas, and direct contact between these cells and ECs is necessary for optimal BBB properties (Janzer and Raff, 1987), but the relationship between the two cell types is complex. As astrocytes have a role regulating the expression of molecules from the junctional complex of the endothelium (Tao-Cheng et al., 1987), ECs also regulate astrocyte function.

Pericytes

Pericytes are perivascular cells with numerous projections involving the adjacent endothelium. Present in a high density in the BBB (1:3 pericytes/EC instead of 1:100 in vessels outside the BBB)(Allt and Lawrenson, 2001), these cells belong to the smooth muscle cell lineage and therefore are able to regulate capillary blood flow through contraction and relaxation (Hamilton et al., 2010; Peppiatt et al., 2006).

Like astrocytes, pericytes interact with ECs and contribute to vessel stability, although the mechanisms are still unclear (Zlokovic, 2008). *In vitro* studies demonstrated that pericytes stabilize the capillaries formed by endothelial cells cultivated with astrocytes by preventing apoptosis of the ECs (Ramsauer et al., 2002). In addition, there is evidence that pericytes induce expression of components of the basement membrane and are required for its functional

deposition and, its assemble (Stratman and Davis, 2012). Pericytes degeneration is associated with neurological conditions such as epilepsy and multiple sclerosis, showing that this cell type is essential for barrier and brain regulation (Claudio et al., 1995; Liwnicz et al., 1990).

Junctional Complexes

The junctional complexes are formed by a group of intricate proteins, linked to each other and to the cell's cytoskeleton. These complexes are important to the endothelial barrier formation and paracellular transport of blood-derived molecules (figure 11).

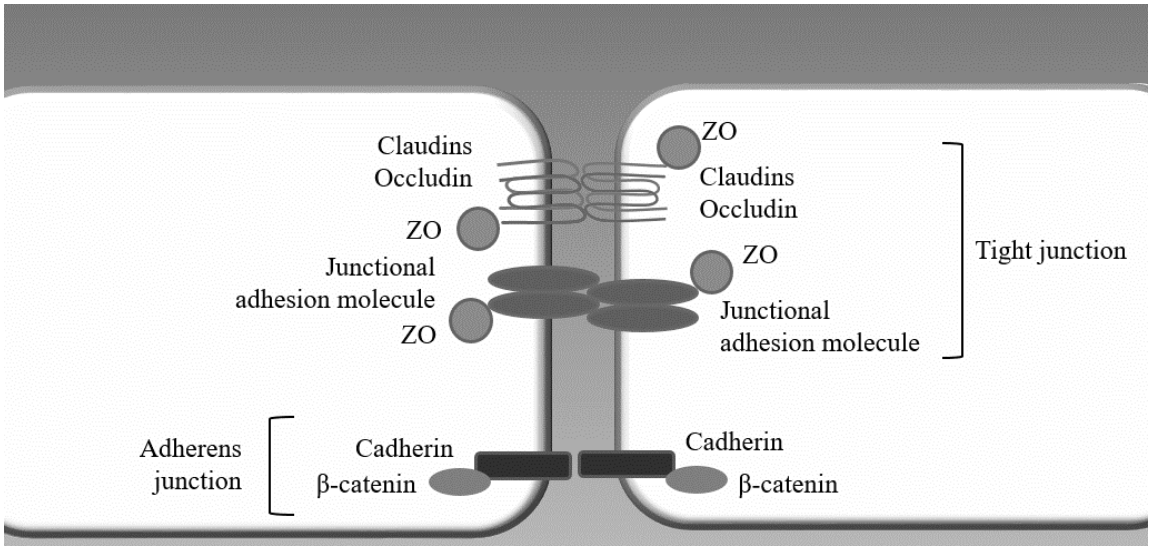

Figure 11: Junctional complexes of the BBB

Tight Junctions

Tight junctions (TJ) are a type of paracellular adhesion complex which play a central role isolating the intercellular space in endothelium and epithelium (Anderson and Van Itallie, 1995). Within the BBB, the tight junctions are specially made to insure proper barrier function, and are unlike any other EC in the body. The TJ are responsible for restricting the passage of molecules through the BBB. TJ are composed by claudins, occludins and junction adhesion

molecules associated with zona occludens (ZO) 1 to 3, cingulin and other accessory proteins (Ballabh et al., 2004).

Part of a family with 24 members, claudins are the main barrier-forming proteins. They form dimers which binds to other claudins in adjacent endothelial cells and to ZO proteins. (Stamatovic et al., 2008). Occludins are integral membrane proteins exclusively found in TJs. This protein forms a dimer that binds to F-actin in the cytoskeleton or to ZO proteins that will then bind to the cell's cytoskeleton (Liu et al., 2012), and its decrease is linked to increased BBB permeability in ALF (Chen et al., 2009). The junctional adhesion molecules are responsible for keeping TJ stability (Bradfield et al., 2007) by participating in TJ formation and binding to other junctional components such as ZO. The ZO interact directly and with most transmembrane proteins bridging the connection between them and the cell cytoskeleton (Liu et al., 2012). This interaction is necessary for TJ's function and stability and, because of that, loss of ZO leads to increased BBB permeability (Hawkins and Davis, 2005).

Adherens Junctions

Adherens junctions (AJ) are composed by numerous membrane proteins, such as catenin and cadherin. Catenin are linked to the cell cytoskeleton and are bound to the cytoplasmic domains of the cadherin (Ballabh et al., 2004). Components of AJ are known to interact and influence TJ. Interactions between catenin from the adherens and ZO from the tight junctions influence TJ assembly through the induction of claudin-5 transcription by VE-cadherin (Matter and Balda, 2003). AJ are responsible for initiating and stabilizing intercellular adhesion and regulation of the actin cytoskeleton and transcriptional regulation among others (Hartsock and Nelson, 2008).

Brain edema

Brain edema is one of the most important feature of HE, being also documented in several neurological disorders such as stroke and traumatic brain injury (Córdoba et al., 2001; Ropper, 1984; Unterberg et al., 2004). In type A HE, edema is associated with a change in brain volume that, due to the rigid skull structure, causes increased intracranial pressure in 20% of patients,

culminating in brain stem herniation and death in up to 55% of these patients (Bernal et al., 2013). In CLD, brain edema is present in compensated (Córdoba et al., 2001) and decompensated patients (Donovan et al., 1998), although rarely progressing to intracranial hypertension.

The development of edema evolves through two different mechanisms: cytotoxic or vasogenic (Figure 12). Vasogenic edema is defined as an accumulation of water in the brain due to disruption of the BBB, and is known to occurs in sepsis (Cotena and Piazza, 2012). Increased permeability due to a physical breakdown of the BBB indicates a severe dysregulation of the tight junctions bridging the endothelial cells together, and consequently molecules that normally do not enter the brain are therefore capable of passing between the cells (paracellular route). Breakdown of the BBB allows the entrance and accumulation of plasma constituents and subsequently water in the extracellular space, leading to edema (Cui et al., 2013).

When BBB breakdown is absent, the increase in osmolytes movement into the brain through an intact BBB causes a change in osmotic pressure inside the cells, which will culminate in water entrance and increase in cell volume, characterizing cytotoxic edema. These molecules (such as NH_4^+ and other ions) pass through the cells (transcellular route) of the BBB possibly due to the regulation of transporters and channels located on the endothelial cells, and then reach the brain. The astrocytes are the most known targets of cytotoxic swelling, being evaluated *in vitro* (Jayakumar et al., 2008) and *in vivo* (Traber et al., 1987).

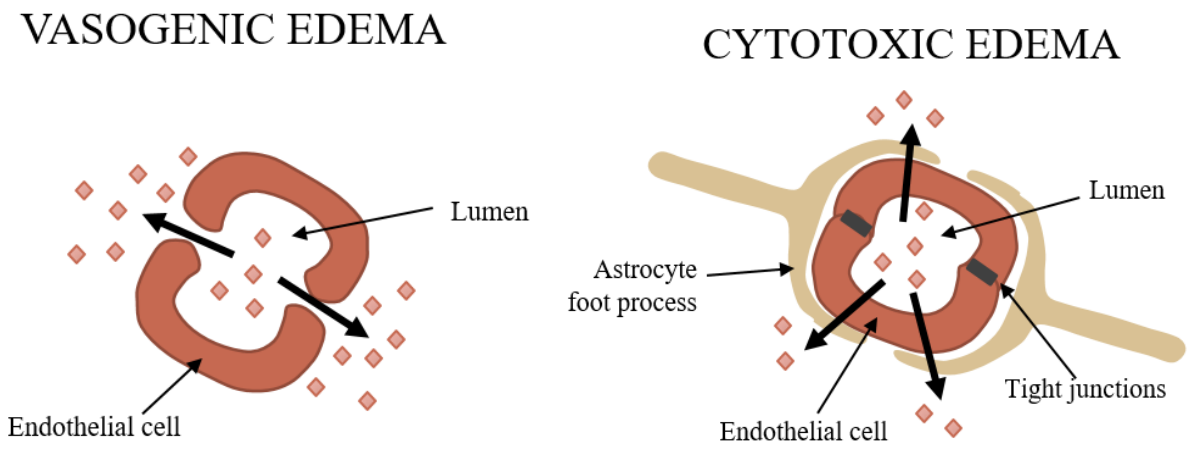

Figure 12: The mechanisms of brain edema

In vasogenic edema osmolytes pass through the BBB paracellularly due to the lack of TJs, while in cytotoxic edema they pass transcellularly. Figure modified from (Tait et al., 2008)

Pathogenesis of brain edema in HE

Several factors are involved in the pathogenesis of brain edema such as inflammation, oxidative stress and hyperammonemia. Two main theories for the role of hyperammonemia and glutamine have been formulated: the "osmolyte" and the "Trojan horse". In the former, the principle is that once ammonia is inside the astrocyte, GS will transform ammonia into glutamine, which will accumulate and change the osmotic pressure inside the astrocyte, provoking water entrance and therefore leading to cell swelling (Scott et al., 2013). In the Trojan's horse hypothesis, glutamine formed by GS is transported into the mitochondria and then converted into glutamate + ammonia by GA. The ammonia build up in the mitochondria causing oxidative stress and impairing the energy metabolism of the cell, which will lead to energy failure and subsequent cellular edema (Albrecht and Norenberg, 2006). Regardless of the mechanism, animal models of HE, when treated with ammonia-lowering agents, showed decrease in brain water, highlighting the importance of this toxin in brain edema (Davies et al., 2009; Ytrebø et al., 2009).

Studies conducted by our laboratory assessed brain edema in the bile duct ligated (BDL), a model of CLD. Results showed that both ammonia and systemic oxidative stress are imperative for the development of brain swelling. Animals that presented only hyperammonemia such as a type B HE model or BDL animals treated with antioxidants (allopurinol) showed less brain water content when compared with hyperammonemia plus ROS, emphasizing the importance of oxidative stress (Bosoi et al., 2012, 2014). On the other hand, the decrease in ammonia concentrations alone, by using the ammonia scavenger AST-120, also caused a decrease in brain water content (Bosoi et al., 2011), showing that ROS alone are not sufficient to cause edema. Finally, the use of pro-oxidant regimens to induce oxidative stress in hyperammonemic type B HE model with no prior edema resulted in the development of brain swelling, stressing the possible synergistic effect between these two toxins. Since the BBB in the BDL rat is not disrupted, it is likely that the origin of the edema is cytotoxic (Bosoi et al., 2012). Finally, because ROS in BDL are only systemic and not central, it is likely that the cells of the BBB, the interface between the blood and the brain, are involved in its pathogenesis.

Na-K–Cl cotransporter

Several blood-derived molecules can affect the proteins of the endothelial cells of the BBB such as receptors (vascular endothelial growth factor, chemokines) and transporters (amino acids, glucose and ions such as the Na–K–2Cl cotransporter (NKCC)), leading to cell dysfunction. Cytotoxic brain edema is caused by increased osmolyte entry into the brain, and ion transporters might play a central role. The NKCC are part of the cation–chloride cotransporter family (Gillen et al., 1996), and are known to be implicated in cell swelling *in vitro* and *in vivo*.

Presentation

Also known as Bumetanide-Sensitive Cotransporter (BSC), NKCCs are integral membrane proteins with 12 transmembrane domains (figure 13). This transporter carry ions across cellular membranes and into the cells (Geck et al., 1980; Haas et al., 1982), depending on the ionic gradient. The binding of the ions is ordered, with the first binding of a Na^+ followed by a $Cl^–$, a K^+ and finally $Cl^–$. Inside the cell, the ions are released in the same order that they were uptaken (Lytle et al., 1998), respecting an electroneutral stoichiometry of 1 Na^+:1 K^+:2 $Cl^–$ for most cells (Haas, 1989; Russell, 2000) or 2 Na^+:1 K^+:3 $Cl^–$ for at least one cell type (Russell, 1983) in normal ionic conditions.

Two isoforms of the Na-K-Cl cotransporter were identified so far, NKCC1 and NKCC2. Although 61% identical to each other (Payne and Forbush, 1994), these isoforms are localized in different membrane domains, where they play different physiological roles. The BSC1 transporter, also known as NKCC2, has 121kDa, with approximately 1100 amino acid residues encoded by the Slc12a1 gene on chromosome 15q15–q21.1 (Payne and Forbush, 1994). It is found mainly in the apical portion of mammalian kidney cells where it has a role in ion reabsorption (Ares et al., 2011; Kaplan et al., 1996). Mutations on this gene in humans are rare and associated with clinically reduced blood pressure and protection from hypertension (Ji et al., 2008).

NKCC1 is the predominant ubiquitary isoform, also known as BSC2, and is the product of the Slc12a2 gene on chromosome 5q23.2. Larger than NKCC2, it is a protein of 1212 amino acid residues and a predicted weight of 132 kDa, but presented as a 160 kDa -190 kDa band,

depending on the species (D'Andrea et al., 1996; Lytle et al., 1992; Tanimura et al., 1995), on sodium dodecyl sulfate polyacrylamide gels (SDS-PAGE) due to its glycosylation.

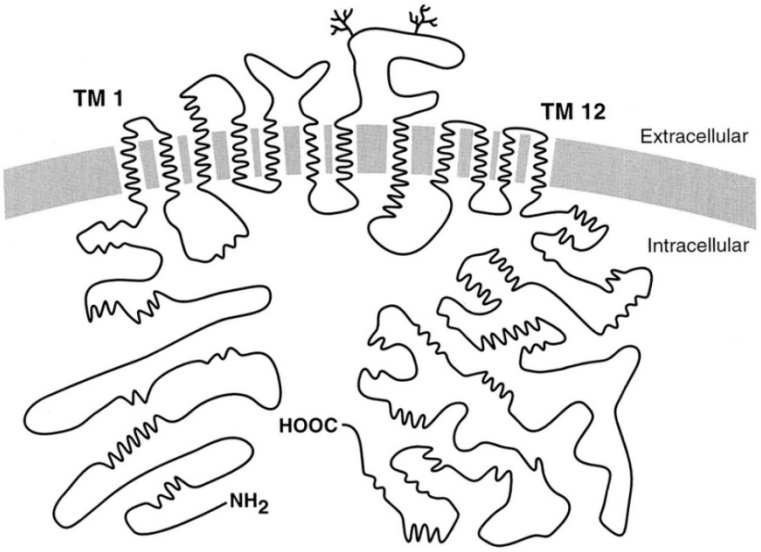

Figure 13: Schematics of NKCC1

TM = transmembrane domain. The transporter possesses a central domain with 12 TM sites, a N- and a C-terminal (Russell, 2000).

Functions

NKCC1 is an ubiquitary transporter that has two important roles: secretory activity and cell volume regulation. In secretory epithelia, NKCC1 from the basolateral cellular membrane internalize ions (active osmolytes), forcing the entry of water into the cells by osmotic pressure. In other locations, such as the endothelial cells of the BBB, NKCC1 is found mostly in the apical membrane, facing the lumen of the vessels (O'Donnell et al., 2004). This location agrees with its role of transporting ions and water from the blood and into the brain, contributing to the formation of the interstitial fluid. Osmolytes have a major influence in water movement across membranes, which give ionic channels such as NKCC1 an important role in cell volume regulation (Russell, 2000). NKCC1 responds to cell volume and ion content and is implicated in regulatory cell volume increase, which consists in gain of ions (KCl) and water after shrinkage, acting towards the regaining of normal cell volume (Hoffmann et al., 2009).

The influence of NKCC1 in cell volume regulation is well documented, and dysregulation of this process is shown to be related to cellular (cytotoxic) edema. In HE, many factors can dysregulate NKCC1, culminating in brain edema. In a model of ALF induced by thioacetamide, with hyperammonemia, inflammation and oxidative stress (Demirel et al., 2012; Sathyasaikumar et al., 2007), an increase in brain NKCC1 total protein and phosphorylation was presented. The increase in NKCC1 protein was also associated with increase in brain water, which was attenuated by bumetanide (Jayakumar et al., 2011). Astrocyte swelling is a central feature of brain edema in HE. When astrocytes were exposed to up to 5mM of ammonia, NKCC1 expression and phosphorylation was found increased and cell swelling was observed. In addition, high ammonia levels are linked with oxidative and nitrosative stress. In fact, NKCC1 was shown to be nitrated/oxidized and treatment with anti-oxidants and nitric oxide synthase decreased swelling and decreased NKCC1 phosphorylation and activity (Jayakumar et al., 2008).

Regulation

Phosphorylation

Activation of NKCC1 occurs following the phosphorylation of serine and threonine residues of its cytosolic terminus (Flatman, 2002). The most relevant kinases involved in the process are Ste20 Proline Alanine-rich Kinase (SPAK) and the Oxidative Stress Response kinase (OSR1). The phosphorylation process starts with physical interaction of the *with no lysine kinase* (WNK) with SPAK/OSR1. WNK phosphorylates SPAK/OSR1 at the catalytic and regulatory domains, activating them. Finally, SPAK/OSR1 activate and phosphorylate NKCC1 (Gagnon et al., 2006). The SPAK/OSR1 phosphorylation sites at NKCC1 are two amino acid residues with a RFxV motif in the N-terminus, being only one motif sufficient and essential for transporter activation (Piechotta et al., 2002). At the same time, activated WNK and activated SPAK/OSR1 act by phosphorylating and inactivating KCC (K^+, $2Cl^-$ extrusion transporter). The regulation of the two ionic transporters respond to cell volume changes (shrinkage) and subsequent increase in intracellular Cl^- levels (Heros et al., 2014). In addition the calcium binding protein-39 (Cab39) stabilizes SPAK in its closed or active form (Filippi et al., 2011),

and it can facilitate its phosphorylation even without upstream WNK activation (Markadieu and Delpire, 2014; Ponce-Coria et al., 2012).

Other kinases might also be involved in the phosphorylation process. In endothelial cells, p38 and Jun amino-terminal Mitogen Activated Protein Kinases (MAPK) activation in ischemic conditions (hypoxia and aglycemia) was linked to increase in NKCC1 activity, and the inhibition of these kinases by specific blockers prevented the effect (Wallace et al., 2012). Brain edema in traumatic brain injury was related to increased NKCC1, and the water content was decreased by bumetanide. In this model, MAPK were related to the increase in NKCC1 mRNA and protein expression (Lu et al., 2008)

Regulation by ion concentration

First, since the functioning of the transporter depends on the simultaneous presence of Na^+, K^+ and Cl^-, the amount of each ion can affect its activity. Hyperammonemia can upregulate the transporter possibly by increasing its substrate, since ammonia and K^+ share similar ionic properties.

Glycosylation

Glycosylation of NKCC1 on the large TM7-TM8 loop is essential for its membrane expression, activity and affinity for loop diuretics (Markadieu and Delpire, 2014). In fact, when glycosylation was inhibited by tunicamycin, a severe reduction of NKCC1 activity was observed. In addition, mutation on the glycosylation sites on the N-terminus site linked to glycosylation (N442) causes increase in Cl^- and a decrease in bumetanide binding (Paredes et al., 2006).

Others

Other factors might play a role in NKCC1 regulation, possibly by implicating one or more of the factors listed above, e.g. hormones, cytokines, signaling cascades, growth factors, oxygen, intracellular Mg^+, pH and calcium (Markadieu and Delpire, 2014; Russell, 2000).

Synthetic Inhibitors

Finally, NKCC1 is known to be inactivated by loop diuretics (furosemide, bumetanide), by binding at the transmembrane domains 2-7 and 11-12 (figure 13) (Payne and Forbush, 1995). Bumetanide is considered the one with highest inhibitory capacity.

Animal models of HE

Studies in humans are challenging due to high costs, sample variability and accessibility and ethical concerns, therefore the use of animal's models remains the most reliable option. Type A HE models results from severe inflammatory and necrotic liver disease with rapid progression of symptoms to coma. Type A models are induced following the acute administration of hepatic toxins (galactosamine, acetaminophen, thioacetamide and azoxymethane), which will lead to rapid hepatic necrosis and severe liver injury (table 3). Type B models are induced surgically following a porto-caval anastomosis in which the portal vein is ligated to the vena cava, enabling gut-derived toxins from the liver to direct enter the systemic circulation. This model presents hyperammonemia and minimal HE without liver injury (Butterworth et al., 2009). There are no optimal models of type C HE so far. Laboratory animals do not respond to hepatitis virus, alcohol or fat intake like humans. Although biliary cirrhosis represents only a small fraction of the CLD aetiologies in humans, the BDL rat is a strong model of type C HE presenting several features of the human disease such as jaundice, portal hypertension, portal-systemic shunting, immune system dysfunction and bacterial translocation (Dunn et al., 1991; Greve et al., 1990; Kountouras et al., 1984).

Table 3: Animal models of HE.

HE type	Model	Mechanism	Characteristics
A	Thioacetamide	Hepatic necrosis	Hyperammonemia, brain edema, oxidative stress (Rama Rao et al., 2010)
A	Azoxymethane	Hepatic necrosis	Hyperammonemia, brain edema (Nguyen et al., 2006)
A	Acetaminophen	Hepatic necrosis	Hyperammonemia, brain edema, oxidative stress (Fontana, 2008)
A	Galactosamine	Hepatic necrosis	Hyperammonemia, brain edema, oxidative stress (Gamal et al., 2014)
B	Porto-caval anastomosis	Non-detoxification of toxins without hepatic injury	Hyperammonemia (Bosoi et al., 2014)
C	Bile duct ligation	Extra-hepatic cholestasis	Hyperammonemia, brain edema, oxidative stress (Bosoi et al., 2012)

The bile duct ligated rat

The bile duct ligated rat (BDL) is a model of extra-hepatic cholestasis, in which a resection of the common bile duct is made resulting in hepatic build-up of bile and subsequent fibrosis and cirrhosis. Marked by the development of minimal/covert HE (4-6 weeks), the BDL rat presents systemic and central hyperammonemia, systemic oxidative stress (Bosoi et al., 2012) and brain pro-inflammatory cytokine TNF-alpha (Sheen et al., 2016).

Brain swelling is a well-known feature of this model (Bosoi et al., 2011; Dhanda et al., 2013). The use of permeability tests by our lab found that the BBB is not broken and the edema in the BDL rat thus arise from cytotoxic origin (Bosoi et al., 2012).

Aim of the project

Brain edema is a serious complication of HE, but its pathogenesis is still unclear. Cytotoxic edema is known to affect astrocytes, with ammonia and ROS toxicity being involved. EC of the BBB are the first cells in contact with possible blood-derived harmful molecules, but surprisingly their role in ammonia metabolism and brain edema has never been thoroughly explored. Therefore, the aim of this study is to evaluate the effects of hyperammonemia and ROS on the BBB in the pathogenesis of brain edema *in vivo* and *in vitro* by:

1- Assessing the effect of liver disease, ammonia and oxidative stress on NKCC1 expression in EC's of BBB *in vitro* and *in vivo*

2- Exploring GS and ammonia metabolism in health and liver disease, with varying ROS and ammonia conditions in EC's of the BBB *in vitro* and *in vivo*.

Material and Methods

Materials

Trichloroacetic acid, β-mercaptoethanol, Ethylenediaminetetraacetic acid (EDTA), Sodium L-glutamate, resazurin sodium salt, diethyl pyrocarbonate (DEPC), dimethyl sulphoxide (DMSO), imidazole, ammonium persulfate, ammonium chloride, potassium chloride, hydroxylamine, HEPES, hydrochloric acid, bovine serum albumin (BSA), sodium pyrophosphate and isopropanol were from Sigma-Aldrich, Canada. Protease inhibitor cocktail (PIC) was from Roche, Canada. Adenosine 5′-triphosphate disodium salt (ATP) was from Bio Basic, USA. Magnesium chloride, sodium chloride, methanol, DL-Dithiothreitol (DTT), tris base, hydrogen peroxide, ferric chloride, Trizol reagent and all rtPCR reagents were from Thermo Fisher Scientific, Canada.

In vivo

The bile duct ligated rat (BDL)

Male Sprague-Dawley rats of approximately 200g (Charles River, Canada) were kept 2 per cage with 12 h day/night cycles with free access to water and rodent chow. For the surgery, animals were anesthetized with isoflurane 3%. A midline incision was made (Figure 14) and the liver lobes were separated so the bile duct could be exposed (panel 2). After its isolation, a ligature on the distal portion of the duct was performed and 100µl of formalin was injected to prevent dilation of the bile duct (panel 3). Rapidly, a second ligature was placed proximal to the liver and the duct was resected between the two ligatures (panel 4). SHAM animals are used as "placebo controls" in surgical models. Here, they underwent the same operational procedures (anesthesia, incision, isolation of the bile duct and fat removal) except for the ligatures, formalin injection and the bile duct resection. The total surgery time was 20 min and at the end, the incision was closed with 4-0 silk thread. The animals received pain medication (carprofen 0,5mg/kg and bupivacaine 0,25%) and weekly vitamin K injections (50µg/kg) subcutaneously. Vitamin K was used to reinforce blood coagulation, since in this model an anticoagulant effect arises. Experiments were conducted following the Guidelines of Canadian Council on Animal

Care and were approved by the Animal Protection Committee (Comité Institutionnel de Protection des Animaux) of CRCHUM. After 6 weeks, the rats were anesthetized with isoflurane and the blood was collected by cardiac puncture, transferred into heparinized tubes and after centrifugation, the plasma was recovered. The animals were sacrificed by decapitation and the brain was removed. The samples were snap frozen with acetone in dry ice and kept at -80°C.

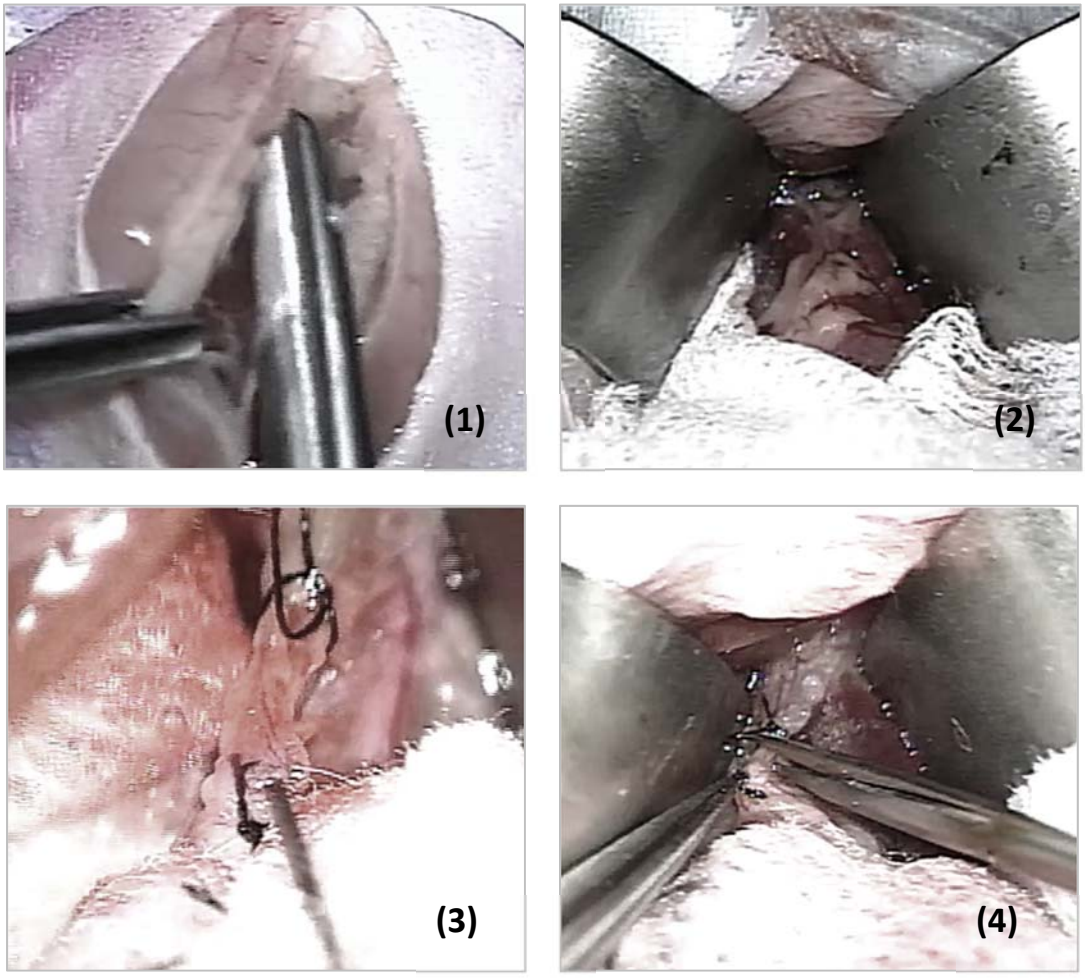

Figure 14: BDL surgery

For the BDL surgery 1) a midline incision is made on rat skin and muscle, 2) the bile duct is exposed and a distal ligature is made, 3) after placing a proximal ligature (kept loose) formalin is injected into the bile duct and the ligature is rapidly fastened, 4) finally, the bile duct is resected.

Samples preparation

Isolation of cerebral microvessels

The microvessel isolation is described in (Faropoulos et al., 2010) and (Krizbai et al., 2005) with modifications. Briefly, the frontal cortex or cerebellum were homogenized at 1300 rpm/min (Heidolph Instruments GmbH & Co., USA) in a sucrose buffer (0,32M sucrose, 3mM HEPES, 1:500 PIC, 50mM potassium fluoride and 10mM sodium pyrophosphate). Potassium fluoride and sodium pyrophosphate were used to inhibit the phosphatases, which was necessary for assessing NKCC1-P expression. All the centrifugation steps were carried out at 4˚C. The homogenized tissue was centrifuged twice at 1000*g* at 4˚C for 10 min. After, it was centrifuged for 30 secs at 100*g*, for 15 secs at 100*g* and three times at 200*g* for 60 sec. After each centrifugation, the supernatant was removed and the pellet was suspended in sucrose buffer. The presence of the microvessels was confirmed by putting a drop of the final sample on a slide and observing under light microscopy (figure 15).

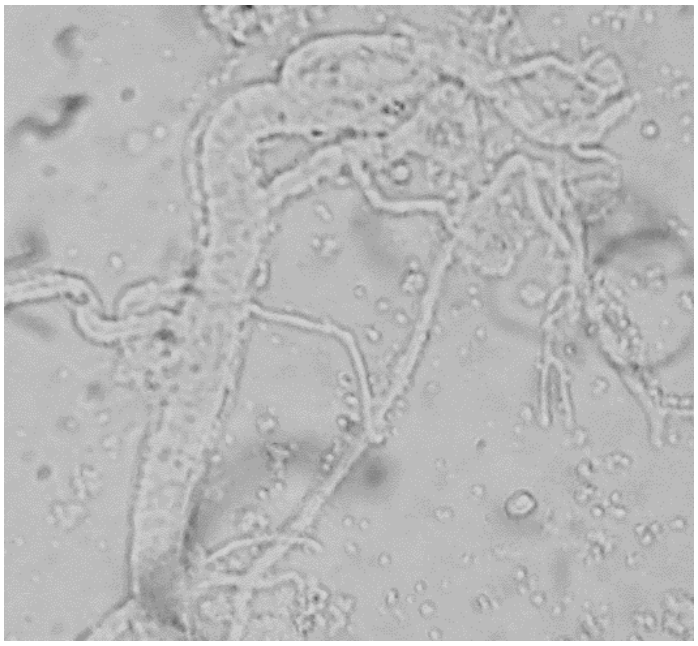

Figure 15 : Cerebral microvessels

Light microscopy picture (20x) of cerebral microvessels isolated from brain frontal cortex by centrifugation using a sucrose gradient.

In vitro

Cell culture

Neonatal Sprague-Dawley rat's primary brain microvascular endothelial cells (RBMEC) were purchased from Cell Biologics (RN-6023, Cell Biologics, USA). Cells were kept in proprietary rat endothelial cell medium (M1266, Cell Biologics, USA) supplemented with 5% fetal bovine serum (FBS), endothelial growth factor, vascular endothelial growth factor, L-glutamine and antibiotics/antimycotic. The culture was expanded and used for experimental procedures until the 8th passage. Cells were grown in T75 flasks until 70% confluence was reached. Cells were washed with warm PBS (WISENT, Canada) and trypsin-EDTA (WISENT, Canada) was added to detach the cells. After 3 min at 37°C, cells were recuperated and cell medium added. An aliquot of the cells suspension was mixed with trypan blue dye (BDH Chemicals) at 1:1 ratio for counting in a Neubauer chamber. The number of cells was calculated and cells were seed at 3000 cells/cm^2 on T75 flasks or stored at -80°C in vials with 5% sterile DMSO for cryopreservation. Cells were grown in an incubator with humidified and controlled atmosphere at 37°C with 5% CO_2 in air.

Treatments

First, cells were seed on 6-well plates at 10000 cells/cm^2 or on 96-well plates at 6000 cells/cm^2 and allowed to attach overnight. Cells were treated with medium containing ammonium chloride diluted in sterile PBS to concentrations ranging from 0,5mM to 5mM and hydrogen peroxide (oxidative stress) to concentration ranging from 10µM to 100µM for 24, 48 or 72 h. Control cells were exposed to cell medium + 5% PBS alone. The cell medium with ammonium and/or hydrogen peroxide was freshly prepared and changed every 24 h to ensure stable concentrations. In a second set of experiments, FBS was replaced by BDL or SHAM plasma, but this resulted in cellular death. Therefore, 5% BDL or SHAM plasma was added to the complete culture medium containing FBS.

Preparation of cells and tissue lysates

Endothelial cells at 80% confluency were washed twice with warm PBS and lysed with Tris-SDS buffer containing 62,5 mM Tris; 2% Sodium dodecyl-sulphate (SDS) and 1:500 PIC.

For NKCC1-P experiments, 50mM potassium fluoride and 10mM sodium pyrophosphate were added to the buffer. For tissue lysate, organs were minced with a scalpel blade. 300µl of ice-cold RIPA buffer (50mM Tris pH 7,4; 150mM sodium chloride; 1mM EDTA; 0,1% SDS; 1:500 PIC) was added, and the tissue was homogenized on ice at 1300 rpm/min by a homogenizer. The samples were centrifuged for 40 min at 4° at 13000*g* and the supernatant was recuperated. All samples were sonicated on ice for 3 times of 10 secs with 30 sec intervals (Vibracell, Sonics and Materials, USA). Protein dosage of CMV, cells and tissues lysates was performed using Bio-Rad DC protein assay kit (Bio-Rad Laboratories, USA).

RNA extraction

Endothelial cells at 80% confluency were washed twice with PBS and lysed with Trizol reagent. Chloroform was added and samples were centrifuged at 13000*g* for 45 min at 4˚C. The supernatant was mixed with ice-cold isopropanol and incubated overnight at -80˚C. Then, the samples were centrifuged at 13000*g* for 30 min at 4˚C. The RNA pellet was washed with 75% ethanol and centrifuged at 6000*g* for 6 min at 4˚C. The supernatant was removed and the pellet was air dried and then re-suspended in 0,1% DEPC-water The RNA concentration was determined by NanoDrop spectrophotometer (Thermo Fisher Scientific).

Viability assessment

Alamar blue assay

Alamar blue is a viability test based on the reduction environment present in viable cells. Once the resazurin dye (blue) is added, viable cells convert it by normal reduction reactions into resorufin, with measurable changes in fluorescence (figure 16).

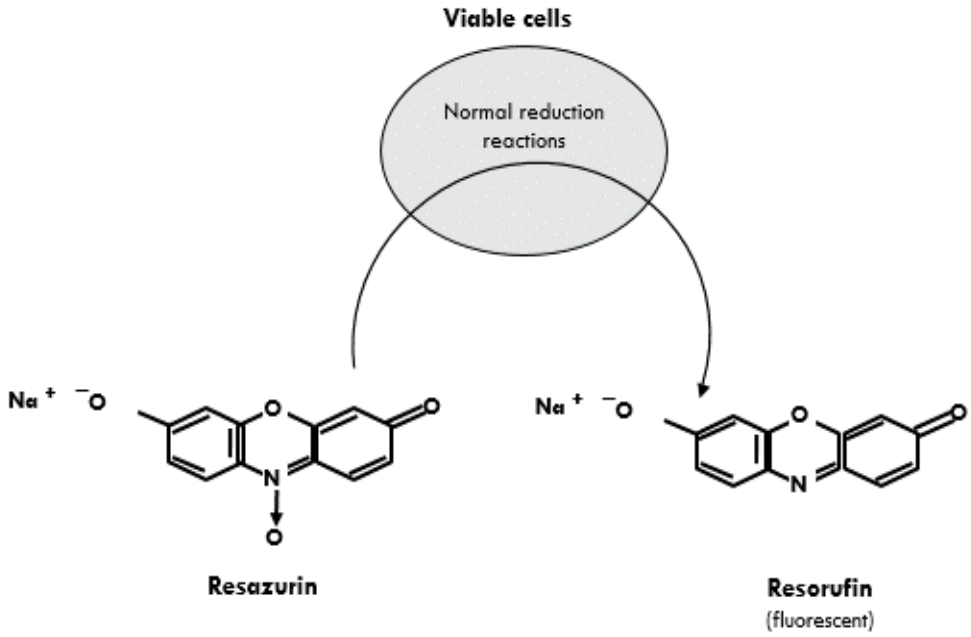

Figure 16: The Alamar blue test's reaction
Conversion of resazurin into resorufin by viable cells, principle of the Alamar blue test.

Endothelial cells were seeded (6000 cells/cm^2) in 96-well plates and allowed to adhere overnight. For ammonia experiments, hydrogen peroxide 100µM was used as a positive control. Cells were then probed with 7-hydroxy-3H-phenoxazin-3-one-10-oxide sodium salt (resazurin sodium salt) to a final concentration of 440µM in phenol red-free endothelial cell medium (PeproGrow Endothelial Cell Basal Medium, ENDO-BM + MicroV Growth supplement, GS-MicroV, PeproTech, USA) for 4h at the incubator and fluorescence was read using a spectrofluometer (Synergy HT, BioTek, USA) at wavelengths of 530nm for excitation and 590nm for emission. The test was done in triplicates and in two independent experiments.

Evaluation of mRNA expression

rtPCR

In rtPCR reaction, RNA of the protein of interest is assessed by reverse transcription through the action of a reverse transcriptase enzyme, capable of synthetizing DNA from RNA,

followed by subsequent polymerase chain reaction, in which the newly formed transcripts are amplified to measurable levels.

Endothelial cells RNA (1µg) was added to a rtPCR mix containing 1x PCR buffer (20mM Tris-HCl, pH 8,4; 50mM KCl; 0,1mM DL-dithiothreitol), 1,5mM $MgCl_2$; 0,1 µg/µl BSA and 0,2mM of deoxynucleotide triphosphate (dNTP), 1µM of each primer (forward and reverse), 1,5U of recombinant DNA Taq Polymerase, 10U of recombinant ribonuclease inhibitor (RNAse out) and 40U of Moloney Murine Leukemia Virus Reverse transcriptase (M-MLV RT). The primer's sequences were designed using BLAST software:

GS forward: 5' CACCAAGGCCATGCGGGAGG 3'

GS reverse: 3' CGGATACTGGCGCTGCGGTT 5'

GAPDH forward: 5' GGGGCTCTCTGCTCCTCCCTGTT 3'

GAPDH reverse: 5' ACTGTGCCGTTGAACTTGCCGT 3'

In a thermal cycler (PTC-100, MJ Research, Canada) the reverse-transcription reaction was initiated by heating samples at 37˚C for 30 min. A first step of denaturation at 94 ˚C for 3 min was followed by 30 cycles of amplification: 1 min at 94˚C to denature the DNA strands, 1 min at 60˚C for primers annealing, 1,5 min at 72 ˚C for strand polymerization. A final extension step of 5 min at 72 ˚C was added. The product of 201 base pairs (GS) or 248 base pairs (glyceraldehyde 3-phosphate dehydrogenase; GAPDH) was then separated by electrophoresis (100 volts for 1 hour) in a 2% agarose gel with incorporated ethidium bromide (0,5µg/ml). Then, the bands were visualized under UV light on a Gel Doc System and analysed with Quantity One software (Bio-Rad Laboratories, USA).

Evaluation of protein expression for GS and NKCC1/NKCC1-P

Western blot

Western blot assays were performed to assess protein levels of GS, α-tubulin, GAPDH, NKCC1 and NKCC1-P in brain endothelial cells or cerebral microvessels. Muscle or brain lysates were used as a positive control for GS expression. Proteins (30µg) were mixed in Laemmli buffer, heated for 5 min at 100˚C and loaded into 8% (NKCC1/NKCC1-P) or 9% (GS) sodium dodecyl-sulfate polyacrylamide gels (SDS-PAGE resolving gel: 0,375M Tris pH 8,8; 0,1% sodium dodecyl sulphate; 8% or 9% acrylamide). The samples were then submitted to

electrophoresis for 1 hour at 90 volts and 45 min at 160 volts. The proteins were transferred to polyvinylidene difluoride (PVDF, Bio-Rad Laboratories, USA) or nitrocellulose (Schleicher & Schuell, USA) membranes for 1 hour at 100 volts in transfer buffer (Tris 48mM; glycine 39mM; 0,037% SDS; 20% methanol). The membranes for actin, GS and NKCC1 were then blocked overnight at 4˚C in a solution of TBST-Milk (1mM Tris; 10mM NaCl; 0,5% Tween-20; 5% skimmed milk) or for NKCC1-P in PBS-BSA (0,3mM KCl; 1mM Na_2HPO_4; 0,2mM KH_2PO_4; 13,7mM NaCl; 1% BSA). Primary antibodies were incubated in their corresponding blocking buffers (TBST-Milk or PBS-BSA) for one hour at room temperature at the following concentrations: 1/2000 mouse anti-GS (BD Biosciences, USA), 1/2000 rabbit anti-β-tubulin and 1/2000 mouse anti-NKCC1 (Developmental Studies Hybridoma Bank, USA), 1/10000 rabbit anti-GAPDH (Sigma-Aldrich) and 1/2000 rabbit anti-NKCC1-P (Flemmer et al., 2002)(courtesy of Dr. Biff Forbush). The membranes were washed with TBST solution for 5 times of 5 min and then incubated with horseradish peroxidase (HRP) conjugated secondary antibodies (goat anti-rabbit or anti-mouse IgG, Jackson ImmunoResearch, USA). After further washes, the membranes were exposed to an antibody detection reagent (HyGLO chemiluminescent HRP, Denville Scientific, USA) and exposed to autoradiography films (HyBlot CL, Denville Scientific). Finally, the bands were scanned and quantified with Quantity One software.

Immunofluorescence

Evaluation of GS in frontal cortex microvessels and *in vitro* endothelial cells was made by immunofluorescence using GS and caveolin-1 (endothelial marker) antibodies. First, naive Sprague-Dawley rats of ~200g (Charles River, Canada) were anesthetized with isoflurane 4% and perfused with saline and with 10% formalin. Brains were extracted and kept in PBS at 4˚C. Frontal cortex brain slices of 50 μm were cut using a vibratome and slices transferred in 24-well plates containing PBS. For *in vitro* assay, endothelial cells were grown in coverslips (10000 cells/cm^2) and allowed to attach overnight. Cells were washed with ice-cold PBS twice, fixed with ice-cold methanol for 15 min, washed three times for 5 min with PBS, permeabilized for 15 min with PBS-Triton 0,5% and washed three times for 5 min. All samples were blocked with PBS-0.5%Triton + 10% donkey serum for 30 min at room temperature and then washed 3 times for 5 min in PBS. Samples were exposed to the primary antibody (1/200 rabbit anti-GS,

Sigma-Aldrich; 1/200 mouse anti-GS, BD Biosciences and 1/300 rabbit anti-caveolin-1, Cell Signaling, USA) in blocking buffer overnight at 4˚C. After 3 washes, samples were then exposed to secondary antibody (1/200 mouse anti-IgG coupled to DyLight™ 488 or 1/200 rabbit anti-IgG coupled to DyLight™ 594, Jackson ImmunoResearch) in PBS-0.5%Triton and incubated for 30 min in the dark and at room temperature. Following washes, 4',6-diamidino-2-phenylindole (DAPI, 1µg/ml) was incubated for 5 min and rinsed with PBS. Slides were mounted with mounting medium (0,1M Tris; 2,5% 1,4-Diazabicyclo [2.2.2] octane; 9,6% Polyvinyl alcohol; 24% glycerol) and analyzed with a Zeiss microscope (Axio Imager M2, Carl Zeiss, Germany) and pictures were taken using the software ZEN. Pictures were processed with Fiji software (Schindelin et al., 2012).

Evaluation of GS activity

Besides catalyzing the reaction of glutamate and ammonia into glutamine, GS is also known to catalyze the formation of γ-glutamylhydroxamate from glutamate and hydroxylamine (reaction below). Here, GS activity was determined indirectly based on the formation of a γ-glutamylhydroxamate ferric chloride complex, according to (Calas et al., 2008).

$$\text{L-glutamate} + \text{Hydroxylamine} + \text{ATP} \xrightarrow[Mg_2^+]{\text{GS}} \text{ADP} + \gamma\text{-glutamylhydroxamate}$$

Briefly, tissue or cell lysates (30 µg of protein) were incubated with 75 µl of reaction mix composed by 100mM Imidazole pH 7,2; 50mM sodium L-glutamate; 10mM β-mercaptoethanol; 20mM disodium ATP; 40mM magnesium chloride; 100mM hydroxylamine pH 7,2 in a 96-well microplate for 1 hour at 37˚C. The reaction was stopped by the addition of 150 µl of a solution containing 0,37 M ferric chloride; 0,67 M hydrochloric acid and 0,2 M trichloroacetic acid and the plate was incubated for 30 min at 4˚C. Finally, absorbance was measured at wavelength of 530 nm in a spectrophotometer and the readings were within the

range of a γ-glutamylhydroxamate's standard curve. The test was done in triplicates and in three independent experiments.

Statistics

Statistics were calculated with GraphPad Prism Software (GraphPad software, USA). Student-t test was used to test the difference between two groups. When analyzing more than two groups, two-way ANOVA or one-way ANOVA was used with Tukey`s post hoc test. The data is expressed as mean ± standard error of the mean (SEM), and significance was considered when $p<0,05$.

Results

1. Viability of endothelial cells of the blood-brain barrier in presence of ammonia and oxidative stress

Alamar Blue Assay

For further tests, the evaluation of the metabolism of living cells exposed to different molecules was required. Although hydrogen peroxide is systemically present in CLD, no breakdown of the BBB is present and therefore no evidence of endothelial cell death. Because of that, it was necessary to determine a non-fatal concentration of hydrogen peroxide for *in vitro* testing. The Alamar blue assay is commonly used to evaluate *in vitro* cell viability as resazurin (oxidized form) is reduced to resorufin in metabolically viable cells.

Here, viability was assessed in RBMEC subjected to concentrations from 10µM to 500µM of hydrogen peroxide, for 24h and 48h (figure 17-A). At all timepoints, concentrations of 100µM and 500µM caused significant decrease in viability when compared to untreated cells ($p<0,05$). In addition, 50µM hydrogen peroxide caused significant loss in viability only after 48h of treatment when compared to untreated cells ($p<0,05$). The concentration of 10µM of hydrogen peroxide did not lead to cell death at any of the timepoints and therefore was used as ROS source for all the subsequent experiments. The concentration of 100µM was therefore used as positive control for all subsequent experiments (figure 17-B and C).

To assess ammonia toxicity, RBMEC were subjected to concentrations ranging from 0,5mM to 5mM of ammonium chloride for 24h and 48h (figure 1 7-B). Cells showed loss of viability with 2mM at 24h and 48h treatment and following 48h treatment with 5mM, with no changes with 0,5mM and 1mM at 24h and 48h. Since the concentrations of 0,5mM and 1mM of ammonium chloride did not lead to cell death at any of the timepoints, they were therefore used in all the subsequent experiments.

Finally, to assess the toxicity of cells submitted to both ammonia and oxidative stress, RBMEC exposed to a mixture of ammonium chloride (0,5mM and 1mM) and hydrogen

peroxide (10μM) were assessed for cell viability (figure 17-C). In this setting, there was no decrease in cell viability at any of the concentrations and timepoints.

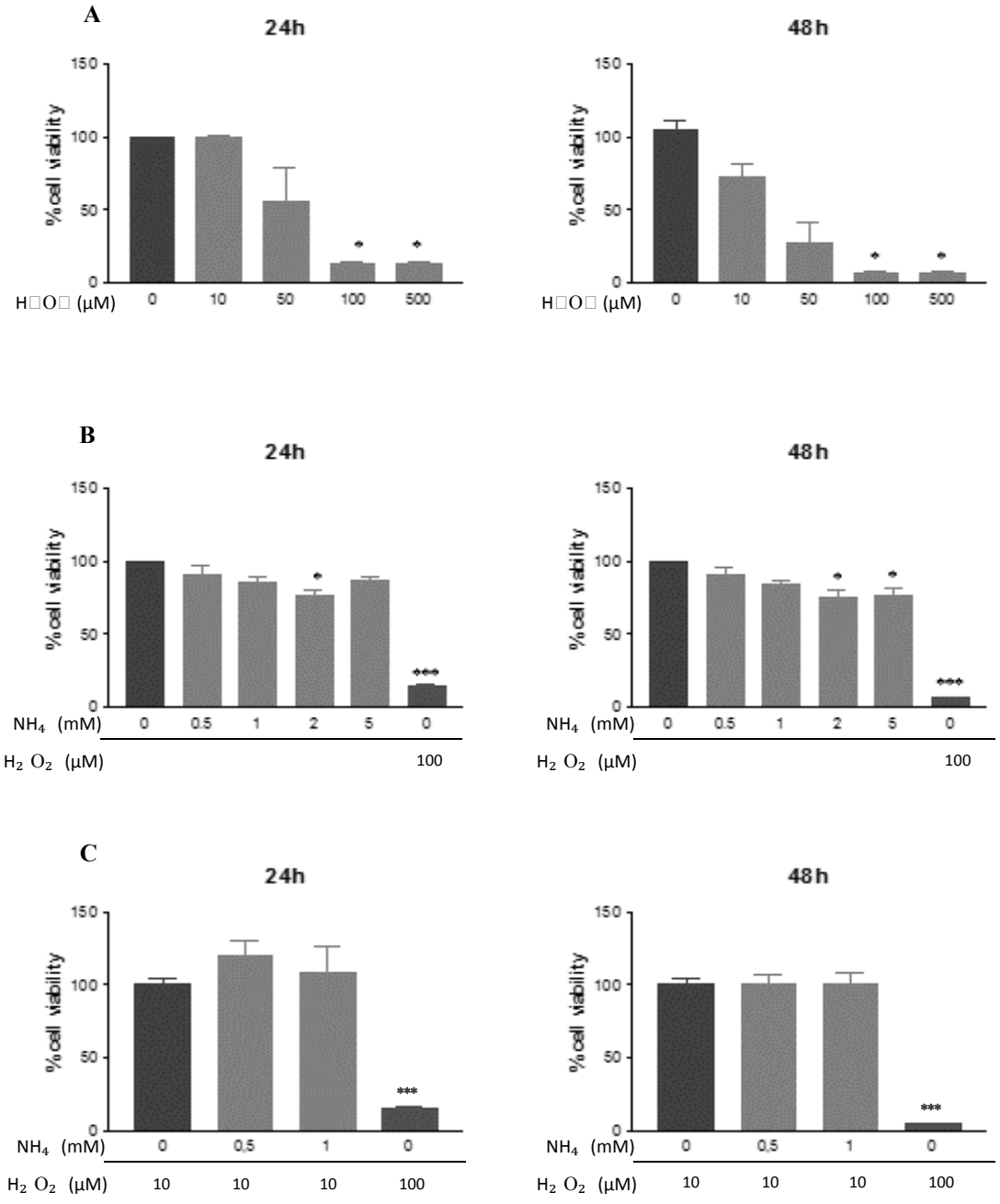

Figure 17 : Cell viability in RBMECS exposed to oxidative stress and ammonia

Cell viability by the Alamar's blue method in RBMEC exposed to hydrogen peroxide (A) ammonium chloride (B) or hydrogen peroxide plus ammonium chloride (C). 100µM hydrogen peroxide was used as positive control for B and C. * $p<0,05$; ** $p<0,01$ and *** $p<0,001$ when compared to untreated cells. Test was done in triplicates and in two independent experiments.

2. NKCC1 expression in the endothelial cells of the blood-brain barrier

NKCC1/NKCC1-P is not upregulated in RBMEC submitted to oxidative stress and/or hyperammonemia.

Since ammonia (NH_4^+) can cross biological barriers through NKCC1 transporters, the upregulation of the expression of these transporters could be vital to ammonia transport. To assess the independent and synergistic roles of ammonia and ROS on NKCC1 regulation, protein expression was measured in RBMEC subjected to 0,5mM-1mM of ammonia chloride with or without 10µM hydrogen peroxide. Treatments with different concentrations of ammonia with or without hydrogen peroxide for 24h and 48h did not upregulate protein expression of NKCC1 or NKCC1-P/NKCC1 (figure 18 A and B).

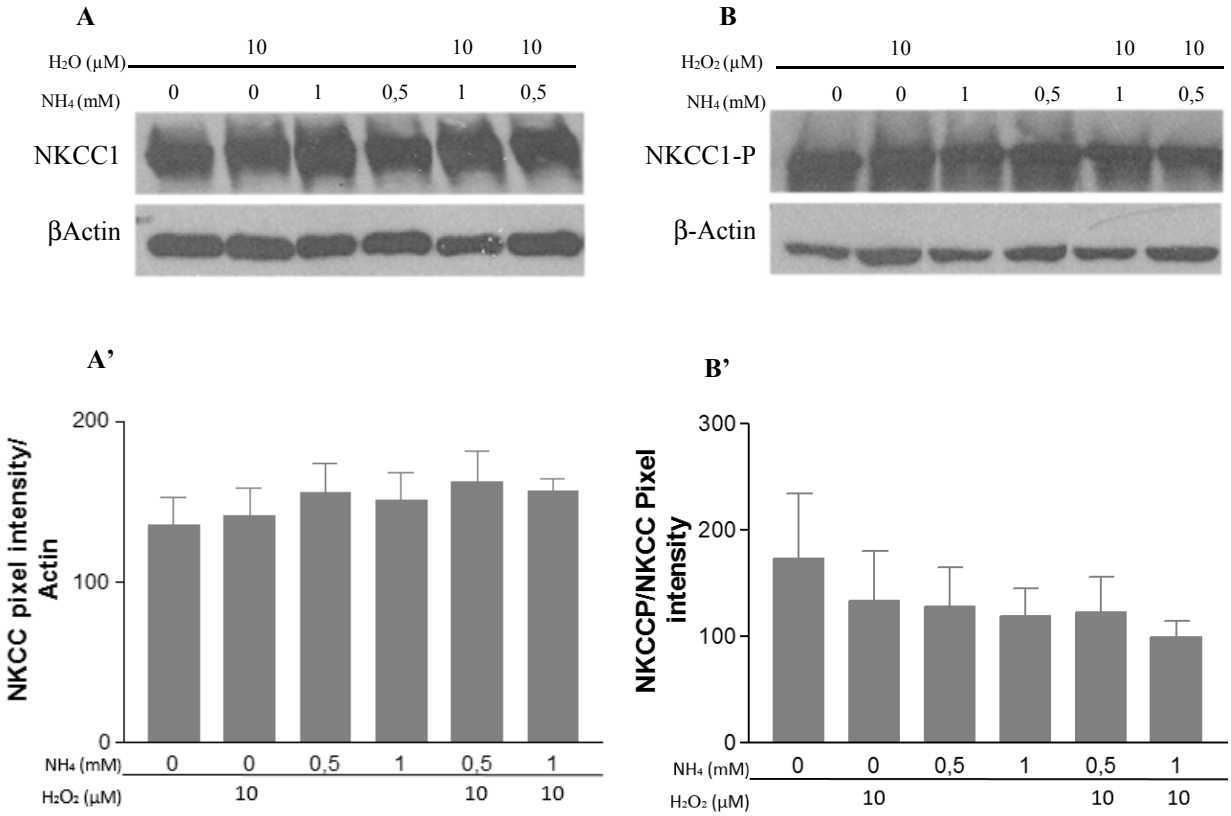

Figure 18: Protein expression of NKCC1/NKCC1-P in RBMEC exposed to ammonia and oxidative stress

Protein expression of NKCC1 (A, A') and NKCC1-P/NKCC1 (B, B') is not upregulated in RBMEC treated with 1 and 0,5mM of ammonia chloride, with or without hydrogen peroxide.

NKCC1/NKCC1-P is not upregulated in endothelial cells of BDL animals

To confirm the *in vitro* results and therefore determine whether NKCC1/NKCC1-P was upregulated in brain endothelium of BDL animals, protein expression was assessed in cerebral microvessels (CMV) from pre-frontal cortex and cerebellum. Here CMV from both brain regions of BDL animals showed no difference in NKCC1 total protein or in its phosphorylated form (figure 19 A and B), demonstrated by the ratio NKCC1/NKCC1-P, compared to SHAM operated controls.

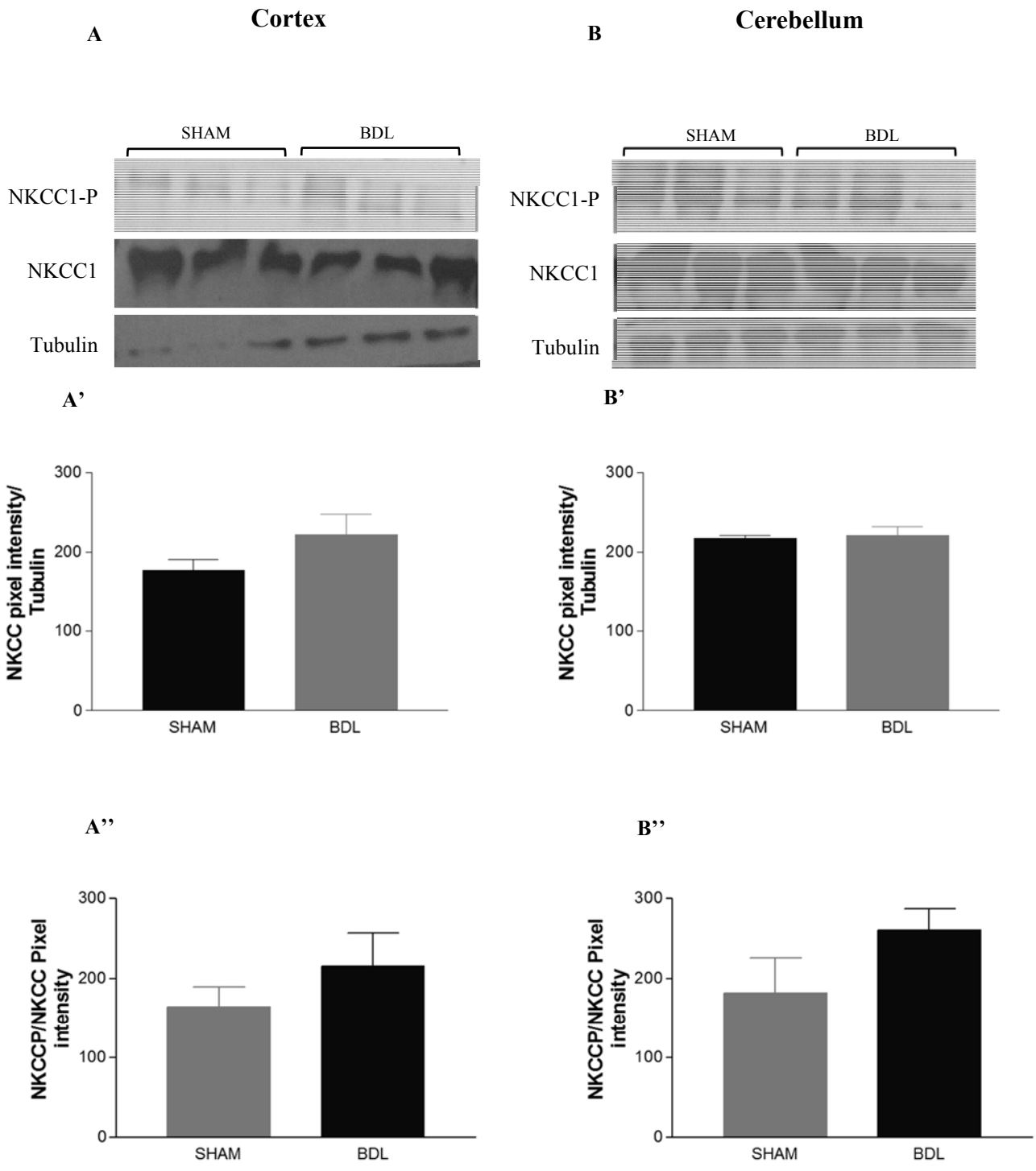

Figure 19: NKCC1 and NKCC1-P/NKCC1 protein expression in CMV

Protein expression from pre-frontal cortex (A, A', A'') and cerebellum (B, B', B'') of BDL (n=3) and SHAM (n=3) animals.

3. GS is present on endothelial cells of the BBB

Since ammonia is transported into RBMEC of the BBB, we explored whether GS could be implicated in ammonia metabolism. In liver disease, the most prominent enzyme involved in ammonia metabolism is GS, which presence has never been reported in BBB's endothelium.

GS mRNA in RBMEC

We first tested for GS mRNA levels in RBMEC using rtPCR. We found GS mRNA in these cells (figure 20-A), although lower than in the liver ($p<0,05$). We included a sample with no reverse transcriptase enzyme to control for DNA contamination and found no band, indicating that the band detection in the RBMEC was indeed GS mRNA.

GS protein expression in brain endothelial cells

Following the presence of mRNA, we then assessed GS protein expression in RBMEC. A band was found, which was less intense than the one found in liver and brain (positive controls) (figure 20-B). In CMV isolated from naive rat pre-frontal cortex (figure 21-A), GS protein was also detected, with levels like brain and liver (positive controls). In addition, when comparing GS protein expression from CMV isolated from two different brain regions (pre-frontal cortex vs cerebellum), no difference in protein levels was found (figure 21-C).

GS activity in brain endothelial cells

We then proceeded to measure GS activity in RBMEC and CMV using a colorimetric assay. The enzyme activity was performed by measuring the conversion of glutamate and hydroxylamine into glutamylhydroxamate, a reaction catalyzed by GS. GS activity was detected in RBMEC, although lower than that found in brain and liver (figure 20-C). In addition, GS activity in CMV was present and significantly lower than liver and brain (figure 21-B). In addition, when comparing GS activity from CMV isolated from two different brain regions (pre-frontal cortex vs cerebellum), no difference was found (figure 21-D).

GS immunofluorescence in brain endothelial cells

To further confirm the presence of GS in RBMEC, immunofluorescence was performed. GS signal was present in both RBMEC (figure 20-D) and in frontal cortical brain slices of naive rats (co-localized with endothelial marker caveolin-1 (figure 21-E), confirming that GS is present in ECs of the BBB *in vitro* and *in vivo*. In addition, when brain's slices from naive rats were probed with second antibodies alone, as a control for unspecific binding, no signal was obtained (data not shown).

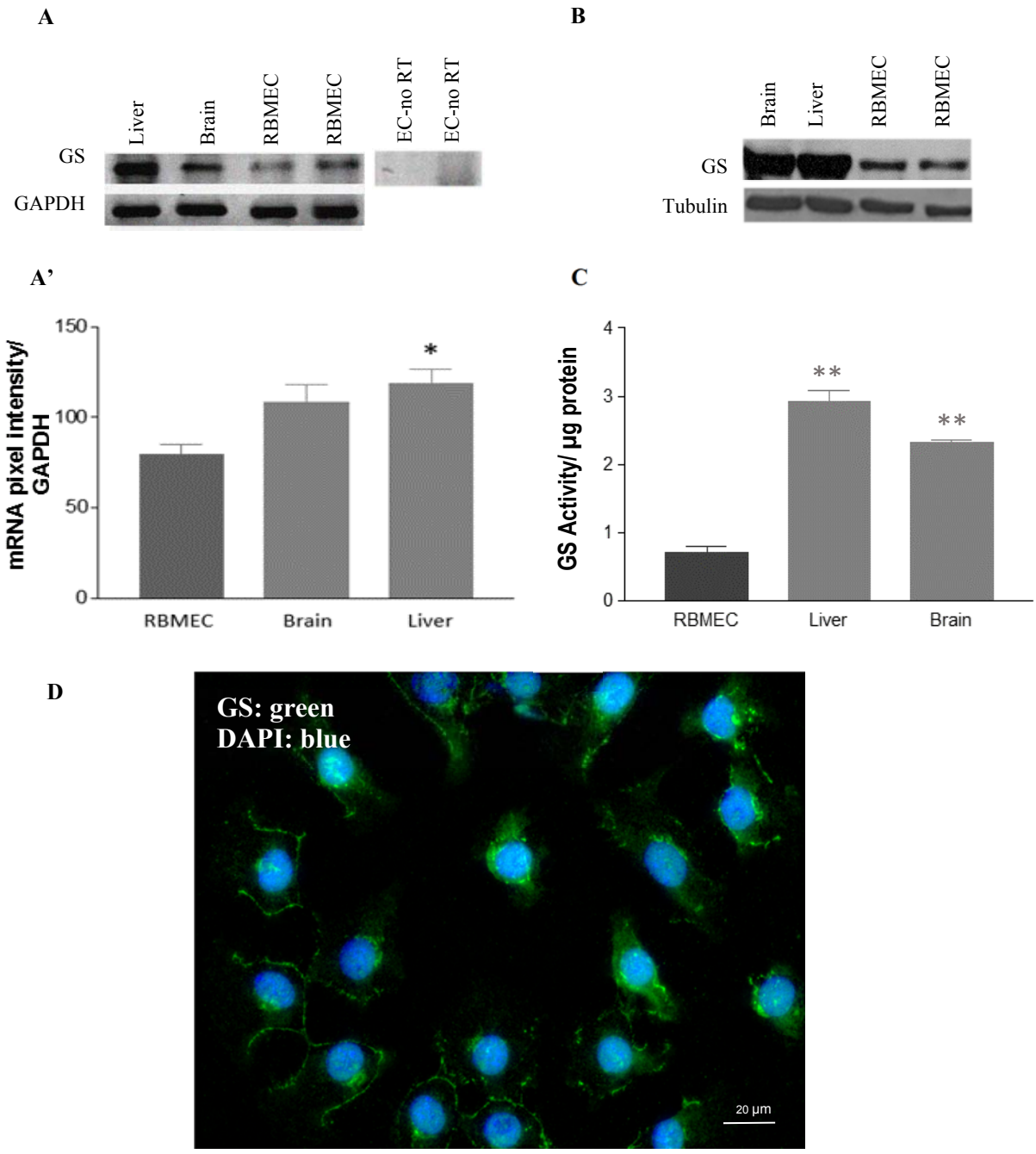

Figure 20: GS is present in RBMEC

GS expression and activity in RBMEC. Cells showed (A, A') mRNA expression (*p<0,05), (B) protein levels and (C) GS activity (**p<0,001). (D) Immunofluorescence showed GS expression in RBMEC. Activity was done in triplicates and in two independent experiments. In mRNA expression, "EC-no RT" is a control for DNA contamination.

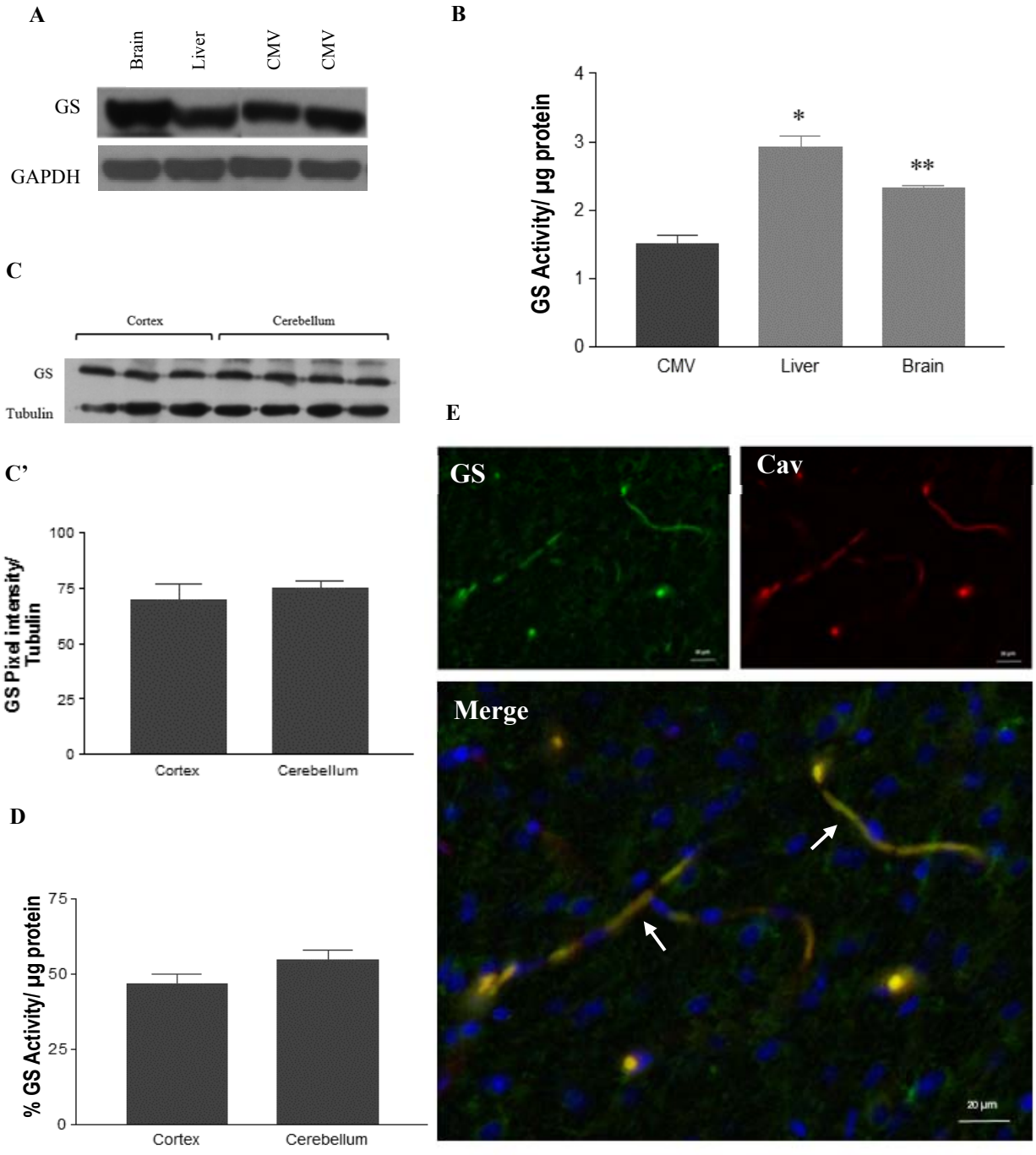

Figure 21: GS expression in CMV from naive rats

(A) Protein expression and (B) activity (* $p<0,01$ and ** $p<0,001$). GS (C, C') protein expression and (D) activity between pre-frontal cortex (n=3) and cerebellum (n=4), of naive rats. (E) Immunofluorescence of GS in brain slices of naive rats, co-localized with the endothelial cell marker caveolin-1.

4. GS in endothelial cells during hyperammonemia, ROS and liver disease

Glutamine synthetase (GS) is an enzyme which has been found to be responsible for up to half of the liver total detoxification in hyperammonemia (Hakvoort et al., 2016) and therefore has an important compensating role in CLD.

GS in chronic liver disease

To assess BBB endothelial cell's GS (expression and activity) in a model of chronic liver disease, CMV were isolated from pre-frontal cortex and cerebellum of both BDL and SHAM rats. When assessed for GS levels, BDL animals showed no significant change in GS protein expression (Figure 22-A and B) or GS activity (Figure 22-C and D) when compared to SHAM-operated controls.

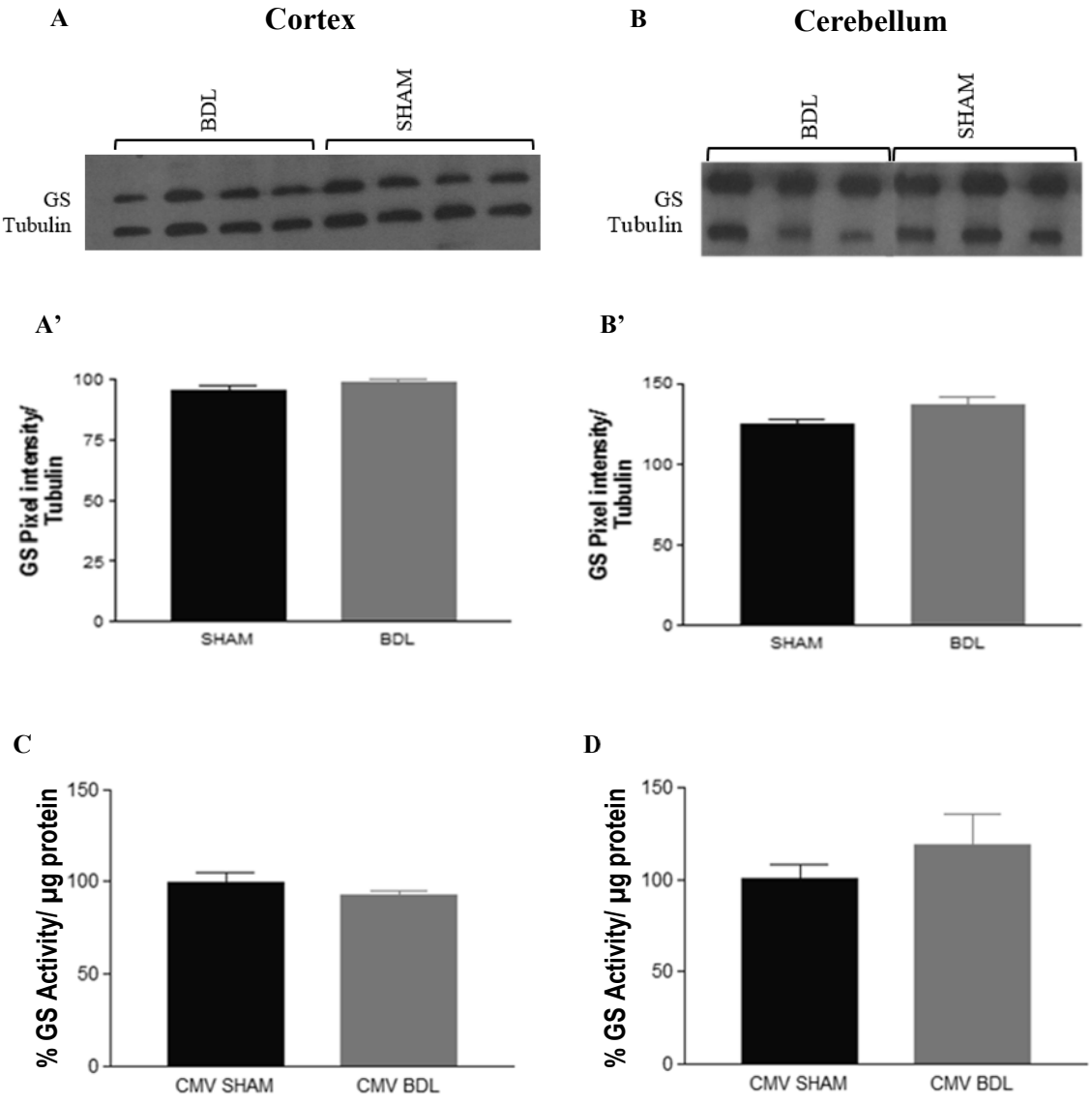

Figure 22: GS protein expression and activity in CMV from BDL and SHAM animals

GS expression in (A, A') pre-frontal cortex and (B, B') cerebellum from BDL (n=3) and SHAM (n=3). GS activity in (C) pre-frontal cortex and (D) cerebellum of BDL (n=3) and SHAM (n=3) animals.

GS in RBMEC following treatment with BDL vs SHAM conditioned media

To further assess the role of chronic liver disease in isolated RBMEC, cultured cells were exposed to 5% BDL or SHAM plasma. Cells exposed to SHAM plasma (but not BDL) showed an upregulation of GS activity and protein expression in a time dependent manner (figure 23-A

and B). In addition, at 72h (not 24h or 48h), proteins levels (figure 23-A) and activity (figure 23-B) of GS were downregulated in BDL compared to SHAM animals.

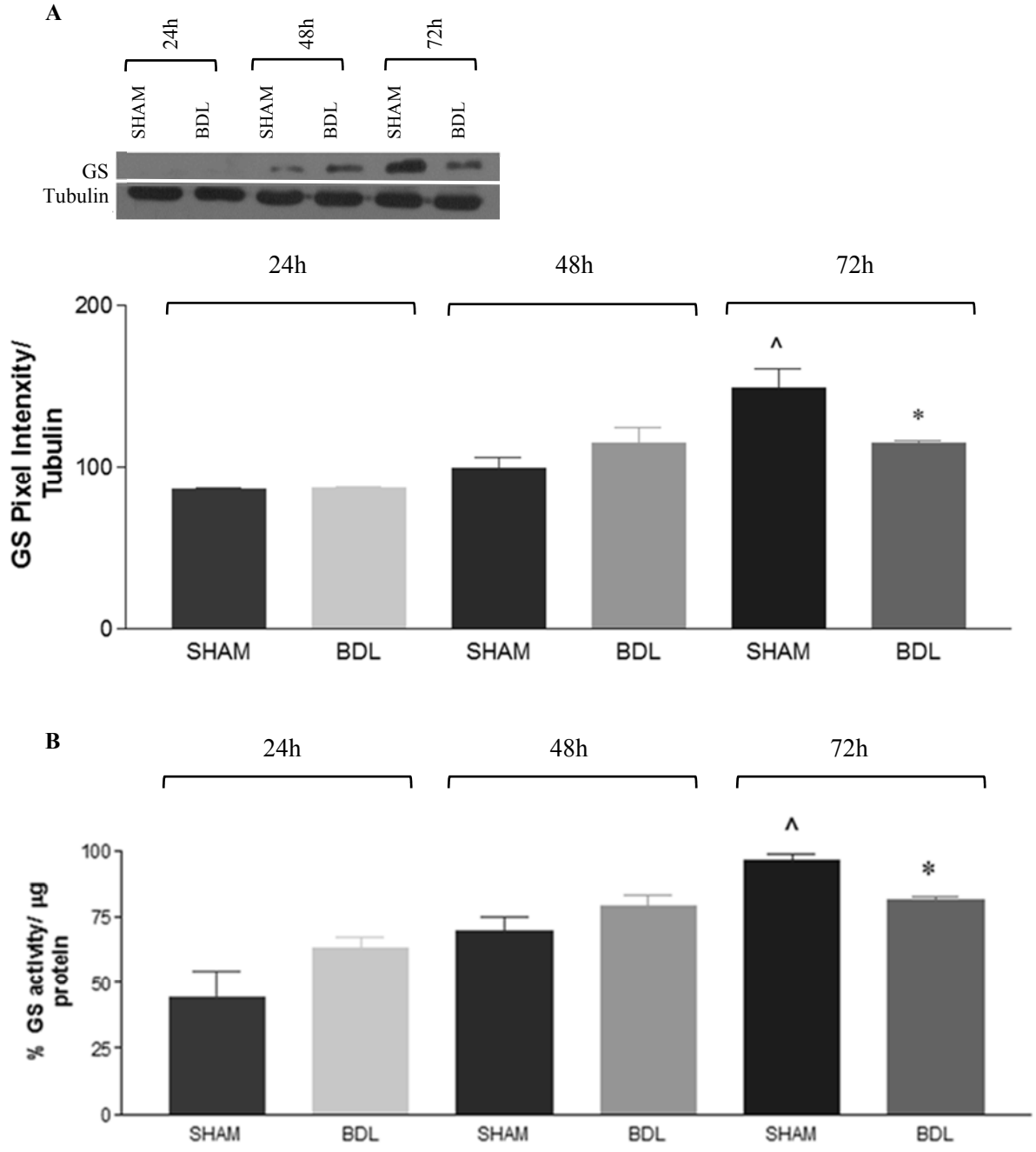

Figure 23: GS expression and activity in RBMEC treated with conditioned medium

GS (A) protein expression and (B) activity were measured after treatment with BDL or SHAM plasma. * $p<0,05$ compared to SHAM 72h and ^ $p<0,05$ compared to SHAM 24h. Activity tests were performed in triplicates with 2 independent experiments (n=6).

GS in RBMEC subjected to ammonia and oxidative stress

Finally, the role of ammonia and oxidative stress was further evaluated in RBMEC. GS activity was upregulated in RBMEC at 48h (not 24h) treated with 1mM of ammonium chloride compared to untreated cells. Treatments of 0,5mM of ammonium chloride at 24h or 48h showed no difference when compared to untreated cells (figure 24). All concentrations of ammonium chloride plus hydrogen peroxide treatments showed downregulated activity when compared to untreated cells at 48h (not 24h) (figure 25).

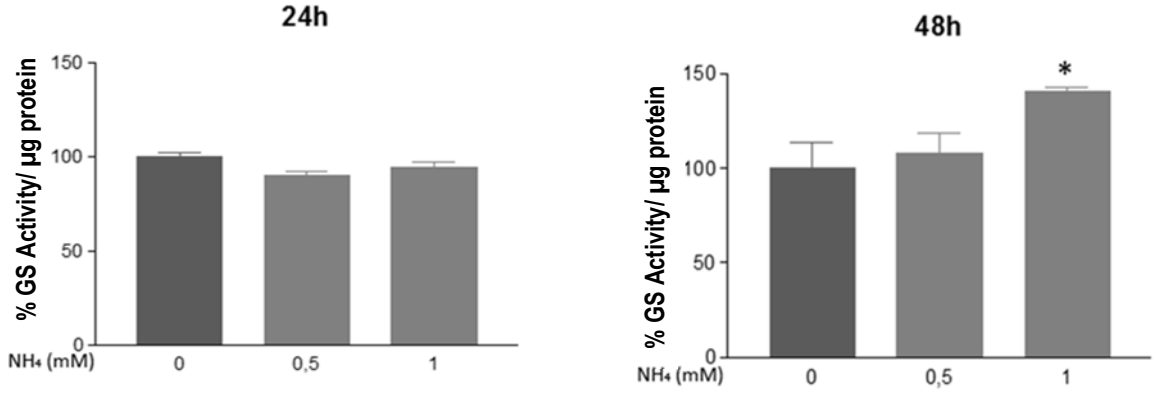

Figure 24: GS activity of RBMEC exposed to ammonia

GS activity of RBMEC exposed to 0, 0,5mM and 1mM of ammonia chloride for 24 and 48h (* $p<0,05$ compared to untreated cells). Tests were performed in triplicates with 2 independent experiments (n=6).

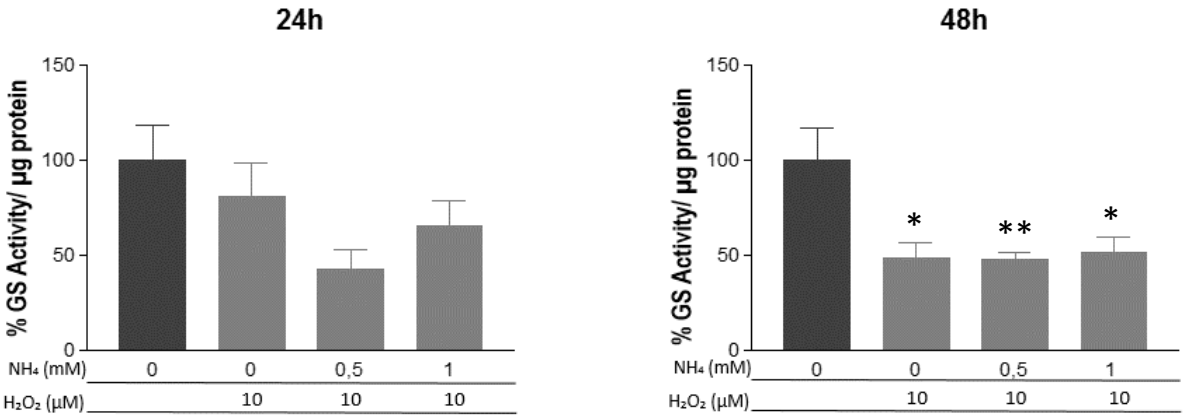

Figure 25: GS activity of RBMEC exposed to oxidative stress with or without ammonia

GS activity of RBMEC exposed to 0, 0,5mM and 1mM of ammonia chloride plus 10µM of hydrogen peroxide for 24 and 48h (* $p<0,05$ and ** $p<0,01$ compared to untreated cells). Tests were performed in triplicates with 2 independent experiments (n=6).

Discussion

To evaluate the effects of ammonia in the context of oxidative stress toxicity on the BBB in the pathogenesis of brain edema, expression of NKCC transporter and ammonia metabolism was assessed *in vitro* and *in vivo*. Here, NKCC was not upregulated in both EC treated with ammonia and oxidative stress and in CMV from BDL rats. Glutamine synthetase, an important ammonia detoxifying enzyme was found in brain EC *in vitro* and *in vivo*. GS mRNA was present in primary endothelial cells. In addition, protein expression, activity and immunofluorescence of GS was found in both cultured EC and CMV from naive rats. GS protein expression and activity in cultured endothelial cells was lower than liver and brain (controls) but mRNA was only lower than in liver. Although GS protein expression in CMV was no different from brain and liver (controls), GS activity in CMV was lower than both controls. Moreover, there was no difference in GS expression in CMV from cerebellum vs pre-frontal cortex. When GS expression was assessed in a model of liver disease, there was no change of protein expression or activity in CMV of BDL animals however, GS downregulation was found when EC were treated with conditioned medium from plasma of BDL rats. Whereas, conditioned medium with SHAM's plasma increased GS expression in a time dependent manner. Furthermore, EC treated with ammonia showed increase in GS activity while EC submitted to oxidative stress presented decreased GS activity.

NKCC1

Ammonia can enter the brain as a gas which passively diffuses through the blood-brain barrier (BBB) and as an ion, carried by potassium transporters such as the Na^+ K^+ $2Cl^-$ (NKCC). The NKCC1 transporter has an important role in cell volume regulation and there is substantial evidence that links its increase in activity and protein expression with brain edema in a number of pathologies such as traumatic brain injury, cerebral ischemia and HE (Kahle et al., 2009; Lu et al., 2008).

HE effects in cortex and cerebellum

Hepatic encephalopathy involves alterations in memory, learning, concentration as well as motor coordination. While the pre-frontal cortex is involved in complex cognition, the

cerebellum has an important role in fine motor coordination and therefore these areas are believed to be highly implicated in the symptoms of HE. The development of brain dysfunction can affect the whole brain or be restricted to one specific area. Cauli and colleagues assessed brain edema in different brain regions following ALF. The authors found that the cerebellum and cortex presented different edema profiles, with frontal cortex developing cytotoxic edema and the cerebellum demonstrating an apparent vasogenic form of edema with early increase in BBB permeability (Cauli et al., 2011). Therefore, it is plausible that the regulation of NKCC1 might differ between these two regions.

Bumetanide and brain edema

Bumetanide is a potent, specific inhibitor of NKCC1. Despite bumetanide's low ability to cross the BBB, it should be enough to inhibit central NKCC1 when administered in high doses (Javaheri et al., 1993), it is likely that reducing ammonia entrance into the brain by inhibiting NKCC1 on EC of the BBB plays an important role preventing brain edema. A study by O'Donnell and coworkers assessed NKCC1 localization in CMVs and discovered that 80% of the transporter is localized in the luminal side of the vessels. The use of the inhibitor bumetanide decreased brain edema in a model of stroke by arterial occlusion (O'Donnell et al., 2004). Furthermore, the effect of bumetanide on reducing brain edema could be attributed to its systemic diuretic effect, but the lack of difference in body weight between animals treated with or without bumetanide points to the beneficial effect of the drug on the BBB (Jayakumar et al., 2011). The effect of bumetanide on brain edema was confirmed in the BDL model by our laboratory where rats were treated with bumetanide lead to a decrease in brain water compared to vehicle-treated BDL (Huynh, 2011, non-published results), stressing the potential role of NKCC1 in the pathogenesis of brain edema.

Role of NKCC1 in edema

In HE, the increase of NKCC1 (activity or expression) may be implicated in the development of brain edema and is possibly upregulated due to hyperammonemia and oxidative stress. It has been shown that astrocytes exposed to high ammonia concentrations exhibit cell swelling, which was correlated with increased NKCC1 protein. Since high ammonia concentrations (5mM) leads to oxidative stress, these cells were treated with antioxidants (*N*-

nitro-l-arginine methyl ester and uric acid) which lead to a decrease in NKCC1 expression and astrocyte swelling (Jayakumar et al., 2008). In a model of ALF (induced by thioacetamide), NKCC1 protein expression, phosphorylation and activity was shown to be increased in brain in relation to brain edema (Jayakumar et al., 2011).

BDL, brain edema and the synergistic effect between ammonia and ROS

The BDL rat is a model of covert HE in which the obstruction of the common bile duct leads to cirrhosis, accumulation of toxins in the blood and development of brain edema. Our laboratory evaluated the role of ammonia and systemic oxidative stress in the pathogenesis of brain edema in this model. We observed decreased brain water when BDL animals were treated with an ammonia-lowering compound (AST-120) for up to 6 weeks (Bosoi et al., 2011). In addition, in the same model, when oxidative stress was attenuated, using the antioxidant allopurinol, a decrease in brain edema was also observed (Bosoi et al., 2012). Finally, a model of type B HE (porto-caval anastomosis), which presents only hyperammonemia with no oxidative stress or brain edema, was used to prove even further the relationship between ammonia, ROS and brain edema. Oxidative stress was induced in this model via injection of diethyl maleate (depletes glutathione stores) and the result was the occurrence of brain edema, confirming the synergistic effect between ammonia and oxidative stress in the setting of brain edema in CLD (Bosoi et al., 2014).

NKCC1 is not regulated in ECs submitted to ammonia and ROS

In vivo models such as the BDL are complex, with numerous cell interactions (e.g. EC-pericytes-astrocytes) and circulating molecules (e.g. bile acids, ROS, cytokines, lactate, ammonia). *In vitro* settings can be used to dissect the effects of specific cells and/or molecules. Here, we used rat brain microvascular EC as a simplified model of the BBB. Since our study aimed to mimic situations found in the BDL model, which demonstrate no physical breakdown of the BBB, it was important to ensure that toxins of interest did not cause loss of viability of brain EC. To find a relevant concentration of ammonia and hydrogen peroxide for *in vitro* treatments, a viability test (Alamar's blue) was performed.

First, cultured cells were exposed for 24h or 48h to concentrations ranging from 10µM to 500µM of hydrogen peroxide, which was used as a ROS source to cause oxidative stress. The

highest concentrations (100µM and 500µM) provoked a loss in viability at both time points, and because of that, the 100µM treatment was used in the other tests as a positive control for the technique. Treatments of 50µM and 10µM did not cause a loss in cell viability at 24h or 48h. Since 10µM was the most physiologically relevant concentration, it was used in the further assays as a source of ROS.

The next step was to assess how EC act in ammonia conditions. Cells were exposed to concentrations from 0,5mM to 5mM of ammonia for 24h and 48h, and viability was assessed. Loss in viability was observed with 2 mM ammonia at 24h and 48h, and with 5mM of ammonia at 48h only. Curiously, cells submitted to 5mM of ammonia for 24h did not show decrease in viability. Concentrations of 1mM and 0,5mM of ammonia did not cause loss in cell viability, and therefore were used in the subsequent tests as ammonia source.

Finally, to assess potential additive effects of ammonia and ROS in the viability of brain endothelium, cells submitted to concentrations of ammonia of 0,5mM and 1mM plus 10 µM of hydrogen peroxide were assessed after 24h and 48h treatments. None of these concentrations at either timepoints resulted in a decrease in viability. The concentrations chosen in this study were based in the fact that they i) represented pathophysiologically relevant levels of these toxins and ii) did not induce cell death, which is uncommonly found in HE.

After exposing EC to the concentrations of ammonia and ROS selected by the viability test for 24 and 48h, NKCC1/NKCC1-P protein expression was assessed. In our study, cells exposed to concentrations of 0,5mM and 1mM of ammonia for up to 48h showed no upregulation of NKCC1/NKCC1-P protein expression. Jayakumar and colleagues found increased NKCC1/NKCC1-P protein expression and activity in astrocytes submitted to ammonia chloride, but the ammonia concentrations used in these studies were up to 10 times higher than the ones used in our study and no viability test was performed (Jayakumar et al., 2008, 2014; Kelly et al., 2009). Therefore, it is possible that only high levels of ammonia or longer exposure are able to regulate NKCC1 expression.

When cells were exposed to 48h with concentrations of 0,5mM and 1mM of ammonium chloride with 10µM of hydrogen peroxide, there was still no change in NKCC1 or NKCC1-P expression compared to untreated control cells. It is possible that the oxidative stress here is not enough intense to trigger NKCC1/NKCC1-P regulation. Finally, it is possible that other factors

such as hormones or cytokines present *in vivo* are involved in the regulation of NKCC1/NKCC1-P, and therefore the expression of the transport should be assessed.

NKCC1 is not upregulated in CMV of BDL rats when compared to SHAM operated controls

To confirm the *in vitro* results and therefore determine whether NKCC1/NKCC1-P was upregulated in brain endothelium of BDL animals, protein expression was assessed in cerebral microvessels (CMV) from pre-frontal cortex and cerebellum. Here, we found no upregulation of NKCC1 or its phosphorylated form in BDL rats compared to SHAM control animals. Considering that inhibition of NKCC1 is beneficial, decreasing edema, no increase in NKCC1 expression does not mean no increase in activity, as NH_4^+ (and possibly Na^+, Ca^+, Cl^-) is elevated in plasma during cirrhosis which could lead to an increase in activity. Furthermore, there are 4 points that could also explain the lack of upregulation of NKCC1:

1) The concentration of ammonia in the BDL rat is not enough to cause a significant change in NKCC1. The BDL (model of CLD) presents around 150-250μM of circulating ammonia (Bosoi et al., 2011). Data showing an upregulation of NKCC1 protein or activity arose from studies involving a model of ALF (Jayakumar et al., 2011), which present up to 4 times higher concentration of systemic ammonia (Rose et al., 2007). It is therefore possible that pathophysiologically relevant levels of ammonia in CLD are not enough to trigger an upregulation of NKCC1;

2) The systemic oxidative stress present in the BDL model might not cause the phosphorylation of NKCC1 at serine and threonine residues by action of the SPAK/OSR1 kinases, resulting in no changes in its phosphorylated form. In addition, since there are no reports that ammonia and oxidative stress regulate NKCC1/NKCC1-P expression in EC, it is possible that this is a feature restricted to astrocytes;

3) The ratio between NKCC1/KCC is more relevant than NKCC1 alone in the setting of brain edema. KCC is an outward transporter from the same family as NKCC1, found in the abluminal membrane of the EC. Since these two transporters can carry ammonia, are both involved in volume regulation and are both regulated by the same pathway (action of SPAK/OSR1 activates NKCC1 and inhibits KCC at the same time) (delos Heros et al., 2014;

Kahle et al., 2010), it is possible that both are involved in the pathogenesis of brain edema. In the same study that found no correlation in blood NKCC1 levels from CLD patients with and without HE, Li and colleagues found a correlation between KCC levels, and the importance of the ratio NKCC1/KCC was stressed. On the other hand, a report of bumetanide treatment showed that decrease in brain edema after cerebral ischemia-reperfusion injury is in fact associated with decrease in NKCC1 expression, with no change in KCC (Wang et al., 2014). Interestingly, this study does not discredit the importance of the NKCC1/KCC ratio, since changes in either one of the transporters is enough to alter the ratio.

4) Finally, other factors such as inflammation might prevent the upregulation of the transporter, compensating and masking a potential increase in NKCC1 expression and activity. The cytokine TNF-α is a well-known pro-inflammatory molecule which is present in BDL animals (Sheen et al., 2016). In an *in vitro* study using colon cells, TNF-α was responsible for the downregulation of NKCC1 transporter (Markossian and Kreydiyyeh, 2005), and therefore it is possible that an opposite effect between the different toxins present in BDL animals (ammonia, ROS, inflammation) act simultaneously, preventing the upregulation of the transporter.

Ammonia metabolism and GS

Implications in disease

GS plays a critical role in nitrogen metabolism and brain function, therefore changes in its expression and activity can lead to multiple disorders.

Inborn GS deficiency

GS deficiency is a syndrome caused by mutations in exon 6 of the GLUL gene. It is marked by moderate hyperammonemia and low systemic levels of glutamine. Because glutamine has a central role regulating neurotransmission by limiting glutamate and serving as a substrate for GABA synthesis, individuals with this syndrome present epileptic encephalopathy with multifocal or generalized seizures. GS deficiency is an extreme severe condition marked by brain malformations, brain atrophy and multiorgan failure leading to

multiple hospital visits and early death. Fortunately, GS inborn deficiency is an extremely rare disorder.

Importance of GS and brain edema

The role of GS in the pathogenesis of brain edema is yet not fully understood. Glutamine synthetase rapidly converts glutamate and ammonia present in the brain into glutamine, which is an active osmolyte. In hyperammonemic conditions, the increase in GS's substrates increase the production of glutamine (Takahashi et al., 1991), which could change brain osmolality. In this case, if the BBB is not disrupted, water could enter the brain through aquaporin channels (Francesca and Rezzani, 2010) and cause astrocytic cytotoxic edema (Rama Rao et al., 2010). The role of GS in brain edema is tightly connected to astrocytic GS, however the role of endothelial GS has never been properly evaluated.

Inhibition with L-Methionine-S-Sulfoximine

L-Methionine-S-Sulfoximine (MSO) is a known inhibitor of GS. MSO competes with glutamate as a GS substrate. Once the inhibitor binds (instead of glutamate), the enzyme becomes phosphorylated, and irreversibly inactivated (Jeitner and Cooper, 2014). MSO presents an efficient inhibition of GS activities in all tissues. Studies regarding the effects of MSO in the central nervous system are extensive, although to some extent contradictory. In hyperammonemic conditions, MSO treatments are known to protect the brain from cytotoxic edema possibly due to the decrease in glutamine, reducing brain (astrocyte) osmolarity (Tanigami et al., 2005). On the other hand, MSO shows multiple deleterious effects such as toxic psychosis (Krakoff, 1961), seizures and neuronal cell loss (Wang et al., 2009a). In addition, MSO treatment was able to induce astrocytic edema (type II Alzheimer's astrocytes), a typical feature of hyperammonemia (Gutierrez and Norenberg, 1975). Since MSO treatment is known to increase ammonia levels by blocking its detoxification by GS (Heeneman and Deutz, 1993), it is possible that the increase in ammonia levels are indeed responsible for such effects.

Extra hepatic GS and importance in hyperammonemia

In liver disease, loss of hepatic function greatly impairs ammonia detoxification. In this state, extra-hepatic GS becomes the main ammonia detoxifying source. GS has been found in several organs, with skeletal muscle being the most important due to its mass. In BDL animals, although GS expression and activity are upregulated in muscle, hyperammonemia still persists (Jover-Cobos et al., 2014). This indicates that GS upregulation in muscle alone cannot compensate entirely for detoxifying ammonia during hepatic dysfunction. Furthermore, ammonia enters the brain and therefore central GS (astrocytic) also might have an important compensatory detoxifying role, but without success.

GS is found in the BBB's EC and CMV

GS mRNA expression

In the central nervous system, glutamine formation by GS is the main pathway for ammonia elimination. So far GS was never identified in EC of the BBB. Several studies confined the presence of GS to astrocytes and even oligodendrocytes, but never in EC (Anlauf and Derouiche, 2013). In our study, primary brain EC demonstrated GS mRNA, although less than compared to the same amount of RNA from whole liver lysate (but not brain) used as positive control. This difference was not surprising considering the important role of GS in ammonia detoxification in liver.

Protein expression of GS

Protein expression of GS was also assessed *in vitro* and *in vivo*. Primary microvascular EC showed lower presence of GS when compared to liver and brain tissue samples. The lower expression of GS compared to brain samples was not significant in mRNA results, which could mean that GS protein translation from mRNA is not 100%. CMV from naive animals behave differently than *in vitro* cells, presenting the same protein levels when compared to whole brain and liver samples (positive controls). The difference in expression of GS between *in vivo* and *in vitro* might be explained by the fact 1) the cultured cells (even if primary cells) might have slight different protein expression compared to what was observed *in vivo* and 2) CMV preparations

might contain small amounts of perivascular elements, such as astrocytes. In fact, CMV from naive rats showed significant higher protein expression when compared to cultured EC (data not shown). Finally, there was no difference in protein expression of GS in cerebellum vs pre-frontal cortex from naive rats, indicating that there is no influence between these brain regions in GS expression levels.

GS activity

GS activity in primary brain EC followed the results of protein expression, with lower activity when compared to whole brain and liver tissue (positive controls). On the other hand, results from CMV from naive rats showed lower GS activity when compared to both brain and liver used as positive controls. It is possible that GS in CMV is less active than in other tissues (brain and liver) and therefore, EC of the BBB have high potential as target for GS activity stimulation. In addition, GS activities from CMVs isolated from pre-frontal cortex and cerebellum were similar as were GS protein levels.

Immunofluorescence

Here *in vitro* immunofluorescence was used to visually confirm the western blot results. On the other hand, immunofluorescence using brain slices of naive rats was the most important step in GS identification *in vivo*. Because CMV might have other perivascular elements, there was a possibility that the results obtained by protein expression were altered by the presence of astrocytes, which are known to have GS. The visual confirmation of GS co-localized with EC marker established that the enzyme assessed by western blot was indeed endothelial. Other studies have assessed the localization of GS in brain tissue by immunohistochemistry (Martinez-Hernandez et al., 1977; Norenberg, 1979) but none of them searched specifically for GS in EC. Because astrocytes present GS, it is likely that GS is overlooked in endothelium cells unless it is localization is determined with a specific EC marker.

Importance of GS in different cell types

GS in astrocytes

The presence of GS in astrocytes was reported multiple times (Anlauf and Derouiche, 2013; Martinez-Hernandez et al., 1977; Norenberg, 1979). GS in astrocytes, different from all the other GS in the body, has an important role in regulating the neuronal glutamate pools via the astrocyte-neuron glutamate-glutamine cycle. Astrocytes play a major role in protecting against excitotoxicity by clearing synaptic cleft of glutamate following synaptic transmission (Maragakis and Rothstein, 2004). The action of GS allows glutamate to be converted to glutamine and shuttled through the extracellular space (in the form of the non-neuroactive glutamine, preventing neurotoxicity) to neurons. Stressing the importance of GS in these cells, several studies indicated that GS activity is decreased in several brain disorders such as epilepsy, ischemia-reperfusion injury, Alzheimer's and Huntington's disease (Eid et al., 2013; Liévens et al., 2001; Oliver et al., 1990; Robinson, 2000).

GS in hepatocytes

Liver GS has perhaps its most notorious function: ammonia detoxification. GS is responsible for as much as half of liver ammonia clearance (Hakvoort et al., 2016). Although important, liver GS might not be essential for survival. Animal models with selective liver inhibition of GS presented relatively normal phenotype, with only 1.9 fold in ammonia levels and decreased muscle-to-fat ratio. Even so, GS has a potential role as a target in urea cycle disorders, by exerting a compensatory role in ammonia detoxification in these patients.

GS in myocytes

Skeletal muscle is the main endogenous source of the amino acid glutamine in the body by the action of GS. Because of that, GS has an central role in muscle build up, recovery and response to fasting (He et al., 2010; Street et al., 2011). Since muscle is an energy demanding tissue and glutamine is a major energy source (Newsholme et al., 2003; Zielke et al., 1984), the importance of GS after fasting is central. A study done by He and colleagues showed that the inhibition of GS prevents the necessary 4-fold increase in muscle glutamine after fasting (He et al., 2010). In addition, inhibition with MSO caused 55% reduction in intracellular muscle

glutamine in normal feeding animals, and this was correlated with a potential increase in muscle protein breakdown (Heeneman and Deutz, 1993). These results show that GS plays a key role in muscle energy metabolism.

GS in EC

The discovery of GS in EC leads to new questions regarding its function and importance in this cell type. Because of its restrictive barrier function, EC of the BBB have high energy requirements. From requiring substrates for numerous transporters, carriers and other critical proteins, to the energy necessary to maintain these systems, these cells demand a rich environment. Glutamine supports the establishment of cells that have high energy demands and synthesize large amounts of proteins. Because of that, the use of glutamine produced by GS as a source of energy in this cell type agrees with its metabolic needs. In addition, the ability to synthesize glutamine would provide a constant source of nutrients to maintain the critical barrier function, even when the individual is submitted to fasting.

Since the BBB is the interface between the blood and the brain, the EC act as a first barrier against central toxicity. Because the brain is susceptible to ammonia insults, GS in EC would protect and therefore limit the passage of ammonia into the brain, preventing deleterious effects such as mitochondrial dysfunctions and subsequent astrocyte swelling. EC of the BBB have excitatory amino acid transporters (EAATs) predominantly in abluminal membranes, carrying glutamate against its electrochemical gradient: from the brain's extracellular space into the EC, thus providing substrate for GS detoxification (Hawkins, 2009). At the same time, the glutamine produced in the EC can be used as an energy source, integrating the two possible GS roles (detoxification and energy production). In this setting, increased GS activity in EC of the BBB might act to prevent the brain's ammonia toxicity by 1) decreasing ammonia entrance into the brain, 2) removing excess of glutamate from the brain and 3) keeping the normal function of the BBB by providing energy as glutamine.

Ammonia-lowering strategies

Since hyperammonemia is a key feature of HE, the use of ammonia-lowering compounds is the first line of treatment in these patients. Ammonia-lowering strategies can be

divided by its mechanism of action in 1) molecules that decrease ammonia generation and 2) molecules that increase ammonia removal.

1) Most treatments used to date for HE patients focusses on decreasing ammonia production. Ammonia is primarily produced in the intestines by the action of the enzyme glutaminase and by ammoniogenic bacteria. Examples of this class of treatments are: a) lactulose, which is a laxative and therefore acts by accelerating the passage of proteins trough the gastrointestinal tract (GIT) and by changing the pH of the intestines, affecting the survival of ammoniogenic bacteria and decreasing protein breakdown by the enzyme glutaminase; b) rifaximin (recently approved in Canada), which is a non-absorbable antibiotic and acts by altering the activity and amount of bacteria in the gut c) probiotics and branched-chain amino acids, which improve the balance of the intestinal flora, decreasing preferentially ammoniogenic bacteria.

2) Treatments that increase ammonia-removal represent very promising strategies, focussing primarily on increasing GS activity. Examples of molecules that belong to this class are:

a) L-ornithine L-aspartate (LOLA) (not available in Canada), which serves as a substrate for the hepatic urea cycle as aspartate, and to the GS activity as ornithine, inducing ammonia excretion (Bai et al., 2014; Ong et al., 2011). These two amino acids lowered blood ammonia and improved HE when administered intravenously (Kircheis et al., 1997), but despite that, this treatment can have a diminished effect in end-stage liver disease, due to lack of functional hepatocytes (Hadjihambi and Jalan, 2015). In addition, glutamine formed as the final product of GS metabolism might be converted in glutamate and ammonia, by the action of the enzyme glutaminase;

b) glycerol phenylbutyrate (GPB) (not clinically available), which is composed by three molecules of phenylbutyric acid plus one molecule of glycerol. Once GPB is in the GIT, it suffers hydrolysis and β-oxidation to form phenylacetate, which will bind to glutamine forming phenylacetylglutamine, a stable molecule that can be excreted in urine, preventing the release of ammonia by glutaminase (figure 26). This drug is already used to treat children with urea cycle disorders, and in clinical trials was shown to reduce ammonia levels and HE events in patients with cirrhosis. (Rockey et al., 2014);

c) ornithine phenylacetate (OP), which presents the best features of LOLA and GPB combined, provides the ornithine to induce GS metabolism and the phenylacetate that will bind the formed glutamine producing phenylacetylglutamine and preventing glutamine from being metabolized by glutaminase and regenerating ammonia. Ornithine can enter muscle cells, where it is converted into glutamate by the enzyme ornithine transcarbamylase, and into glutamine by GS. After that, the glutamine joins the phenylacetate forming the stable phenylacetylglutamine, which cannot be metabolized by glutaminase and therefore will be excreted in urine. OP present reduced ammonia levels and brain edema and upregulation of muscle GS in animal models and liver-diseased patients (Ventura-Cots et al., 2013; Ytrebø et al., 2009), but is still in trial phase. The most impressive characteristic of OP is its ability to penetrate diverse tissues and provide GS with a substrate, acting towards its upregulation. Because of that, OP would make an interesting therapy targeting GS of any organ or cell type, including the BBB EC.

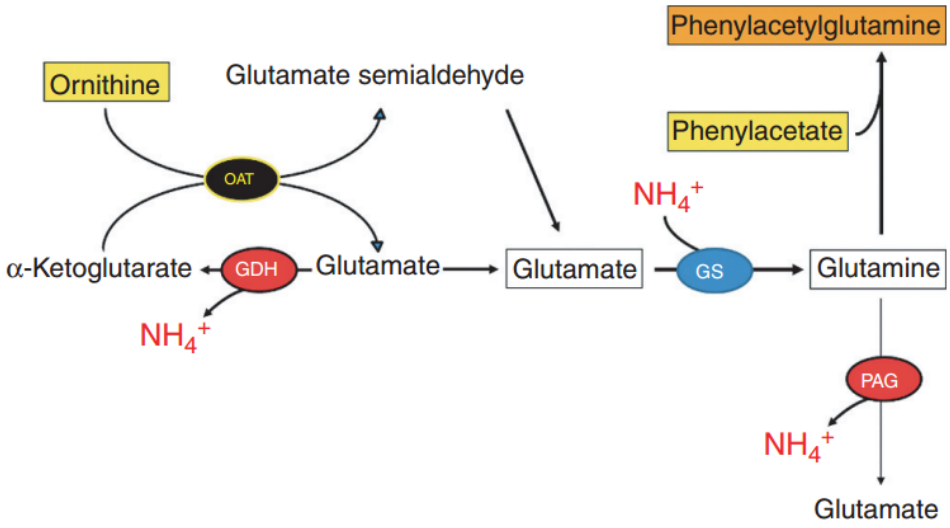

Figure 26 : Ornithine-phenylacetate mechanism of action

Differently from glutamate, ornithine can penetrate muscle tissue, acting as a source of substrate for glutamine synthesis by GS. Figure from (Rose, 2012).

GS regulation

Due to GS importance in homeostasis, it is imperative to have a tightly regulated activity of the enzyme, which is achieved by the combination of transcriptional and post-transcriptional mechanisms, with oxidative stress having an influential role.

Tyrosine nitration

The relationship between GS activity and tyrosine nitration is well established. GS activity is highly susceptible to regulation due to ROS (Görg et al., 2007), which was demonstrated by the decrease in GS activity in cultured astrocytes exposed to increased nitric oxide (Miñana et al., 1997). The nitration of tyrosine residues to 3-nitrotyrosine is a posttranslational modification caused by an imbalance in nitric oxide signaling and metabolism favoring nitrosative and oxidative stress. Nitric oxide metabolites in the presence of ROS leads to the formation of nitrating molecules like peroxynitrite (Radi, 2013). These molecules bind to GS likely Tyr-335 residues (Görg et al., 2007) and can lead to structural and functional changes that might culminate in altered cell homeostasis.

Lysine acetylation

Recently Nguyen and colleagues (Nguyen et al., 2016) demonstrated the regulation of GS by glutamine through lysine acetylation. The regulation of GS degradation starts with the acetylation of lysine 11 and 14 in the presence of high glutamine. After the lysine-acetylated domains bind to the receptor for the cullin-RING ubiquitin ligase 4 (CRL4), a signaling for proteasome degradation starts with GS ubiquitylation.

Other factors

GS can also be regulated by β-catenin, which in liver was shown to be necessary for normal GS mRNA and protein expression (Sekine et al., 2006). GS cellular distribution was also parallel to that of β-catenin activity (Cadoret et al., 2002). Changes in pH can regulate GS by modifying ammonia and glutamate/glutamine balance (Nissim, 1999).

GS regulation by liver disease and ammonia/ROS

GS is not altered in CMV in BDL vs SHAM

There was no difference in GS protein levels and activity in CMVs isolated from cortex or cerebellum of BDL animals when compared to SHAM, which corroborates other studies using brain homogenates. A study from Jover-Cobos and colleagues, also found no difference in brain GS protein and activity in BDL animals when compared to SHAM operated controls (Jover-Cobos et al., 2014). On the other hand, studies using an animal model of type B HE presented a decrease in GS levels (Butterworth et al., 1988; Desjardins et al., 1999). Finally, Montes and colleagues reported in 2-week BDL rat, a decrease in whole brain GS activity, which subsequently recovered at 4 and 6 weeks (Montes et al., 2003). This supports our findings at 6 weeks, but the changes that occur at 2 weeks post-BDL remains unclear.

GS is downregulated in RBMEC exposed to conditioned medium from plasma of BDL and SHAM rats

GS is downregulated in RBMEC submitted to conditioned medium from BDL rats when compared with SHAM controls

BDL rat models express several systemic pathogenic factors that might play a role in the pathogenesis of brain edema, therefore we proceeded to treat EC's with conditioned media from BDL and SHAM rats. The use of conditioned medium allows to explore blood-derived factors that might influence GS protein expression and activity. Also, conditioned medium is used to rule out the effects of cell-cell signaling and brain-derived molecules. In our study, medium containing plasma from BDL and SHAM animals was used to expose cultured endothelial cells only to systemic factors. ECs treated at 24 hours with either BDL or SHAM plasma showed the same protein expression than untreated ECs (data not shown). EC's exposed to plasma from BDL for 72 hours presented downregulation in GS protein expression and activity compared to 72h SHAM's plasma. This shows that BDL animals either present circulating factors that can downregulate endothelial GS expression and activity or possess less factors that can upregulate GS expression and activity in CLD.

Under cholestatic conditions such as in the BDL rat, elevated levels of bile acids in the liver and consequently in the circulation lead to oxidative stress (Qin et al., 2006), which might play a role in GS regulation. In a study conducted by Nakajima and colleagues, treatment with the bile acids deoxycholic and chenodeoxycholic acid enhanced NO_2^- production in vascular EC (Nakajima et al., 2000). So, bile acids are also responsible for producing oxidative stress and might have an effect in GS levels. Both GS main regulatory mechanisms (tyrosine nitration and lysine acetylation) might be influenced by oxidative stress and therefore, might be the cause of the lack of GS upregulation in BDL animals presented here.

The non-significant change of GS in CMV from BDL vs SHAM animals might be explained by compensation of other cells (such as astrocytes) in the detoxification of toxins and therefore protection of EC or by the effect of other brain molecules that might prevent GS downregulation. Finally, when CMVs are isolated from brain tissue, a small portion of other perivascular cells can remain present (data not shown). Since astrocytes have a large pool of GS, even a low percentage of these cells might interfere with the detection of small changes in EC's.

GS is upregulated with 72h compared to 24h plasma treatment from SHAM animals

Treatments with SHAM plasma (but not BDL) for 72h caused upregulation of GS protein expression when compared to SHAM 24h, which was accompanied with an increase in activity. There was a trend for the same effect in BDL plasma treated cells (72h vs 24h), bur significance was not achieved due to the lack of upregulation found in BDL 72h treated cells.

Several toxins, nutrients, hormones and other signaling molecules are present in plasma from living animals that might have a potential effect on protein expression. Hormonal regulation of GS represents the transcriptional regulatory mechanism in which glucocorticoids are known to increase GS transcription. The studies were made by Labow and colleagues in rat lung epithelial cells and indicated regulation of the enzyme by a receptor-dependent mechanism. The GS response is given by a region around 6kb upstream of the transcription initiation site, and the other within the first intron of the gene (Labow et al., 2001). Endogenous glucocorticoids present in plasma of both animal models might be accountable for the increase in GS levels.

GS is regulated in RBMEC treated with ammonia and ROS

GS is upregulated by ammonia

Hyperammonemia is known to influence GS in astrocytes; (i) astrocytes localized in glutaminergic areas show increased GS expression, protecting these areas from neurotoxicity while astrocytes from non-glutaminergic zones show a decrease in GS (Suárez et al., 2002). Here when EC were exposed to 1mM of ammonia for 48h, cells displayed an increase in GS activity. That increase might represent an adaptive response of the BBB in order to protect the brain from ammonia insult by increasing its detoxification by GS. Our results demonstrate high levels of ammonia for at least 48 hours are necessary to induce GS in ECs, since treatments of 1 mM for 24 hours and 0,5 mM for 24 and 48 hours showed no upregulation of GS activity.

GS is downregulated by oxidative stress

Oxidative stress is known to regulate GS activity. In liver disease patients, systemic oxidative stress is correlated with the presence of minimal HE (Gimenez-Garzó et al., 2015). Those patients showed increased levels of oxidative stress in blood, with increased lipid peroxidation, DNA oxidation and tyrosine nitration levels. Supporting this study, Negru and colleagues found in HE patients due to alcoholic liver disease elevated blood levels of free radicals and decreased antioxidant capacity (Negru et al., 1999).

Our results demonstrated a decrease in GS activity in EC following 48 hours (not 24 hours) of hydrogen peroxide with or without ammonia. Considering the potential role of GS as a source of energy in the EC, the inhibition of the enzyme due to ROS could possibly culminate in energy failure and subsequent cellular edema, as demonstrated in astrocytes. In addition, glutamine levels protect cells from oxidative injury caused by hydrogen peroxide (Hinshaw and Burger, 1990), therefore the decrease in GS activity can exacerbate deleterious effects.

Future studies

NKCC1 and edema

The two ionic co-transporters NKCC and KCC work together to maintain cell volume regulation. As upregulation of NKCC would cause increase in ammonia entrance, a change in KCC would lead ammonia transfer into the brain or accumulation in the endothelial cells. With GS present in ECs, it is possible that an increase in GS (due to ammonia) could lead to EC swelling. Therefore, assessing KCC levels in CMV of BDL animals is worth investigating and evaluation of endothelial cell swelling in ammonia and oxidative stress conditions is also merited. A 3D volume assessment technique would be used to monitor cell volume changes in real time. The method developed by Boudreault and Grygorczyk allows to assess single cell volume changes in adherent cells while infusing with ammonia and oxidative stress (Boudreault and Grygorczyk, 2004).

GS and ammonia metabolism in EC

GS is the most important enzyme involved in extra-hepatic ammonia detoxification, and our study clearly identified for the first time GS presence in BBB endothelial cells. There still a lot to learn about this enzyme and its role in EC metabolism. However, it would be of great interest to evaluate whether the beneficial effect of the treatments LOLA and OP also involve the activity of GS in the BBB.

Isolating CMV

The isolated CMV are central in the assessment of the BBB. With some perivascular elements present in the enriched solution, this could interfere with the results. Therefore, better (cleaner) isolation techniques are required. Fluorescence-activated cell sorting (FACS) provide a robust method for cell sorting and therefore could be used to increase the purity of CMV.

Ammonia metabolism enzymes

GS is one of the most important enzymes in ammonia detoxification, but is not the only one. Other enzymes are responsible for previous steps in ammonia detoxification, but their presence in endothelial cells of the BBB is unknown. Glutamate dehydrogenase is the enzyme responsible for converting ketoglutaric acid into glutamate, which will serve as a GS substrate. Ornithine aminotransferase is responsible for the conversation of ornithine into glutamate, and might have an important effect in GS substrate availability. In addition, this enzyme is crucial for the use of ammonia-lowering drug OP. In addition, it would be interesting to evaluate these enzymes in liver disease conditions.

Increase expression on GS

Finally, here we showed that oxidative stress downregulates GS activity, but the mechanisms involved in this process are still unknown. GS activity is regulated by protein tyrosine nitration, which is affected by oxidative stress. Therefore, assessing GS tyrosine nitration in CMV from the BDL model and *in vitro* on ammonia and oxidative stress conditions is interesting. In addition, we could try to stimulate GS activity with antioxidants and evaluate its effect of *in vivo* and *in vitro.*

Conclusion

In conclusion, our results demonstrate that NKCC1 located on the EC of the BBB is likely not involved in the pathogenesis of brain edema in the BDL model. Protein and activity of the enzyme GS was found for the first time in EC of the BBB *in vitro* and *in vivo*. Ammonia (< 1mM) treatments lead to an increase in GS activity while in combination with oxidative stress, caused a decrease in activity. CMV from BDL rats showed no differential expression of GS when compared to SHAM operated controls. Nevertheless, GS in EC have the potential to be stimulated to help increase ammonia clearance and protect the brain in conditions of hyperammonemia. Finally, the discovery of GS in this cell type presents a breakthrough in the understanding of brain ammonia metabolism and poses a potential target for ammonia-lowering strategies.

Bibliography

Abdel-Misih, S.R.Z., and Bloomston, M. (2010). Liver Anatomy. Surg. Clin. North Am. *90*, 643–653.

Ah Mew, N., Lanpher, B.C., Gropman, A., Chapman, K.A., Simpson, K.L., Urea Cycle Disorders Consortium, and Summar, M.L. (1993). Urea Cycle Disorders Overview. In GeneReviews(®), R.A. Pagon, M.P. Adam, H.H. Ardinger, S.E. Wallace, A. Amemiya, L.J. Bean, T.D. Bird, N. Ledbetter, H.C. Mefford, R.J. Smith, et al., eds. (Seattle (WA): University of Washington, Seattle), p.

Ahabrach, H., Piedrafita, B., Ayad, A., El Mlili, N., Errami, M., Felipo, V., and Llansola, M. (2010). Chronic hyperammonemia alters the circadian rhythms of corticosteroid hormone levels and of motor activity in rats. J. Neurosci. Res. *88*, 1605–1614.

Albrecht, J., and Norenberg, M.D. (2006). Glutamine: A Trojan horse in ammonia neurotoxicity. Hepatology *44*, 788–794.

Alfadda, A.A., and Sallam, R.M. (2012). Reactive Oxygen Species in Health and Disease. BioMed Res. Int. *2012*, e936486.

Allen, S.N. (2013). Urea cycle disorder. Ment. Health Clin. *2*, 398–401.

Allt, G., and Lawrenson, J.G. (2001). Pericytes: cell biology and pathology. Cells Tissues Organs *169*, 1–11.

Anderson, J.M., and Van Itallie, C.M. (1995). Tight junctions and the molecular basis for regulation of paracellular permeability. Am. J. Physiol. *269*, G467-475.

Anlauf, E., and Derouiche, A. (2013). Glutamine synthetase as an astrocytic marker: its cell type and vesicle localization. Front. Endocrinol. *4*, 144.

Ares, G.R., Caceres, P.S., and Ortiz, P.A. (2011). Molecular regulation of NKCC2 in the thick ascending limb. Am. J. Physiol. Renal Physiol. *301*, F1143-1159.

Arias, N., Fidalgo, C., Felipo, V., and Arias, J.L. (2014). The effects of hyperammonemia in learning and brain metabolic activity. Metab. Brain Dis. *29*, 113–120.

Bai, M., He, C., Yin, Z., Niu, J., Wang, Z., Qi, X., Liu, L., Yang, Z., Guo, W., Tie, J., et al. (2014). Randomised clinical trial: L-ornithine-L-aspartate reduces significantly the increase of venous ammonia concentration after TIPSS. Aliment. Pharmacol. Ther. *40*, 63–71.

Bajaj, J.S. (2008). Management options for minimal hepatic encephalopathy. Expert Rev. Gastroenterol. Hepatol. *2*, 785–790.

Bajaj, J.S., Cordoba, J., Mullen, K.D., Amodio, P., Shawcross, D.L., Butterworth, R.F., Morgan, M.Y., and International Society for Hepatic Encephalopathy and Nitrogen Metabolism (ISHEN) (2011). Review article: the design of clinical trials in hepatic encephalopathy--an International Society for Hepatic Encephalopathy and Nitrogen Metabolism (ISHEN) consensus statement. Aliment. Pharmacol. Ther. *33*, 739–747.

Bajaj, J.S., Ridlon, J.M., Hylemon, P.B., Thacker, L.R., Heuman, D.M., Smith, S., Sikaroodi, M., and Gillevet, P.M. (2012). Linkage of gut microbiome with cognition in hepatic encephalopathy. Am. J. Physiol. Gastrointest. Liver Physiol. *302*, G168-175.

Ballabh, P., Braun, A., and Nedergaard, M. (2004). The blood–brain barrier: an overview: Structure, regulation, and clinical implications. Neurobiol. Dis. *16*, 1–13.

Bernal, W., Hall, C., Karvellas, C.J., Auzinger, G., Sizer, E., and Wendon, J. (2007). Arterial ammonia and clinical risk factors for encephalopathy and intracranial hypertension in acute liver failure. Hepatol. Baltim. Md *46*, 1844–1852.

Bernal, W., Hyyrylainen, A., Gera, A., Audimoolam, V.K., McPhail, M.J.W., Auzinger, G., Rela, M., Heaton, N., O'Grady, J.G., Wendon, J., et al. (2013). Lessons from look-back in acute liver failure? A single centre experience of 3300 patients. J. Hepatol. *59*, 74–80.

Bismuth, H. (1982). Surgical anatomy and anatomical surgery of the liver. World J. Surg. *6*, 3–9.

Boksha, I.S., Schönfeld, H.-J., Langen, H., Müller, F., Tereshkina, E.B., and Burbaeva, G.S. (2002). Glutamine synthetase isolated from human brain: octameric structure and homology of partial primary structure with human liver glutamine synthetase. Biochem. Biokhimiia *67*, 1012–1020.

Bosoi, C.R., and Rose, C.F. (2009). Identifying the direct effects of ammonia on the brain. Metab. Brain Dis. *24*, 95–102.

Bosoi, C.R., Parent-Robitaille, C., Anderson, K., Tremblay, M., and Rose, C.F. (2011). AST-120 (spherical carbon adsorbent) lowers ammonia levels and attenuates brain edema in bile duct-ligated rats. Hepatol. Baltim. Md *53*, 1995–2002.

Bosoi, C.R., Yang, X., Huynh, J., Parent-Robitaille, C., Jiang, W., Tremblay, M., and Rose, C.F. (2012). Systemic oxidative stress is implicated in the pathogenesis of brain edema in rats with chronic liver failure. Free Radic. Biol. Med. *52*, 1228–1235.

Bosoi, C.R., Tremblay, M., and Rose, C.F. (2014). Induction of systemic oxidative stress leads to brain oedema in portacaval shunted rats. Liver Int. *34*, 1322–1329.

Boudreault, F., and Grygorczyk, R. (2004). Evaluation of rapid volume changes of substrate-adherent cells by conventional microscopy 3D imaging. J. Microsc. *215*, 302–312.

Bradfield, P.F., Nourshargh, S., Aurrand-Lions, M., and Imhof, B.A. (2007). JAM Family and Related Proteins in Leukocyte Migration (Vestweber Series). Arterioscler. Thromb. Vasc. Biol. *27*, 2104–2112.

Brownson, E.A., Abbruscato, T.J., Gillespie, T.J., Hruby, V.J., and Davis, T.P. (1994). Effect of peptidases at the blood brain barrier on the permeability of enkephalin. J. Pharmacol. Exp. Ther. *270*, 675–680.

Burton, B.K. (2000). UREA CYCLE DISORDERS. Clin. Liver Dis. *4*, 815–830.

Bustamante, J., Rimola, A., Ventura, P.J., Navasa, M., Cirera, I., Reggiardo, V., and Rodés, J. (1999). Prognostic significance of hepatic encephalopathy in patients with cirrhosis. J. Hepatol. *30*, 890–895.

Butterworth, R.F., Girard, G., and Giguère, J.F. (1988). Regional differences in the capacity for ammonia removal by brain following portocaval anastomosis. J. Neurochem. *51*, 486–490.

Butterworth, R.F., Norenberg, M.D., Felipo, V., Ferenci, P., Albrecht, J., Blei, A.T., and Members of the ISHEN Commission on Experimental Models of HE (2009). Experimental models of hepatic encephalopathy: ISHEN guidelines. Liver Int. Off. J. Int. Assoc. Study Liver *29*, 783–788.

Cadoret, A., Ovejero, C., Terris, B., Souil, E., Lévy, L., Lamers, W.H., Kitajewski, J., Kahn, A., and Perret, C. (2002). New targets of beta-catenin signaling in the liver are involved in the glutamine metabolism. Oncogene *21*, 8293–8301.

Calas, A.-G., Richard, O., Même, S., Beloeil, J.-C., Doan, B.-T., Gefflaut, T., Même, W., Crusio, W.E., Pichon, J., and Montécot, C. (2008). Chronic exposure to glufosinate-ammonium induces spatial memory impairments, hippocampal MRI modifications and glutamine synthetase activation in mice. NeuroToxicology *29*, 740–747.

Caley, D.W., and Maxwell, D.S. (1970). Development of the blood vessels and extracellular spaces during postnatal maturation of rat cerebral cortex. J. Comp. Neurol. *138*, 31–47.

Cauli, O., López-Larrubia, P., Rodrigo, R., Agusti, A., Boix, J., Nieto-Charques, L., Cerdán, S., and Felipo, V. (2011). Brain region-selective mechanisms contribute to the progression of cerebral alterations in acute liver failure in rats. Gastroenterology *140*, 638–645.

Chen, F., Ohashi, N., Li, W., Eckman, C., and Nguyen, J.H. (2009). Disruptions of occludin and claudin-5 in brain endothelial cells in vitro and in brains of mice with acute liver failure. Hepatol. Baltim. Md *50*, 1914–1923.

Chen, Y., Yang, F., Lu, H., Wang, B., Chen, Y., Lei, D., Wang, Y., Zhu, B., and Li, L. (2011). Characterization of fecal microbial communities in patients with liver cirrhosis. Hepatol. Baltim. Md *54*, 562–572.

Claudio, L., Raine, C.S., and Brosnan, C.F. (1995). Evidence of persistent blood-brain barrier abnormalities in chronic-progressive multiple sclerosis. Acta Neuropathol. (Berl.) *90*, 228–238.

Cooper, A.J.L., and Jeitner, T.M. (2016). Central Role of Glutamate Metabolism in the Maintenance of Nitrogen Homeostasis in Normal and Hyperammonemic Brain. Biomolecules *6*, 16.

Córdoba, J., Alonso, J., Rovira, A., Jacas, C., Sanpedro, F., Castells, L., Vargas, V., Margarit, C., Kulisewsky, J., Esteban, R., et al. (2001). The development of low-grade cerebral edema in cirrhosis is supported by the evolution of (1)H-magnetic resonance abnormalities after liver transplantation. J. Hepatol. *35*, 598–604.

Cotena, S., and Piazza, O. (2012). Sepsis-Associated Encephalopathy. Transl. Med. UniSa *2*, 20–27.

Cui, W., Sun, C.-M., and Liu, P. (2013). Alterations of blood-brain barrier and associated factors in acute liver failure. Gastroenterol. Res. Pract. *2013*, 841707.

D'Andrea, L., Lytle, C., Matthews, J.B., Hofman, P., Forbush, B., and Madara, J.L. (1996). Na:K:2Cl cotransporter (NKCC) of intestinal epithelial cells. Surface expression in response to cAMP. J. Biol. Chem. *271*, 28969–28976.

Davies, N.A., Wright, G., Ytrebø, L.M., Stadlbauer, V., Fuskevåg, O.-M., Zwingmann, C., Davies, D.C., Habtesion, A., Hodges, S.J., and Jalan, R. (2009). L-ornithine and phenylacetate synergistically produce sustained reduction in ammonia and brain water in cirrhotic rats. Hepatology *50*, 155–164.

Demirel, U., Yalniz, M., Aygün, C., Orhan, C., Tuzcu, M., Sahin, K., Ozercan, I.H., and Bahçecioğlu, I.H. (2012). Allopurinol ameliorates thioacetamide-induced acute liver failure by regulating cellular redox-sensitive transcription factors in rats. Inflammation *35*, 1549–1557.

Desjardins, P., Rao, K.V.R., Michalak, A., Rose, C., and Butterworth, R.F. (1999). Effect of Portacaval Anastomosis on Glutamine Synthetase Protein and Gene Expression in Brain, Liver and Skeletal Muscle. Metab. Brain Dis. *14*, 273–280.

Devrajani, B.R., Shah, S.Z.A., Devrajani, T., and Kumar, D. (2009). Precipitating factors of hepatic encephalopathy at a tertiary care hospital Jamshoro, Hyderabad. JPMA J. Pak. Med. Assoc. *59*, 683–686.

Dhanda, S., Kaur, S., and Sandhir, R. (2013). Preventive effect of N-acetyl-L-cysteine on oxidative stress and cognitive impairment in hepatic encephalopathy following bile duct ligation. Free Radic. Biol. Med. *56*, 204–215.

Donovan, J.P., Schafer, D.F., Shaw, B.W., and Sorrell, M.F. (1998). Cerebral oedema and increased intracranial pressure in chronic liver disease. The Lancet *351*, 719–721.

Dunn, C.W., Horton, J.W., Megison, S.M., and Vuitch, M.F. (1991). Contribution of portal systemic shunt to Kupffer cell dysfunction in obstructive jaundice. J. Surg. Res. *50*, 234–239.

Eid, T., Tu, N., Lee, T.-S.W., and Lai, J.C.K. (2013). Regulation of astrocyte glutamine synthetase in epilepsy. Neurochem. Int. *63*, 670–681.

ElAli, A., and Hermann, D.M. (2011). ATP-binding cassette transporters and their roles in protecting the brain. Neurosci. Rev. J. Bringing Neurobiol. Neurol. Psychiatry *17*, 423–436.

Elgadi, K.M., Meguid, R.A., Qian, M., Souba, W.W., and Abcouwer, S.F. (1999). Cloning and analysis of unique human glutaminase isoforms generated by tissue-specific alternative splicing. Physiol. Genomics *1*, 51–62.

Faropoulos, K., Chroni, E., Assimakopoulos, S.F., Mavrakis, A., Stamatopoulou, V., Toumpeki, C., Drainas, D., Grintzalis, K., Papapostolou, I., Georgiou, C.D., et al. (2010). Altered occludin expression in brain capillaries induced by obstructive jaundice in rats. Brain Res. *1325*, 121–127.

Filippi, B.M., de los Heros, P., Mehellou, Y., Navratilova, I., Gourlay, R., Deak, M., Plater, L., Toth, R., Zeqiraj, E., and Alessi, D.R. (2011). MO25 is a master regulator of SPAK/OSR1 and MST3/MST4/YSK1 protein kinases. EMBO J. *30*, 1730–1741.

Fine, E.J., Ionita, C.C., and Lohr, L. (2002). The History of the Development of the Cerebellar Examination. Semin. Neurol. *22*, 375–384.

Flatman, P.W. (2002). Regulation of Na–K–2Cl cotransport by phosphorylation and protein–protein interactions. Biochim. Biophys. Acta BBA - Biomembr. *1566*, 140–151.

Flemmer, A.W., Gimenez, I., Dowd, B.F.X., Darman, R.B., and Forbush, B. (2002). Activation of the Na-K-Cl cotransporter NKCC1 detected with a phospho-specific antibody. J. Biol. Chem. *277*, 37551–37558.

Fontana, R.J. (2008). Acute Liver Failure including Acetaminophen Overdose. Med. Clin. North Am. *92*, 761–794.

Francesca, B., and Rezzani, R. (2010). Aquaporin and Blood Brain Barrier. Curr. Neuropharmacol. *8*, 92–96.

Gagnon, K.B.E., England, R., and Delpire, E. (2006). Volume sensitivity of cation-Cl- cotransporters is modulated by the interaction of two kinases: Ste20-related proline-alanine-rich kinase and WNK4. Am. J. Physiol. Cell Physiol. *290*, C134-142.

Gamal, M., Abdel Wahab, Z., Eshra, M., Rashed, L., and Sharawy, N. (2014). Comparative Neuroprotective Effects of Dexamethasone and Minocycline during Hepatic Encephalopathy. Neurol. Res. Int. *2014*.

Geck, P., Pietrzyk, C., Burckhardt, B.-C., Pfeifferl, B., and Heinz, E. (1980). Electrically silent cotransport of Na+, K+ and Cl− in ehrlich cells. Biochim. Biophys. Acta BBA - Biomembr. *600*, 432–447.

Gillen, C.M., Brill, S., Payne, J.A., and Forbush, B. (1996). Molecular Cloning and Functional Expression of the K-Cl Cotransporter from Rabbit, Rat, and Human A NEW MEMBER OF THE CATION-CHLORIDE COTRANSPORTER FAMILY. J. Biol. Chem. *271*, 16237–16244.

Gimenez-Garzó, C., Urios, A., Agustí, A., González-López, O., Escudero-García, D., Escudero-Sanchis, A., Serra, M.A., Giner-Durán, R., Montoliu, C., and Felipo, V. (2015). Is cognitive impairment in cirrhotic patients due to increased peroxynitrite and oxidative stress? Antioxid. Redox Signal. *22*, 871–877.

Görg, B., Qvartskhava, N., Voss, P., Grune, T., Häussinger, D., and Schliess, F. (2007). Reversible inhibition of mammalian glutamine synthetase by tyrosine nitration. FEBS Lett. *581*, 84–90.

Görg, B., Morwinsky, A., Keitel, V., Qvartskhava, N., Schrör, K., and Häussinger, D. (2010a). Ammonia triggers exocytotic release of L-glutamate from cultured rat astrocytes. Glia *58*, 691–705.

Görg, B., Qvartskhava, N., Bidmon, H.-J., Palomero-Gallagher, N., Kircheis, G., Zilles, K., and Häussinger, D. (2010b). Oxidative Stress Markers in the Brain of Patients with Cirrhosis and Hepatic Encephalopathy. Hepatol. Baltim. Md *52*, 256–265.

Government of Canada, P.H.A. of C. (2013). Chronic Diseases and Injuries in Canada - Evolution of the determinants of chronic liver disease in Quebec - Public Health Agency of Canada.

Greve, J.W., Gouma, D.J., Soeters, P.B., and Buurman, W.A. (1990). Suppression of cellular immunity in obstructive jaundice is caused by endotoxins: a study with germ-free rats. Gastroenterology *98*, 478–485.

Gropman, A.L., Summar, M., and Leonard, J.V. (2007). Neurological implications of urea cycle disorders. J. Inherit. Metab. Dis. *30*, 865–879.

Gutierrez, J.A., and Norenberg, M.D. (1975). Alzheimer II Astrocytosis Following Methionine Sulfoximine. Arch. Neurol. *32*, 123–126.

Guzy, R.D., and Schumacker, P.T. (2006). Oxygen sensing by mitochondria at complex III: the paradox of increased reactive oxygen species during hypoxia. Exp. Physiol. *91*, 807–819.

Haas, M. (1989). Properties and diversity of (Na-K-Cl) cotransporters. Annu. Rev. Physiol. *51*, 443–457.

Haas, M., Schmidt, W.F., and McManus, T.J. (1982). Catecholamine-stimulated ion transport in duck red cells. Gradient effects in electrically neutral [Na + K + 2Cl] Co-transport. J. Gen. Physiol. *80*, 125–147.

Häberle, J. (2011). Clinical practice. Eur. J. Pediatr. *170*, 21–34.

Häberle, J., Görg, B., Rutsch, F., Schmidt, E., Toutain, A., Benoist, J.-F., Gelot, A., Suc, A.-L., Höhne, W., Schliess, F., et al. (2005). Congenital glutamine deficiency with glutamine synthetase mutations. N. Engl. J. Med. *353*, 1926–1933.

Hadjihambi, A., and Jalan, R. (2015). Hepatic encephalopathy: New treatments. Clin. Liver Dis. *5*, 109–111.

Hakvoort, T.B.M., He, Y., Kulik, W., Vermeulen, J.L.M., Duijst, S., Ruijter, J.M., Runge, J.H., Deutz, N.E.P., Koehler, S.E., and Lamers, W.H. (2016). Pivotal role of glutamine synthetase in ammonia detoxification. Hepatology n/a-n/a.

Hamilton, N.B., Attwell, D., and Hall, C.N. (2010). Pericyte-Mediated Regulation of Capillary Diameter: A Component of Neurovascular Coupling in Health and Disease. Front. Neuroenergetics *2*.

Hartsock, A., and Nelson, W.J. (2008). Adherens and Tight Junctions: Structure, Function and Connections to the Actin Cytoskeleton. Biochim. Biophys. Acta *1778*, 660–669.

Hashizume, R., Maki, Y., Mizutani, K., Takahashi, N., Matsubara, H., Sugita, A., Sato, K., Yamaguchi, S., and Mikami, B. (2011). Crystal structures of protein glutaminase and its pro forms converted into enzyme-substrate complex. J. Biol. Chem. *286*, 38691–38702.

Hawkins, R.A. (2009). The blood-brain barrier and glutamate1234. Am. J. Clin. Nutr. *90*, 867S–874S.

Hawkins, B.T., and Davis, T.P. (2005). The blood-brain barrier/neurovascular unit in health and disease. Pharmacol. Rev. *57*, 173–185.

He, Y., Hakvoort, T.B.M., Köhler, S.E., Vermeulen, J.L.M., de Waart, D.R., de Theije, C., ten Have, G.A.M., van Eijk, H.M.H., Kunne, C., Labruyere, W.T., et al. (2010). Glutamine synthetase in muscle is required for glutamine production during fasting and extrahepatic ammonia detoxification. J. Biol. Chem. *285*, 9516–9524.

Heeneman, S., and Deutz, N.E.P. (1993). The effect of 4 days methionine sulfoximine administration on net muscle protein breakdown in rats. Clin. Nutr. *12*, 182–190.

Helou, K., Das, A.T., Lamers, W.H., Hoovers, J.M., Szpirer, C., Szpirer, J., Klinga-Levan, K., and Levan, G. (1997). FISH mapping of three ammonia metabolism genes (Glul, Cps1, Glud1) in rat, and the chromosomal localization of GLUL in human and Cps1 in mouse. Mamm. Genome Off. J. Int. Mamm. Genome Soc. *8*, 362–364.

Hermenegildo, C., Monfort, P., and Felipo, V. (2000). Activation of N-methyl-D-aspartate receptors in rat brain in vivo following acute ammonia intoxication: Characterization by in vivo brain microdialysis. Hepatology *31*, 709–715.

Heros, P. de los, Alessi, D.R., Gourlay, R., Campbell, D.G., Deak, M., Macartney, T.J., Kahle, K.T., and Zhang, J. (2014). The WNK-regulated SPAK/OSR1 kinases directly phosphorylate and inhibit the K+–Cl− co-transporters. Biochem. J. *458*, 559–573.

delos Heros, P., Alessi, D.R., Gourlay, R., Campbell, D.G., Deak, M., Macartney, T.J., Kahle, K.T., and Zhang, J. (2014). The WNK-regulated SPAK/OSR1 kinases directly phosphorylate and inhibit the K+–Cl− co-transporters. Biochem. J. *458*, 559–573.

Hinshaw, D.B., and Burger, J.M. (1990). Protective effect of glutamine on endothelial cell ATP in oxidant injury. J. Surg. Res. *49*, 222–227.

Hoffmann, E.K., Lambert, I.H., and Pedersen, S.F. (2009). Physiology of Cell Volume Regulation in Vertebrates. Physiol. Rev. *89*, 193–277.

Huang, C.-H., and Liu, P.Z. (2001). New Insights into the Rh Superfamily of Genes and Proteins in Erythroid Cells and Nonerythroid Tissues. Blood Cells. Mol. Dis. *27*, 90–101.

Iadecola, C., and Nedergaard, M. (2007). Glial regulation of the cerebral microvasculature. Nat. Neurosci. *10*, 1369–1376.

Iqbal, K., and Ottaway, J.H. (1970). Glutamine synthetase in muscle and kidney. Biochem. J. *119*, 145–156.

Irimia, R., Ciobica, A., Stanciu, C., and Trifan, A. (2013). The relevance of oxidative stress in cirrhotic patients with different forms of hepatic encephalopathy. ResearchGate *65*, 1245–1252.

Janzer, R.C., and Raff, M.C. (1987). Astrocytes induce blood-brain barrier properties in endothelial cells. Nature *325*, 253–257.

Javaheri, S., Davis, C., and Rogers, D.H. (1993). Ionic Composition of Cisternal CSF in Acute Respiratory Acidosis: Lack of Effect of Large Dose Bumetanide. J. Neurochem. *61*, 1525–1529.

Jayakumar, A.R., Liu, M., Moriyama, M., Ramakrishnan, R., Forbush, B., Reddy, P.V.B., and Norenberg, M.D. (2008). Na-K-Cl Cotransporter-1 in the mechanism of ammonia-induced astrocyte swelling. J. Biol. Chem. *283*, 33874–33882.

Jayakumar, A.R., Valdes, V., and Norenberg, M.D. (2011). The Na-K-Cl cotransporter in the brain edema of acute liver failure. J. Hepatol. *54*, 272–278.

Jayakumar, A.R., Tong, X.Y., Curtis, K.M., Ruiz-Cordero, R., Abreu, M.T., and Norenberg, M.D. (2014). Increased toll-like receptor 4 in cerebral endothelial cells contributes to the astrocyte swelling and brain edema in acute hepatic encephalopathy. J. Neurochem. *128*, 890–903.

Jeitner, T.M., and Cooper, A.J.L. (2014). Inhibition of human glutamine synthetase by L-methionine-S,R-sulfoximine – relevance to the treatment of neurological diseases. Metab. Brain Dis. *29*, 983–989.

Ji, W., Foo, J.N., O'Roak, B.J., Zhao, H., Larson, M.G., Simon, D.B., Newton-Cheh, C., State, M.W., Levy, D., and Lifton, R.P. (2008). Rare independent mutations in renal salt handling genes contribute to blood pressure variation. Nat. Genet. *40*, 592–599.

Jiang, S.-M., Jia, L., and Zhang, M.-H. (2015). Probiotic and lactulose: influence on gastrointestinal flora and pH value in minimal hepatic encephalopathy rats. Int. J. Clin. Exp. Med. *8*, 9996–10000.

Jover-Cobos, M., Noiret, L., Lee, K., Sharma, V., Habtesion, A., Romero-Gomez, M., Davies, N., and Jalan, R. (2014). Ornithine phenylacetate targets alterations in the expression and activity of glutamine synthase and glutaminase to reduce ammonia levels in bile duct ligated rats. J. Hepatol. *60*, 545–553.

Kahle, K.T., Simard, J.M., Staley, K.J., Nahed, B.V., Jones, P.S., and Sun, D. (2009). Molecular mechanisms of ischemic cerebral edema: role of electroneutral ion transport. Physiol. Bethesda Md *24*, 257–265.

Kahle, K.T., Rinehart, J., and Lifton, R.P. (2010). Phosphoregulation of the Na-K-2Cl and K-Cl cotransporters by the WNK kinases. Biochim. Biophys. Acta *1802*, 1150–1158.

Kaplan, M.R., Plotkin, M.D., Lee, W.S., Xu, Z.C., Lytton, J., and Hebert, S.C. (1996). Apical localization of the Na-K-Cl cotransporter, rBSC1, on rat thick ascending limbs. Kidney Int. *49*, 40–47.

Katunuma, N., Okada, M., and Nishii, Y. (1966). Regulation of the urea cycle and TCA cycle by ammonia. Adv. Enzyme Regul. *4*, 317–336.

Kelly, T., Kafitz, K.W., Roderigo, C., and Rose, C.R. (2009). Ammonium-evoked alterations in intracellular sodium and pH reduce glial glutamate transport activity. Glia *57*, 921–934.

Kircheis, G., Nilius, R., Held, C., Berndt, H., Buchner, M., Görtelmeyer, R., Hendricks, R., Krüger, B., Kuklinski, B., Meister, H., et al. (1997). Therapeutic efficacy of L-ornithine-L-aspartate infusions in patients with cirrhosis and hepatic encephalopathy: results of a placebo-controlled, double-blind study. Hepatol. Baltim. Md *25*, 1351–1360.

Kountouras, J., Billing, B.H., and Scheuer, P.J. (1984). Prolonged bile duct obstruction: a new experimental model for cirrhosis in the rat. Br. J. Exp. Pathol. *65*, 305–311.

Krajewski, W.W., Collins, R., Holmberg-Schiavone, L., Jones, T.A., Karlberg, T., and Mowbray, S.L. (2008). Crystal structures of mammalian glutamine synthetases illustrate substrate-induced conformational changes and provide opportunities for drug and herbicide design. J. Mol. Biol. *375*, 217–228.

Krakoff, I.H. (1961). Effect of methionine sulfoximine in man. Clin. Pharmacol. Ther. *2*, 599–604.

Krizbai, I.A., Lenzser, G., Szatmari, E., Farkas, A.E., Wilhelm, I., Fekete, Z., Erdos, B., Bauer, H., Bauer, H.-C., Sandor, P., et al. (2005). Blood-brain barrier changes during compensated and decompensated hemorrhagic shock. Shock Augusta Ga *24*, 428–433.

Kvamme, E., Roberg, B., and Torgner, I.A. (2000). Phosphate-Activated Glutaminase and Mitochondrial Glutamine Transport in the Brain. Neurochem. Res. *25*, 1407–1419.

Labow, B.I., Souba, W.W., and Abcouwer, S.F. (2001). Mechanisms Governing the Expression of the Enzymes of Glutamine Metabolism—Glutaminase and Glutamine Synthetase. J. Nutr. *131*, 2467S–2474S.

Lee, W.M. (2012). Acute liver failure. Semin. Respir. Crit. Care Med. *33*, 36–45.

Liévens, J.C., Woodman, B., Mahal, A., Spasic-Boscovic, O., Samuel, D., Kerkerian-Le Goff, L., and Bates, G.P. (2001). Impaired glutamate uptake in the R6 Huntington's disease transgenic mice. Neurobiol. Dis. *8*, 807–821.

Liu, W.-Y., Wang, Z.-B., Zhang, L.-C., Wei, X., and Li, L. (2012). Tight junction in blood-brain barrier: an overview of structure, regulation, and regulator substances. CNS Neurosci. Ther. *18*, 609–615.

Liwnicz, B.H., Leach, J.L., Yeh, H.S., and Privitera, M. (1990). Pericyte degeneration and thickening of basement membranes of cerebral microvessels in complex partial seizures: electron microscopic study of surgically removed tissue. Neurosurgery *26*, 409–420.

Lockwood, A.H., Finn, R.D., Campbell, J.A., and Richman, T.B. (1980). Factors that affect the uptake of ammonia by the brain: the blood-brain pH gradient. Brain Res. *181*, 259–266.

Lu, K.-T., Cheng, N.-C., Wu, C.-Y., and Yang, Y.-L. (2008). NKCC1-mediated traumatic brain injury-induced brain edema and neuron death via Raf/MEK/MAPK cascade. Crit. Care Med. *36*, 917–922.

Lytle, C., Xu, J.C., Biemesderfer, D., Haas, M., and Forbush, B. (1992). The Na-K-Cl cotransport protein of shark rectal gland. I. Development of monoclonal antibodies, immunoaffinity purification, and partial biochemical characterization. J. Biol. Chem. *267*, 25428–25437.

Lytle, C., McManus, T.J., and Haas, M. (1998). A model of Na-K-2Cl cotransport based on ordered ion binding and glide symmetry. Am. J. Physiol. *274*, C299-309.

Madoff, D.C., Wallace, M.J., Ahrar, K., and Saxon, R.R. (2004). TIPS-related Hepatic Encephalopathy: Management Options with Novel Endovascular Techniques. RadioGraphics *24*, 21–36.

Maragakis, N.J., and Rothstein, J.D. (2004). Glutamate transporters: animal models to neurologic disease. Neurobiol. Dis. *15*, 461–473.

Markadieu, N., and Delpire, E. (2014). Physiology and Pathophysiology of SLC12A1/2 transporters. Pflugers Arch. *466*.

Markossian, S., and Kreydiyyeh, S.I. (2005). TNF-alpha down-regulates the Na+-K+ ATPase and the Na+-K+-2Cl-cotransporter in the rat colon via PGE2. Cytokine *30*, 319–327.

Márquez, J., Cardona, C., Campos-Sandoval, J.A., Peñalver, A., Tosina, M., Matés, J.M., and Martín-Rufián, M. (2012). Mammalian glutaminase isozymes in brain. Metab. Brain Dis. *28*, 133–137.

Martinez-Hernandez, A., Bell, K.P., and Norenberg, M.D. (1977). Glutamine synthetase: glial localization in brain. Science *195*, 1356–1358.

Martín-Rufián, M., Tosina, M., Campos-Sandoval, J.A., Manzanares, E., Lobo, C., Segura, J.A., Alonso, F.J., Matés, J.M., and Márquez, J. (2012). Mammalian Glutaminase Gls2 Gene Encodes Two Functional Alternative Transcripts by a Surrogate Promoter Usage Mechanism. PLoS ONE *7*.

MatÉs, J.M., Pérez-Gómez, C., and De Castro, I.N. (1999). Antioxidant enzymes and human diseases. Clin. Biochem. *32*, 595–603.

Matter, K., and Balda, M.S. (2003). Signalling to and from tight junctions. Nat. Rev. Mol. Cell Biol. *4*, 225–236.

Matthews, G.D., Gur, N., Koopman, W.J.H., Pines, O., and Vardimon, L. (2010). Weak mitochondrial targeting sequence determines tissue-specific subcellular localization of glutamine synthetase in liver and brain cells. J. Cell Sci. *123*, 351–359.

McMaster, P.D. (1922). DO SPECIES LACKING A GALL BLADDER POSSESS ITS FUNCTIONAL EQUIVALENT? J. Exp. Med. *35*, 127–140.

Miller, E.K., Freedman, D.J., and Wallis, J.D. (2002). The prefrontal cortex: categories, concepts and cognition. Philos. Trans. R. Soc. B Biol. Sci. *357*, 1123–1136.

Miñana, M.D., Kosenko, E., Marcaida, G., Hermenegildo, C., Montoliu, C., Grisolía, S., and Felipo, V. (1997). Modulation of glutamine synthesis in cultured astrocytes by nitric oxide. Cell. Mol. Neurobiol. *17*, 433–445.

Misel, M.L., Gish, R.G., Patton, H., and Mendler, M. (2013). Sodium Benzoate for Treatment of Hepatic Encephalopathy. Gastroenterol. Hepatol. *9*, 219–227.

Montes, S., Alcaraz-Zubeldia, M., Muriel, P., and Rios, C. (2003). Role of Manganese Accumulation in Increased Brain Glutamine of the Cirrhotic Rat. Neurochem. Res. *28*, 911–917.

Montoliu, C., Cauli, O., Urios, A., ElMlili, N., Serra, M.A., Giner-Duran, R., González-Lopez, O., Del Olmo, J.A., Wassel, A., Rodrigo, J.M., et al. (2011). 3-Nitro-Tyrosine as a Peripheral Biomarker of Minimal Hepatic Encephalopathy in Patients With Liver Cirrhosis. Am. J. Gastroenterol. *106*, 1629–1637.

Nakajima, T., Okuda, Y., Chisaki, K., Shin, W.-S., Iwasawa, K., Morita, T., Matsumoto, A., Suzuki, J., Suzuki, S., Yamada, N., et al. (2000). Bile acids increase intracellular Ca2+ concentration and nitric oxide production in vascular endothelial cells. Br. J. Pharmacol. *130*, 1457–1467.

Nakhoul, N.L., and Hamm, L.L. (2013). Characteristics of Mammalian Rh Glycoproteins (SLC42 transporters) and Their Role in Acid-Base Transport. Mol. Aspects Med. *34*, 629–637.

Neff, G. (2010a). Pharmacoeconomics of hepatic encephalopathy. Pharmacotherapy *30*, 28S–32S.

Neff, G. (2010b). Factors affecting compliance and persistence with treatment for hepatic encephalopathy. Pharmacotherapy *30*, 22S–7S.

Negru, T., Ghiea, V., and Păsărică, D. (1999). Oxidative injury and other metabolic disorders in hepatic encephalopathy. Romanian J. Physiol. Physiol. Sci. *36*, 29–36.

Newsholme, P., Procopio, J., Lima, M.M.R., Pithon-Curi, T.C., and Curi, R. (2003). Glutamine and glutamate--their central role in cell metabolism and function. Cell Biochem. Funct. *21*, 1–9.

Nguyen, J.H., Yamamoto, S., Steers, J., Sevlever, D., Lin, W., Shimojima, N., Castanedes-Casey, M., Genco, P., Golde, T., Richelson, E., et al. (2006). Matrix metalloproteinase-9 contributes to brain extravasation and edema in fulminant hepatic failure mice. J. Hepatol. *44*, 1105–1114.

Nguyen, T.V., Lee, J.E., Sweredoski, M.J., Yang, S.-J., Jeon, S.-J., Harrison, J.S., Yim, J.-H., Lee, S.G., Handa, H., Kuhlman, B., et al. (2016). Glutamine Triggers Acetylation-Dependent Degradation of Glutamine Synthetase via the Thalidomide Receptor Cereblon. Mol. Cell *61*, 809–820.

Nissim, I. (1999). Newer aspects of glutamine/glutamate metabolism: the role of acute pH changes. Am. J. Physiol. - Ren. Physiol. *277*, F493–F497.

Norenberg, M.D. (1979). Distribution of glutamine synthetase in the rat central nervous system. J. Histochem. Cytochem. Off. J. Histochem. Soc. *27*, 756–762.

Norenberg, M.D., Jayakumar, A.R., and Rao, K.V.R. (2004). Oxidative Stress in the Pathogenesis of Hepatic Encephalopathy. Metab. Brain Dis. *19*, 313–329.

O'Donnell, M.E., Tran, L., Lam, T.I., Liu, X.B., and Anderson, S.E. (2004). Bumetanide Inhibition of the Blood-Brain Barrier Na-K-Cl Cotransporter Reduces Edema Formation in the

Rat Middle Cerebral Artery Occlusion Model of Stroke. J. Cereb. Blood Flow Metab. *24*, 1046–1056.

Olalla, L., Gutiérrez, A., Campos, J.A., Khan, Z.U., Alonso, F.J., Segura, J.A., Márquez, J., and Aledo, J.C. (2002). Nuclear Localization of L-type Glutaminase in Mammalian Brain. J. Biol. Chem. *277*, 38939–38944.

Oldendorf, W.H., and Brown, W.J. (1975). Greater number of capillary endothelial cell mitochondria in brain than in muscle. Proc. Soc. Exp. Biol. Med. Soc. Exp. Biol. Med. N. Y. N *149*, 736–738.

Oliver, C.N., Starke-Reed, P.E., Stadtman, E.R., Liu, G.J., Carney, J.M., and Floyd, R.A. (1990). Oxidative damage to brain proteins, loss of glutamine synthetase activity, and production of free radicals during ischemia/reperfusion-induced injury to gerbil brain. Proc. Natl. Acad. Sci. U. S. A. *87*, 5144–5147.

Ong, J.P., Aggarwal, A., Krieger, D., Easley, K.A., Karafa, M.T., Van Lente, F., Arroliga, A.C., and Mullen, K.D. (2003). Correlation between ammonia levels and the severity of hepatic encephalopathy. Am. J. Med. *114*, 188–193.

Ong, J.P., Oehler, G., Krüger-Jansen, C., Lambert-Baumann, J., and Younossi, Z.M. (2011). Oral L-ornithine-L-aspartate improves health-related quality of life in cirrhotic patients with hepatic encephalopathy: an open-label, prospective, multicentre observational study. Clin. Drug Investig. *31*, 213–220.

Ostapowicz, G., Fontana, R.J., Schiødt, F.V., Larson, A., Davern, T.J., Han, S.H.B., McCashland, T.M., Shakil, A.O., Hay, J.E., Hynan, L., et al. (2002). Results of a prospective study of acute liver failure at 17 tertiary care centers in the United States. Ann. Intern. Med. *137*, 947–954.

Paredes, A., Plata, C., Rivera, M., Moreno, E., Vázquez, N., Muñoz-Clares, R., Hebert, S.C., and Gamba, G. (2006). Activity of the renal Na+-K+-2Cl- cotransporter is reduced by mutagenesis of N-glycosylation sites: role for protein surface charge in Cl- transport. Am. J. Physiol. Renal Physiol. *290*, F1094-1102.

Patidar, K.R., and Bajaj, J.S. (2015). Covert and Overt Hepatic Encephalopathy: Diagnosis and Management. Clin. Gastroenterol. Hepatol. Off. Clin. Pract. J. Am. Gastroenterol. Assoc. *13*, 2048–2061.

Payne, J.A., and Forbush, B. (1994). Alternatively spliced isoforms of the putative renal Na-K-Cl cotransporter are differentially distributed within the rabbit kidney. Proc. Natl. Acad. Sci. U. S. A. *91*, 4544–4548.

Payne, J.A., and Forbush, B. (1995). Molecular characterization of the epithelial Na□K□Cl cotransporter isoforms. Curr. Opin. Cell Biol. *7*, 493–503.

Pellerin, L., Pellegri, G., Bittar, P.G., Charnay, Y., Bouras, C., Martin, J.L., Stella, N., and Magistretti, P.J. (1998). Evidence supporting the existence of an activity-dependent astrocyte-neuron lactate shuttle. Dev. Neurosci. *20*, 291–299.

Pellicoro, A., Ramachandran, P., Iredale, J.P., and Fallowfield, J.A. (2014). Liver fibrosis and repair: immune regulation of wound healing in a solid organ. Nat. Rev. Immunol. *14*, 181–194.

Peppiatt, C.M., Howarth, C., Mobbs, P., and Attwell, D. (2006). Bidirectional control of CNS capillary diameter by pericytes. Nature *443*, 700–704.

Piechotta, K., Lu, J., and Delpire, E. (2002). Cation Chloride Cotransporters Interact with the Stress-related Kinases Ste20-related Proline-Alanine-rich Kinase (SPAK) and Oxidative Stress Response 1 (OSR1). J. Biol. Chem. *277*, 50812–50819.

Ponce-Coria, J., Gagnon, K.B., and Delpire, E. (2012). Calcium-binding protein 39 facilitates molecular interaction between Ste20p proline alanine-rich kinase and oxidative stress response 1 monomers. Am. J. Physiol. Cell Physiol. *303*, C1198-1205.

Prasad, S., Dhiman, R.K., Duseja, A., Chawla, Y.K., Sharma, A., and Agarwal, R. (2007). Lactulose improves cognitive functions and health-related quality of life in patients with cirrhosis who have minimal hepatic encephalopathy. Hepatol. Baltim. Md *45*, 549–559.

Qin, P., Tang, X., Elloso, M.M., and Harnish, D.C. (2006). Bile acids induce adhesion molecule expression in endothelial cells through activation of reactive oxygen species, NF-κB, and p38. Am. J. Physiol. - Heart Circ. Physiol. *291*, H741–H747.

Qureshi, M.O., Khokhar, N., and Shafqat, F. (2014). Ammonia levels and the severity of hepatic encephalopathy. J. Coll. Physicians Surg.--Pak. JCPSP *24*, 160–163.

Radi, R. (2013). Protein tyrosine nitration: biochemical mechanisms and structural basis of functional effects. Acc. Chem. Res. *46*, 550–559.

Rama Rao, K.V., and Norenberg, M.D. (2012). BRAIN ENERGY METABOLISM AND MITOCHONDRIAL DYSFUNCTION IN ACUTE AND CHRONIC HEPATIC ENCEPHALOPATHY. Neurochem. Int. *60*, 697–706.

Rama Rao, K.V., Reddy, P.V.B., Tong, X., and Norenberg, M.D. (2010). Brain Edema in Acute Liver Failure. Am. J. Pathol. *176*, 1400–1408.

Ramsauer, M., Krause, D., and Dermietzel, R. (2002). Angiogenesis of the blood-brain barrier in vitro and the function of cerebral pericytes. FASEB J. Off. Publ. Fed. Am. Soc. Exp. Biol. *16*, 1274–1276.

Rao, K.V., Mawal, Y.R., and Qureshi, I.A. (1997). Progressive decrease of cerebral cytochrome C oxidase activity in sparse-fur mice: role of acetyl-L-carnitine in restoring the ammonia-induced cerebral energy depletion. Neurosci. Lett. *224*, 83–86.

Riggio, O., Varriale, M., Testore, G.P., Di Rosa, R., Di Rosa, E., Merli, M., Romiti, A., Candiani, C., and Capocaccia, L. (1990). Effect of lactitol and lactulose administration on the fecal flora in cirrhotic patients. J. Clin. Gastroenterol. *12*, 433–436.

Robinson, S.R. (2000). Neuronal expression of glutamine synthetase in Alzheimer's disease indicates a profound impairment of metabolic interactions with astrocytes. Neurochem. Int. *36*, 471–482.

Rockey, D.C., Vierling, J.M., Mantry, P., Ghabril, M., Brown, R.S., Alexeeva, O., Zupanets, I.A., Grinevich, V., Baranovsky, A., Dudar, L., et al. (2014). Randomized, double-blind, controlled study of glycerol phenylbutyrate in hepatic encephalopathy. Hepatol. Baltim. Md *59*, 1073–1083.

Ropper, A.H. (1984). Brain Edema After Stroke: Clinical Syndrome and Intracranial Pressure. Arch. Neurol. *41*, 26–29.

Rose, C.F. (2012). Ammonia-lowering strategies for the treatment of hepatic encephalopathy. Clin. Pharmacol. Ther. *92*, 321–331.

Rose, C., Ytrebø, L.M., Davies, N.A., Sen, S., Nedredal, G.I., Belanger, M., Revhaug, A., and Jalan, R. (2007). Association of reduced extracellular brain ammonia, lactate, and intracranial pressure in pigs with acute liver failure. Hepatol. Baltim. Md *46*, 1883–1892.

Russell, J.M. (1983). Cation-coupled chloride influx in squid axon. Role of potassium and stoichiometry of the transport process. J. Gen. Physiol. *81*, 909–925.

Russell, J.M. (2000). Sodium-Potassium-Chloride Cotransport. Physiol. Rev. *80*, 211–276.

Sangeetha, K., Krishnasamy, N., Padma, K., and Rajendran, K. (2016). Evaluation of Oxidative Stress in Liver Cirrhosis Patients to Early Diagnosis of Minimal Hepatic Encephalopathy. ResearchGate *5*, 1–9.

Sathyasaikumar, K.V., Swapna, I., Reddy, P.V.B., Murthy, C.R.K., Dutta Gupta, A., Senthilkumaran, B., and Reddanna, P. (2007). Fulminant hepatic failure in rats induces oxidative stress differentially in cerebral cortex, cerebellum and pons medulla. Neurochem. Res. *32*, 517–524.

Schindelin, J., Arganda-Carreras, I., Frise, E., Kaynig, V., Longair, M., Pietzsch, T., Preibisch, S., Rueden, C., Saalfeld, S., Schmid, B., et al. (2012). Fiji: an open-source platform for biological-image analysis. Nat. Methods *9*, 676–682.

Schousboe, A., Bak, L.K., and Waagepetersen, H.S. (2013). Astrocytic Control of Biosynthesis and Turnover of the Neurotransmitters Glutamate and GABA. Front. Endocrinol. *4*, 102.

Scott, T.R., Kronsten, V.T., Hughes, R.D., and Shawcross, D.L. (2013). Pathophysiology of cerebral oedema in acute liver failure. World J. Gastroenterol. WJG *19*, 9240–9255.

Sekine, S., Lan, B.Y.-A., Bedolli, M., Feng, S., and Hebrok, M. (2006). Liver-specific loss of beta-catenin blocks glutamine synthesis pathway activity and cytochrome p450 expression in mice. Hepatol. Baltim. Md *43*, 817–825.

Sharma, B.C., Sharma, P., Agrawal, A., and Sarin, S.K. (2009). Secondary prophylaxis of hepatic encephalopathy: an open-label randomized controlled trial of lactulose versus placebo. Gastroenterology *137*, 885–891, 891.e1.

Sheen, J.-M., Chen, Y.-C., Hsu, M.-H., Tain, Y.-L., Yu, H.-R., and Huang, L.-T. (2016). Combined Intraperitoneal and Intrathecal Etanercept Reduce Increased Brain Tumor Necrosis Factor-Alpha and Asymmetric Dimethylarginine Levels and Rescues Spatial Deficits in Young Rats after Bile Duct Ligation. Front. Cell. Neurosci. *10*.

Sotil, E.U., Gottstein, J., Ayala, E., Randolph, C., and Blei, A.T. (2009). Impact of preoperative overt hepatic encephalopathy on neurocognitive function after liver transplantation. Liver Transplant. Off. Publ. Am. Assoc. Study Liver Dis. Int. Liver Transplant. Soc. *15*, 184–192.

Spodenkiewicz, M., Diez-Fernandez, C., Rüfenacht, V., Gemperle-Britschgi, C., and Häberle, J. (2016). Minireview on Glutamine Synthetase Deficiency, an Ultra-Rare Inborn Error of Amino Acid Biosynthesis. Biology *5*.

Stamatovic, S.M., Keep, R.F., and Andjelkovic, A.V. (2008). Brain Endothelial Cell-Cell Junctions: How to "Open" the Blood Brain Barrier. Curr. Neuropharmacol. *6*, 179–192.

Stewart, P.A. (2000). Endothelial Vesicles in the Blood–Brain Barrier: Are They Related to Permeability? Cell. Mol. Neurobiol. *20*, 149–163.

Stewart, C.A., Malinchoc, M., Kim, W.R., and Kamath, P.S. (2007). Hepatic encephalopathy as a predictor of survival in patients with end-stage liver disease. Liver Transpl. *13*, 1366–1371.

Stratman, A.N., and Davis, G.E. (2012). Endothelial cell-pericyte interactions stimulate basement membrane matrix assembly: influence on vascular tube remodeling, maturation, and stabilization. Microsc. Microanal. Off. J. Microsc. Soc. Am. Microbeam Anal. Soc. Microsc. Soc. Can. *18*, 68–80.

Street, B., Byrne, C., and Eston, R. (2011). Glutamine Supplementation in Recovery From Eccentric Exercise Attenuates Strength Loss and Muscle Soreness. J. Exerc. Sci. Fit. *9*, 116–122.

Suárez, I., Bodega, G., and Fernández, B. (2002). Glutamine synthetase in brain: effect of ammonia. Neurochem. Int. *41*, 123–142.

Tait, M.J., Saadoun, S., Bell, B.A., and Papadopoulos, M.C. (2008). Water movements in the brain: role of aquaporins. Trends Neurosci. *31*, 37–43.

Takahashi, H., Koehler, R.C., Brusilow, S.W., and Traystman, R.J. (1991). Inhibition of brain glutamine accumulation prevents cerebral edema in hyperammonemic rats. Am. J. Physiol. *261*, H825-829.

TANIGAMI, H., REBEL, A., MARTIN, L.J., CHEN, T.-Y., BRUSILOW, S.W., TRAYSTMAN, R.J., and KOEHLER, R.C. (2005). EFFECT OF GLUTAMINE SYNTHETASE INHIBITION ON ASTROCYTE SWELLING AND ALTERED ASTROGLIAL PROTEIN EXPRESSION DURING HYPERAMMONEMIA IN RATS. Neuroscience *131*, 437–449.

Tanimura, A., Kurihara, K., Reshkin, S.J., and Turner, R.J. (1995). Involvement of Direct Phosphorylation in the Regulation of the Rat Parotid Na+-K+-2Cl− Cotransporter. J. Biol. Chem. *270*, 25252–25258.

Tao-Cheng, J.H., Nagy, Z., and Brightman, M.W. (1987). Tight junctions of brain endothelium in vitro are enhanced by astroglia. J. Neurosci. Off. J. Soc. Neurosci. *7*, 3293–3299.

Tivers, M.S., Handel, I., Gow, A.G., Lipscomb, V.J., Jalan, R., and Mellanby, R.J. (2014). Hyperammonemia and Systemic Inflammatory Response Syndrome Predicts Presence of Hepatic Encephalopathy in Dogs with Congenital Portosystemic Shunts. PLoS ONE *9*.

Torlot, F.J., McPhail, M.J.W., and Taylor-Robinson, S.D. (2013). Meta-analysis: the diagnostic accuracy of critical flicker frequency in minimal hepatic encephalopathy. Aliment. Pharmacol. Ther. *37*, 527–536.

Traber, P.G., Dal Canto, M., Ganger, D.R., and Blei, A.T. (1987). Electron microscopic evaluation of brain edema in rabbits with galactosamine-induced fulminant hepatic failure: ultrastructure and integrity of the blood-brain barrier. Hepatol. Baltim. Md *7*, 1272–1277.

Unterberg, A.W., Stover, J., Kress, B., and Kiening, K.L. (2004). Edema and brain trauma. Neuroscience *129*, 1019–1027.

Vaquero, J., Chung, C., Cahill, M.E., and Blei, A.T. (2003). Pathogenesis of hepatic encephalopathy in acute liver failure. Semin. Liver Dis. *23*, 259–269.

Ventura-Cots, M., Arranz, J.A., Simón-Talero, M., Torrens, M., Blanco, A., Riudor, E., Fuentes, I., Suñé, P., Soriano, G., and Córdoba, J. (2013). Safety of ornithine phenylacetate in cirrhotic decompensated patients: an open-label, dose-escalating, single-cohort study. J. Clin. Gastroenterol. *47*, 881–887.

Vilstrup, H., Amodio, P., Bajaj, J., Cordoba, J., Ferenci, P., Mullen, K.D., Weissenborn, K., and Wong, P. (2014). Hepatic encephalopathy in chronic liver disease: 2014 Practice Guideline by the American Association for the Study of Liver Diseases and the European Association for the Study of the Liver. Hepatol. Baltim. Md *60*, 715–735.

Wallace, B.K., Jelks, K.A., and O'Donnell, M.E. (2012). Ischemia-induced stimulation of cerebral microvascular endothelial cell Na-K-Cl cotransport involves p38 and JNK MAP kinases. Am. J. Physiol. Cell Physiol. *302*, C505-517.

Wang, G., Huang, H., He, Y., Ruan, L., and Huang, J. (2014). Bumetanide protects focal cerebral ischemia-reperfusion injury in rat. Int. J. Clin. Exp. Pathol. *7*, 1487–1494.

Wang, Y., Kudoh, J., Kubota, R., Asakawa, S., Minoshima, S., and Shimizu, N. (1996). Chromosomal Mapping of a Family of Human Glutamine Synthetase Genes: Functional Gene (GLUL) on 1q25, Pseudogene (GLULP) on 9p13, and Three Related Genes (GLULL1, GLULL2, GLULL3) on 5q33, 11p15, and 11q24. Genomics *37*, 195–199.

Wang, Y., Zaveri, H.P., Lee, T.-S.W., and Eid, T. (2009a). The development of recurrent seizures after continuous intrahippocampal infusion of methionine sulfoximine in rats: A video-intracranial electroencephalographic study. Exp. Neurol. *220*, 293–302.

Wang, Y.-Y., Lui, P.C.W., and Li, J.Y. (2009b). Receptor-mediated therapeutic transport across the blood-brain barrier. Immunotherapy *1*, 983–993.

Ytrebø, L.M., Kristiansen, R.G., Mæhre, H., Fuskevåg, O.M., Kalstad, T., Revhaug, A., Cobos, M.J., Jalan, R., and Rose, C.F. (2009). L-ornithine phenylacetate attenuates increased arterial and extracellular brain ammonia and prevents intracranial hypertension in pigs with acute liver failure. Hepatology *50*, 165–174.

Yudkoff, M. (1999). Urea Cycle.

Zielke, H.R., Zielke, C.L., and Ozand, P.T. (1984). Glutamine: a major energy source for cultured mammalian cells. Fed. Proc. *43*, 121–125.

Zlokovic, B.V. (2008). The Blood-Brain Barrier in Health and Chronic Neurodegenerative Disorders. Neuron *57*, 178–201.

Zwirner, K., Thiel, C., Thiel, K., Morgalla, M.H., Königsrainer, A., and Schenk, M. (2010). Extracellular brain ammonia levels in association with arterial ammonia, intracranial pressure and the use of albumin dialysis devices in pigs with acute liver failure. Metab. Brain Dis. *25*, 407–412.

Junqueira, Carneiro - Basic Histology - Text and Atlas 11e.